A review of anode materials development in solid oxide fuel cells

SAN PING JIANG, SIEW HWA CHAN
Fuel Cells Strategic Research Program, School of Mechanical and Production Engineering, Nanyang Technological University, Nanyang Avenue, Singapore 639798
E-mail: mspjiang@ntu.edu.sg

High temperature solid oxide fuel cell (SOFC) has prospect and potential to generate electricity from fossil fuels with high efficiency and very low greenhouse gas emissions as compared to traditional thermal power plants. In the last 10 years, there has been significant progress in the materials development and stack technologies in SOFC. The objective of this paper is to review the development of anode materials in SOFC from the viewpoint of materials microstructure and performance associated with the fabrication and optimization processes. Latest development and achievement in the Ni/Y$_2$O$_3$-ZrO$_2$ (Ni/YSZ) cermet anodes, alternative and conducting oxide anodes and anode-supported substrate materials are presented. Challenges and research trends based on the fundamental understanding of the materials science and engineering for the anode development for the commercially viable SOFC technologies are discussed. © *2004 Kluwer Academic Publishers*

1. Introduction

Solid oxide fuel cell (SOFC) is an all solid device that converts the chemical energy of gaseous fuels such as hydrogen and natural gas to electricity through electrochemical processes. SOFC, being an electrochemical device, has unique advantages over the traditional power generation technologies. The efficiency of SOFC is inherently high as it is not limited by the Carnot cycle of a heat engine. The greenhouse gas emissions from SOFC are much lower than those emitted from conventional power plants. Due to the high operating temperature, SOFC can be used as a co-generation to produce hot water or steam and to couple with microturbines or gas turbines to produce electrical power which enhance the system efficiency and the range of applications. The momentum of the intensive research and development of SOFC technology started in the middle seventies with the Westinghouse (now Siemens-Westinghouse) tubular SOFC development program [1]. Minh, almost a decade ago in 1993, gave a comprehensive overview on the whole spectra of the SOFC technologies [2]. Since then there have been tremendous progresses and achievements in both the SOFC technologies in materials, design and fabrication and in the fundamental understanding of the mechanism and kinetics of electrode reactions in SOFC. This has been reflected by a number of reviews on various topics of SOFC in recent years. Yokokawa *et al.* [3, 4] reviewed the development of materials from the view point of chemical interactions between various fuel cell component materials. Various aspects of material related issues were also discussed by Badwal and Foger [5], Kawada and Yokokawa [6], Steele [7], Huijsmans [8] and Badwal [9]. Carrette *et al.* [10], Yamamoto [11], Singhal [12]

and De Jonghe *et al.* [13] reviewed some fundamental and technological issues in SOFC. For a comprehensive and general treatment of fundamentals and latest development of SOFC technology, readers should refer to a very recent book by Singhal and Kendall [14].

Current activities in the areas of materials development for SOFC are increasingly focused on the decrease of operating temperatures of the SOFC from traditionally 1000°C to 500–800°C to reduce materials cost and improve the performance stability. To compensate for the increase in ohmic losses at reduced temperatures, electrolytes with higher ionic conductivity or thinner electrolyte structures are needed. As the electrolyte thickness decreases, the overall cell polarization losses are increasingly dominated by the losses of the electrochemical reactions at anodes and cathodes. Therefore it is crucial to understand the important issues associated with anode materials and anode-supported cell structures in the development and optimization of intermediate temperature SOFC (ITSOFC).

In SOFC, anode is the electrode for the electrochemical oxidation of fuels such as hydrogen and natural gas. Hydrogen oxidation is one of the most important electrode reactions in SOFC. The electrochemical oxidation of H$_2$ can be written, following Kröger-Vink notation, as:

$$H_2 + O_{YSZ}^{2-} = H_2O + 2e + V_{\ddot{O},YSZ} \qquad (1)$$
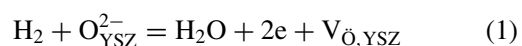
where O_{YSZ}^{2-} is an oxygen ion in the Y$_2$O$_3$-ZrO$_2$ (YSZ) electrolyte lattice site and $V_{\ddot{O},YSZ}$ is an oxygen vacancy in YSZ. To minimize the polarization losses of the H$_2$ oxidation reaction, anode materials should meet the basic requirements of high electronic conductivity,

sufficient electrocatalytic activity for fuel oxidation reactions, chemically stable and thermally compatible with other cell components and has sufficient porosity for efficient gas transportation in high-temperature reducing environment [2].

Due to the requirements of operating in reducing environment and high electronic conductivity, pure porous metallic electrodes, in principle, can be used as anode. Several metals such as Ni [15–17], Pt [17–19] and Ru [20] have been studied as anode materials. Setoguchi et al. [21] studied the electrochemical activity of Ni, Co, Fe, Pt, Mn and Ru and found that Ni exhibits the highest electrochemical activity for H_2 oxidation reaction. Pure nickel has a melting point of 1453°C, a thermal expansion coefficient of 13.3×10^{-6} cm·cm^{-1}k^{-1} and electronic conductivities of 138×10^4 S cm^{-1} and $\sim 2 \times 10^4$ S cm^{-1} at 25° and 1000°C, respectively. Relatively low melting temperature results in the tendency of lower sintering temperature (1000°C) and the thermal expansion coefficient of Ni is much higher than that of YSZ electrolyte (the thermal expansion coefficient of YSZ is in the range of $\sim 10.5 \times 10^{-6}$ cm·cm^{-1}K^{-1}). Addition of YSZ electrolyte phase into Ni significantly reduces the thermal expansion of the composite material in order to be thermally compatible with the electrolyte [22, 23]. It is generally accepted that the electrochemical activity of Ni anodes for H_2 oxidation reaction depends strongly on the three phase boundary (TPB where fuel gas, Ni and YSZ phases are met) areas [24–26]. De Boer et al. [27] observed the significant reduction of electrode polarization resistance of porous Ni electrode modified by deposition of fine YSZ particle as compared to pure Ni electrode. This indicates that YSZ phase in the cermet plays an important electrocatalytic role in the creation of additional reaction sites by extending the two-dimensional reaction zone into three-dimensional reaction zone, significantly enhancing the reaction kinetics in addition to the inhibiting of the coarsening and grain growth of the Ni phase [28–30]. Therefore the system of composite anode usually consisting of metal-oxide cermet structure has been overwhelmingly accepted. Today, the Ni/Y_2O_3-ZrO_2 (Ni/YSZ) cermet materials are still the most common anodes for SOFC.

Fuel cells that directly use hydrocarbon fuels such as natural gas, without first reforming those hydrocarbons to hydrogen, will have enormous advantages over conventional hydrogen-based fuel cells [31]. Removing the need either to supply hydrogen to the fuel cell or to include a hydrocarbon-reforming system greatly decreases the complexity, size and cost of the fuel cell system. Natural gas is regarded as a relatively cheap and clean fuel. The advantage of SOFC over other fuel cells is that the natural gas can be directly used without the need to external fuel reformer and water-gas shift reactor. The main component of natural gas is methane and following reforming reactions can take place directly inside a Ni/YSZ cermet anode:

$$CH_4 + H_2O = 3H_2 + CO \qquad (2)$$

$$CO + H_2O = CO_2 + H_2 \qquad (3)$$
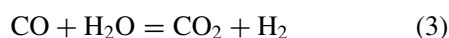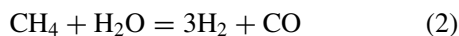
Internal reforming of hydrocarbon fuels is often accompanied by carbon deposition. Carbon deposition covers the active sites of the anodes, resulting in the loss of cell performance [32, 33]. High steam/carbon (S/C) ratios (e.g., up to 3) are typically used in conventional steam reformers to suppress the carbon formation. However, high S/C ratio is unattractive for fuel cells as it lowers the electrical efficiency of the fuel cell by steam dilution of the fuel. The endothermic nature of steam reforming reaction (Equation 2) can cause local cooling and steep thermal gradients potentially capable of mechanically damaging the cell stack [34]. Nevertheless, the impact of the endothermicity of methane steam reforming process on the cell stability can be reduced by the combination of both external and internal reforming activity [35] or by using the so called gradual internal reforming (GIR) of methane [36, 37].

Despite the excellent electrocatalytic properties of Ni/YSZ cermet materials for operation in H_2 fuel, Ni/YSZ based anode suffers a number of drawbacks in systems where natural gas is used as the fuel, notably the sulfur poisoning and carbon deposition caused by cracking of methane. Under high carbon activity environment iron, nickel, cobalt and alloys based on these metals could corrode by a process known as metal dusting. Metal dusting involves the disintegration of bulk metals and alloys into metal particles at high temperatures (300–850°C) in environment that are supersaturated with carbon. Ni corrosion process strongly depends on the temperature and the gas composition and in general Ni corrosion rate increases with temperature [38]. The form of carbon deposited on Ni in wet methane was found to be graphite as observed by in situ Raman microspectroscopy and the deposited carbon cannot be burned by electrochemically permeated oxygen [39]. There is also increased possibility for nickel oxidation at temperatures below 700°C as the result of the increased partial pressure of oxygen under typical operating conditions [40]. The large volume change involved in the oxidation and reduction cycle of Ni/NiO (theoretical density is 8.9 gcm^{-3} for Ni and 6.96 gcm^{-3} for NiO) could cause the instability of the Ni/YSZ cermet microstructure. The performance of conventional Ni/YSZ cermet anode is also not satisfactory at temperature range of 500 to 600°C due to the low ionic conductivity of YSZ phase in the cermet. Thus, the driving force for the development of alternative anodes is mainly due to the need to replace Ni/YSZ cermet anodes for the direct oxidation of hydrocarbon fuels such as methane and to develop dimensionally stable anodes with high mixed electronic and ionic conductivity for low temperature SOFC [41, 42].

The purpose of this paper is to review the achievements and progresses in the development of Ni/YSZ based anode materials and alternative conducting oxide anode materials in solid oxide fuel cells. Materials development for anode-supported structures is also reviewed. Emphasis will be placed on the development and progress in the last 10 years. Finally the direction and strategies in the development and optimization of SOFC anode materials are discussed.
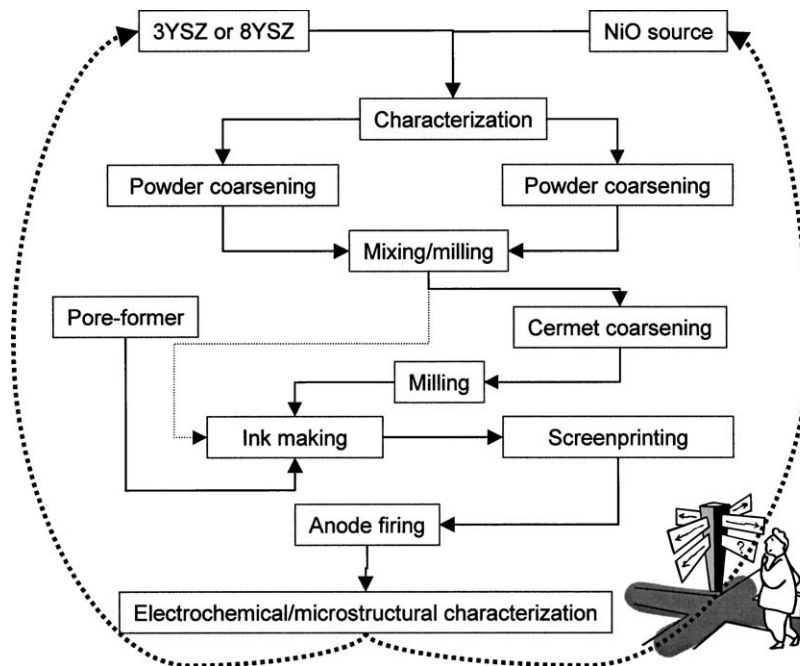
Figure 1 A generalized processing route for the preparation of Ni/YSZ cermet anodes.

2. Development of Ni/YSZ cermet anodes
2.1. Issues in the fabrication of Ni/YSZ cermet anodes

Conventional Ni/YSZ cermet anodes are usually made of commercial NiO and YSZ powders, which are then homogenized by mechanical mixing and milling. The NiO/YSZ ink is applied to the YSZ electrolyte and sintered to form a porous Ni/YSZ cermet electrode. Extensive literature shows that performance and electric properties of Ni/YSZ cermet anodes are critically dependent on the microstructure and distribution of Ni and YSZ phases. This in turn is dependent on the fabrication process, characteristics of the starting NiO and YSZ powders, sintering behavior of YSZ powders, etc. [43, 44]. Fig. 1 shows a general processing route for the preparation of Ni/YSZ cermet anodes, based on the conventional ceramic powder mixing process. Due to its general application in the fabrication and optimization of SOFC anodes, important issues in the fabrication and optimization of Ni/YSZ cermet anodes are discussed first.

2.1.1. Starting powder

Characteristics of the NiO and YSZ powders have significant effect on the fabrication process and the electrochemical performance of the Ni/YSZ cermet anodes. This is due to the fact that the properties such as the average particle size, the particle size distribution and sintering behavior (e.g., shrinkage and shrinkage rate) of NiO and YSZ powders are very different from different suppliers. Fig. 2 shows example of particle size distribution of various commercial NiO powders. NiO powders are ranging from very fine and broad distribution (e.g., AJAX NiO) to coarse and symmetric distribution (e.g., QN NiO). Difference in the powder characteristics will have significant effect on the sintering behavior and physical properties of the powder. Tietz *el al.* [45] eval-
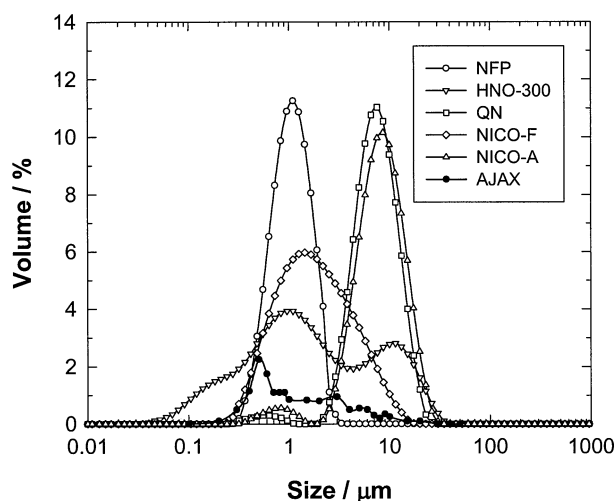
Figure 2 Particle size distribution of as-received commercial NiO powders. The particle size distribution was measured by laser scattering method.

uated eight different commercial NiO powders. The average grain size varied greatly from 0.5 to 14.7 μm with BET surface area from 0.2 to 47 m^2/g. Consequently, the sintering behavior of the powder differed significantly. The shrinkage of NiO powder ranged from 12 to 27% and the maximum shrinkage rate occurred between 660 to 1085°C, depending on the supplier. In general, high surface area corresponds to a high shrinkage and low starting sintering temperature. Similarly for commercial YSZ powders such as 3 mol% Y$_2$O$_3$-ZrO$_2$ (3YSZ) and 8 mol% Y$_2$O$_3$-ZrO$_2$ (8YSZ), the characteristics of the powder also vary considerably. For example, Ciacchi *et al.* [46] found that the specific surface areas of commercial YSZ powders change from 7.5 to 26 m^2 g^{-1}.

In the conventional powder mixing process, electrode performance was found to be affected by the initial particle size of YSZ and NiO powders. Hikita

[47] showed that the electrochemical performance of Ni/8YSZ cermet anodes is related to the particle size ratio of 8YSZ/NiO of starting oxide powders. The minimum anode overpotential losses were obtained at initial 8YSZ/NiO particle size ratio of ~0.01. Murakami *et al.* [48] found that 8YSZ particle size not only affects the electrode performance but also the stability and the volume concentration of the cermet. The larger the 8YSZ size is, the higher the 8YSZ content in the cermet will be required to achieve the best performance. The best performance was observed on the Ni/8YSZ cermet anodes prepared from starting 8YSZ and NiO powders with particle size of 0.5 and 2.5 μm, respectively. This corresponds to an 8YSZ/NiO particle size ratio of ~0.2. In the case of Ni/3YSZ cermet anodes, the effect of particle size of the 3YSZ powder on the polarization performance of Ni/3YSZ cermet anodes is almost linear and the best Ni/3YSZ cermet anode for the H_2 oxidation was prepared from 3YSZ and NiO powders with particle size of 0.06 and 0.14 μm, respectively [49]. As NiO particle size did not change in this case, this means that the polarization performance (or the electrode polarization conductivity) decreases with the increase in 3YSZ/NiO ratio. The discrepancies may be due to the fact that the particle size ratio in the cermet (or the final anode morphology) is significantly affected by the processing steps such as coarsening treatment of YSZ and Ni/YSZ cermet powders.

2.1.2. Powder coarsening treatment

Coarsening treatment of starting powder is one of the most important steps in the preparation of Ni/YSZ cermet anodes and is frequently used to control the powder characterization (e.g., particle size and size distribution) and the shrinkage profile of the cermet coating in order to have high coating quality and reproducibility.

Careful control of shrinkage profile of the Ni/YSZ cermet powders is particularly important in the production scale-up process. In practice, sintering profile of the cermet powder can be adjusted in certain degrees by heat treatment of starting NiO and zirconia powders. Jiang *et al.* [44, 49] studied the effect of coarsening NiO powders on the polarization performance of Ni/3YSZ cermet anodes. Fig. 3 illustrates a typical particle size distribution of NiO as a function of coarsening temperatures for three commercial NiO powders. As-received AJAX NiO powder shows very fine particles and broad particle size distribution (see Fig. 2). Average particle size determined from distribution measurement was ~1 μm. Coarsening AJAX NiO powder at 900°C dramatically changed the powder characteristics, indicated by the increased average particle size and narrowed particle size distribution (Fig. 3a). On the other hand, heat treatment at temperatures below 900°C has much less effect on the characteristics of HNO-300 NiO powders (Fig. 3b). As-received NFP NiO powder has narrow and symmetric particle size distribution and coarsening treatment is mainly to increase the average particle size (Fig. 3c). The difference in the characteristics of the NiO powders in relation to the coarsening treatment has direct effect on the electrode performance.
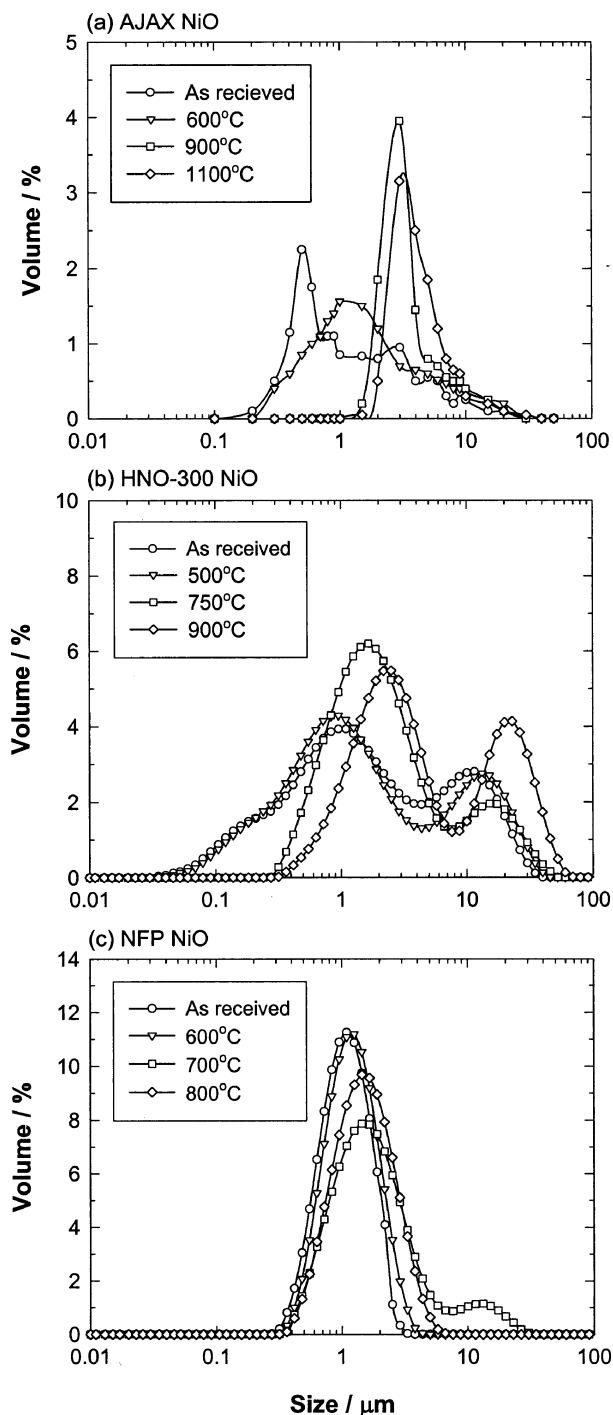
Figure 3 Change of particle size distribution of NiO as a function of coarsening temperatures for three different commercial NiO powders: (a) AJAX NiO, (b) HNO-300 NiO, and (c) NFP NiO.

For Ni/3YSZ cermet anodes prepared from AJAX NiO powder, the polarization losses reached the minimum for the anode prepared from NiO coarsened at ~600°C (Fig. 4a). For Ni/3YSZ cermet anodes prepared from HNO-300 NiO powder, the electrode performance remained more or less the same for the NiO coarsened at temperatures below 900°C (Fig. 4b).

Particle size and distribution of YSZ powder are an important factor in the performance of Ni/YSZ cermet anodes. Heat treatment or coarsening of YSZ powders is an effective way to control the particle size distribution of YSZ powders. Van Herle *et al.* [50] reported the performance of Ni/8YSZ cermet anodes prepared from
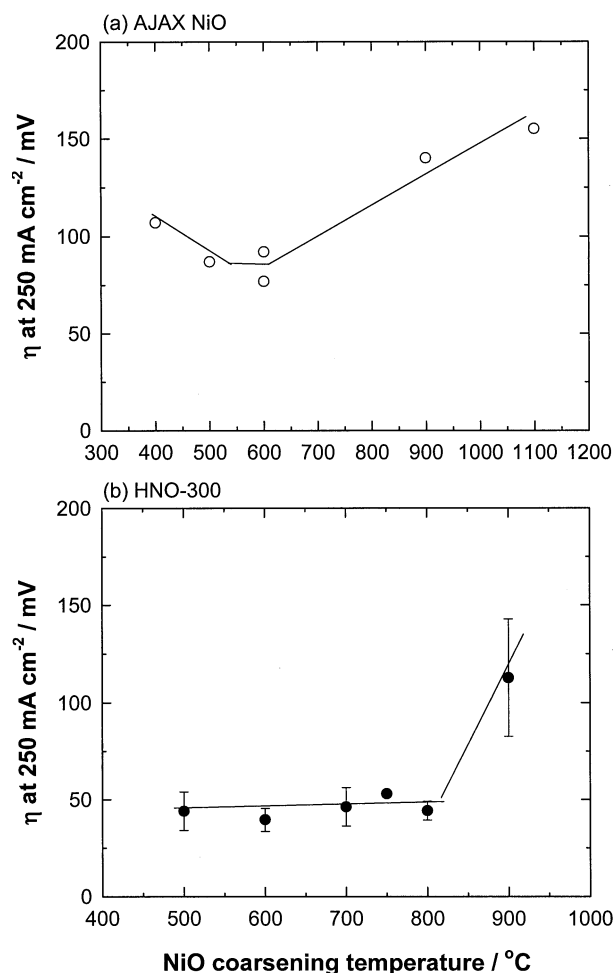
Figure 4 Electrode performance of Ni (50 vol%)/3YSZ (50 vol%) cermet anodes as a function of coarsening temperature of (a) AJAX NiO and (b) HNO-300 NiO. Overpotential was measured under a current density of 250 mA cm^{-2} at 1000°C in 97%H$_2$/3%H$_2$O.

Figure 5 Polarization performance of Ni (70 vol%)/3YSZ (30 vol%) and Ni (50 vol%)/8YSZ (50 vol%) cermet anodes prepared from cermet powders coarsened at different temperatures. Polarization curves were measured at 1000°C in 98%H$_2$/2%H$_2$O and anodes were sintered at 1400°C in air.

8YSZ powder with size distribution of 0.2–15 μm and specific area of 0.52 m^2 g^{-1}. The particle size distribution of 8YSZ powder was obtained by coarsening of the powder at 1400°C and followed by milling. The anode displayed a good stability and performance (overpotential loss of 150 mV at 1 A cm^{-2} and 800°C). Itoh *et al.* [51] showed that by combining large (27 μm) and fine (0.6 μm) YSZ particles, stability and performance of Ni/YSZ cermet anodes were improved substantially. Nevertheless, there may be some limitation in the use of large YSZ particles as large YSZ particles could precipitate from the ink suspension and the separation in the ink will make the quality control of the anode very difficult during the screenprinting or ink coating process. A large volume of coarse YSZ particles could also incur week contact at anode and YSZ electrolyte interface.

In Ni/YSZ cermet anodes, performance of the anode is affected by the coarsening treatment of YSZ and NiO/YSZ cermet powders and the sintering temperature of the cermet coating. However, the effect of coarsening of Ni/YSZ cermet powders appears to be related to the nature of YSZ powder in the cermet [52]. Fig. 5 shows the polarization performance of Ni/3YSZ and Ni/8YSZ cermet anodes prepared from cermet powders coarsened at different temperatures.

The anodes were sintered at 1400°C in air. Polarization performance was measured in wet H$_2$ at 1000°C and iR components were not distracted from the polarization potentials. For Ni/8YSZ cermet anodes, the best performance was obtained on the anode prepared from cermet powder coarsened at 1300°C. In the case of Ni (40 vol%)/8YSZ (60 vol%) cermet anodes, Kawada *et al.* [53] observed the best performance of electrode polarization resistance (R_E) of 0.29 Ωcm^2 as measured at 1000°C in wet hydrogen for the Ni/8YSZ cermet anodes prepared with cermet powder coarsening temperature of 1400°C and anode sintering temperature of 1500°C. On the other hand, the coarsening treatment of NiO/3YSZ cermet powder show little effect on the polarization performance of the Ni/3YSZ cermet anodes (Fig. 5a), in contrast to that of the Ni/8YSZ cermet anodes [49, 52].

The fundamental reason for this significant difference in heat treatment effect of YSZ and Ni/YSZ cermet powder on the anode performance is most likely related to the very different sintering behavior of YSZ powders. In the case of YSZ powders, the sintering behavior is related to the yttria content. Fig. 6 shows the change of the average particle size of Tosoh 3YSZ, Tosoh 8YSZ powder and AJAX NiO with the heat treatment temperature [52]. The significant grain growth as observed for 8YSZ powders indicates that the grain growth kinetics
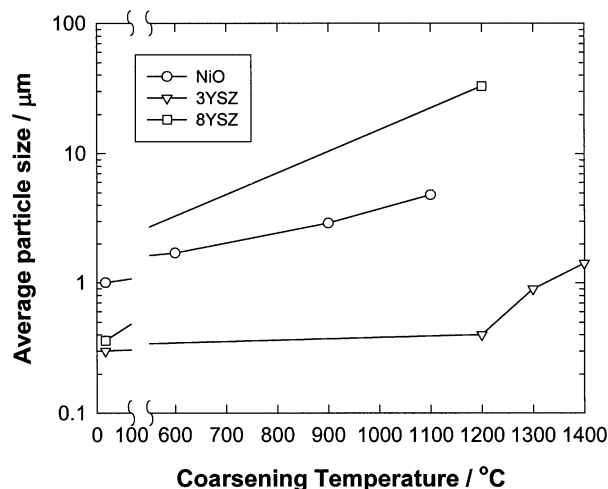
Figure 6 Change of the average particle size of Tosoh 3YSZ, Tosoh 8YSZ and AJAX NiO powders with coarsening temperature.

of 8YSZ powder is much faster as compared to the relatively sluggish grain growth of 3YSZ and NiO powders. Matsushima *et al.* [54] studied the effect of sinterability of 8YSZ powders on the electrode performance of Ni/8YSZ cermet anodes. 8YSZ powder has shrinkage rate of 26% which is close to that of the NiO powder. However, the sintering profile of the NiO/8YSZ cermets is primarily dominated by that of the 8YSZ phase rather than that of the NiO phase. The maximum sintering rate for 8YSZ was found to occur at $\sim$1300°C. Upadhyaya *et al.* [55] studied the densification behavior of 3 mol% Y_2O_3-ZrO_2 powder prepared by the co-precipitation method. They found that the maximum shrinkage occurred at 1020°C; about 150 to 200°C degrees lower than that of 8YSZ powders. As suggested by Lange [56], the maximum sintering rate corresponds to a transition from densification kinetics to coarsening (i.e., grain growth) kinetics. Thus, reducing the sintering and grain growth of 8YSZ powders in the cermet to the level comparable to that of NiO powder would benefit the establishment of the effective Ni-to-Ni contact in the cermet, indicated by the significant reduction in the electrode ohmic resistance of Ni/8YSZ cermet anodes prepared from the coarsened cermet powders [52].

2.1.3. Sintering temperature of anode coatings

Sintering of the Ni/YSZ cermet coating at high temperatures (e.g., 1400°C) is essential to achieve high electrode performance and low electrode ohmic resistance. Jiang [52] showed recently that the formation of Ni-to-Ni electronic contact and YSZ-to-YSZ ionic contact networks are closely related to the sintering temperatures of the anode. Fig. 7 shows the polarization performance of Ni/3YSZ and Ni/8YSZ cermet anodes sintered at different temperatures in wet H_2 at 1000°C. In the case of Ni/8YSZ cermet anodes, the anodes were prepared from cermet powder coarsened at 1300°C. Fig. 8 shows the SEM pictures of Ni/8YSZ cermet electrodes sintered at different temperatures after fuel cell testing. The lowest electrode ohmic and
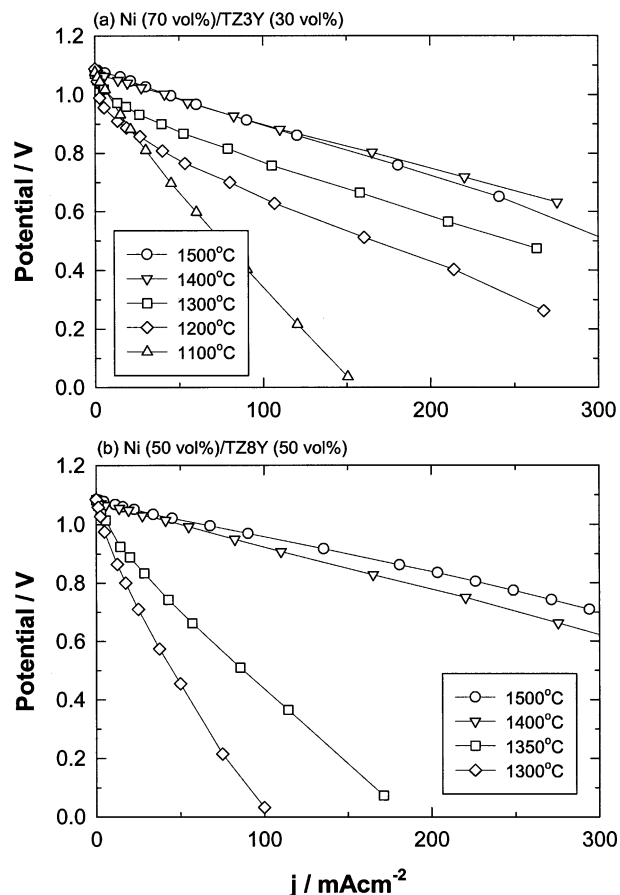
Figure 7 Polarization curves of Ni (70 vol%)/3YSZ (30 vol%) and Ni (50 vol%)/8YSZ (50 vol%) cermet anodes sintered at different temperatures. The performance was measured at 1000°C in 97%H_2/3%H_2O.

polarization resistance was observed for Ni/3YSZ and Ni/8YSZ cermet anodes sintered at 1400°C (Fig. 7). This corresponds to the formation of good YSZ-to-YSZ network for the anodes sintered at 1400°C (Fig. 8). The observation that high sintering temperature basically has no effect on the conductivity of pure Ni anode [52] indicates that sintering of YSZ phase in the cermet has significant effect not only on the formation of Ni-to-Ni electronic contact network in the cermet but also on the formation of electrical contact between the Ni phase in the cermet and YSZ electrolyte. On the other hand, high sintering temperature is essential to create a good bonding between the YSZ phase in the cermet and the YSZ electrolyte, leading to the formation of a rigid YSZ structure to support the Ni phase and the formation of Ni-to-Ni electronic contact network. This appears to be the reasonable explanation for the high electrode performance and high electronic conductivity of the anode coatings sintered at high temperatures. Fukui *et al.* [57] studied the sintering behavior of Ni/YSZ cermet anodes prepared by spray pyrolysis. Electrode ohmic resistance and anode overpotential decreased significantly with the increase of anode sintering temperature. The best performance was observed for Ni/YSZ cermet anode sintered at 1350°C with lowest iR and polarization losses. Similar effect of anode sintering temperature on the electrode ohmic and polarization resistance was also reported by Primdahl *et al.* [58].
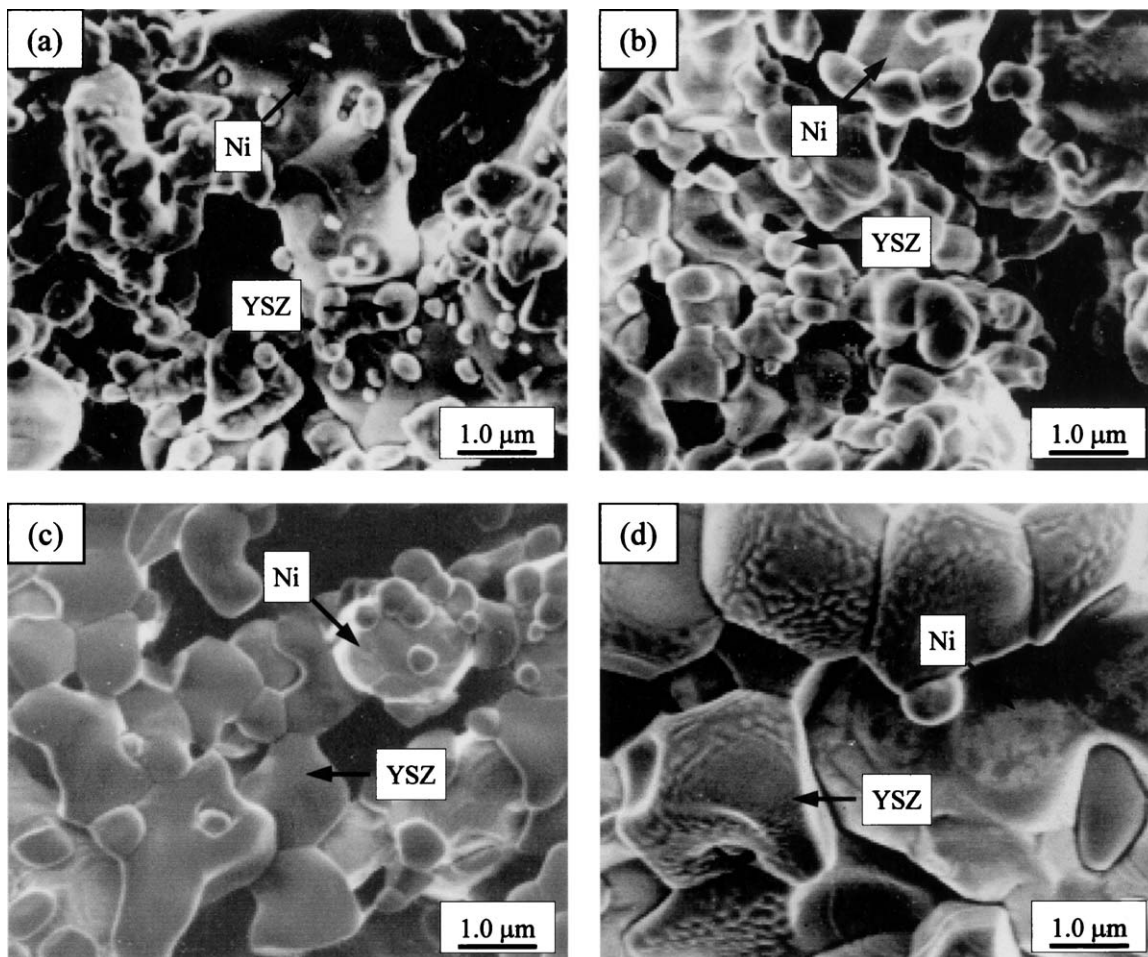
Figure 8 SEM pictures of Ni (50 vol%)/8YSZ (50 vol%) cermet anodes sintered at (a) 1300°C, (b) 1350°C, (c) 1400°C and (d) 1500°C different temperatures after the fuel cell testing. The anodes were prepared from cermet powder coarsened at 1300°C.

2.1.4. Synthesis of cermet powders

In addition to the conventional ceramic mixing process based on commercial NiO and YSZ powders, Ni/YSZ materials can also be prepared by other methods such as wet chemical synthesis process. The purpose of the synthesis of the Ni/YSZ cermet powders is primarily to improve the homogeneity of Ni and YSZ phase distribution, to reduce the sintering temperature of the cermet coating and to increase the electrode performance and stability. A major consideration in the synthesis of Ni/YSZ powders is the effect of the process on the powder morphology and phase distribution. Millini *et al.* [59] showed that the powder morphology of NiO/YSZ powders prepared by citrate route could change from spherical shape by spray-drier to irregular aggregates by rotary evaporation. Li *et al.* [60] employed $NH_3 \cdot H_2O$-NH_4HCO_3 buffer-solution to co-precipitate Ni/YSZ powder with improved homogeneity of the powder composition and uniformity of the particle size. Using NaOH as the co-precipitation agent can avoid the Ni loss, resulting in the accurate control of the cermet composition [61]. Fine Ni/YSZ cermet powder with surface area of 27–32 $m^2\,g^{-1}$ and average particle size of 0.25–0.8 μm, prepared by solution combustion of nitrate salt and carbohydrazide fuel followed by hydrogen reduction at 800°C [62], have been reported. Combustion synthesis method is also commonly employed to produce Ni/YSZ and (Ni,M = Co,Fe,Cu)/YSZ cermet

powder [63–65]. In this method, nitrate precursors of the cermet constitutes such as $ZrO(NO_3)_2 \cdot 6H_2O$, $Y(NO_3)_3 \cdot 6H_2O$ and $Ni(NO_3)_2 \cdot 6H_2O$ are mixed intimately, melted together with urea ($CO(NH_2)_2$) on a hot plate and the combustion takes place in a furnace pre-heated at 600°C. Reported results showed that the specific area of Ni/YSZ powder with 50 vol% YSZ phase was 26 m^2/g and decreased to 17 $m^2\,g^{-1}$ with the addition of 2% Cu. The electrode polarization resistance of a symmetrical cell was estimated to be 0.2 Ωcm^2 at 1000°C, a reasonable value compared to those reported for optimized Ni/YSZ cermet anodes prepared by conventional powders [66]. Ni/YSZ cermet powders could also be prepared by mixed citrate/nitrate combustion synthesis [67].

Spray pyrolysis was used to prepare Ni/YSZ composite powders from 8 mol% Y_2O_3-ZrO_2 and $Ni(CH_3COO)_2 \cdot 4H_2O$ solution [68, 69]. The Ni/YSZ powder obtained by this method showed spherical morphology with average particle size of $\sim$1 μm. The cermet anode prepared from the synthesized composite powder has good distribution of Ni and YSZ phases and the cell prepared from the Ni/YSZ cermet anodes using the spray pyrolysis powder showed no deterioration over 8000 h at 1000°C in moist H_2/air. The same method was also used to prepare Ni/SDC cermet powder with $Ce(NO_3)_3$, Sm_2O_3 and $Ni(CH_3COO)_2 \cdot 4H_2O$ raw materials. Ni/SDC powder obtained by this method

4411

had average particle size of ∼0.5 μm and specific area higher than 2 m^2 g^{-1} [70, 71]. Chung *et al.* [72] used gas atomization method to prepare Ni/CeO$_2$ as potential materials for internal reforming anodes. Gas atomization can be defined as the break up of a liquid into fine droplets by the impringement of gas. The product is a suspension of very fine liquid droplets which then solidify very quickly. The rapid cooling intrinsic to gas atomization allows very little time for segregation to occur. Using intermetallic precursor, CeNi$_5$, Chung *et al.* [72] produced Ni/CeO$_2$ particles with grain size ranging from 5 μm to as large as 100 μm. However, the electrochemical performance of the anodes prepared from the gas atomized Ni/CeO$_2$ powder was not as good as Ni/CeO$_2$ anodes prepared by conventional ceramic mixing method. Chen and Liu [73] reported the preparation of mesoporous YSZ/NiO composite with very high surface area of 108 m^2 g^{-1} using Pluronic P103 surfactant as structure-directing agents and metal chlorides as precursors. Ultrafine Ni/YSZ powder and nano-sized NiO and SDC powder can also be prepared by sol-gel and liquid mixture methods [74] and by heating the oxalate precursors at 300 to 1200°C in air [75], respectively. Gd-doped CeO$_2$ (GDC) powders produced by metal nitrate-glycine process can be densified at temperatures as low as 1250°C and this led to the decrease in sintering temperature of the Ni/GDC cermet anodes [76]. Moon *et al.* [77] reported the preparation of ZrO$_2$-coated NiO powder by thermal hydrolysis of Zr(NO$_3$)$_2$·6H$_2$O in a mixed solvent of iso-PrOH/water. Using advanced mechanical method in dry process can also produce YSZ-covered submicron NiO composite powders [78]. The presence of fine YSZ particles on the surface of NiO would significantly inhibit the grain growth of NiO phase in the cermet. Other methods employed to prepare Ni/YSZ cermet anodes include vapor-deposition [79], wet-powder spraying [80] and mechanical milling and plasma spray [81].

Cracium *et al.* [82] reported a new method for the fabrication of SOFC anodes. In this method, a porous YSZ coating was formed using a mixture of YSZ powder and YSZ fibers, followed by impregnation of the porous YSZ coating with aqueous solution of Ni, or Cu. Performance of the Ni/YSZ and Cu/YSZ cermet anodes prepared by this method was comparable to those of conventional Ni/YSZ cermet anode. The advantage of this method is the high freedom of adding metal or other additives such as CeO$_2$ to the cermet structure. The feasibility of this method in the development of Cu/ceria/YSZ cermet anodes for the direct oxidation of methane has been demonstrated by Park *et al.* [83].

However, considerations in the selection of the synthesis of the Ni/YSZ cermet powders or simply to use conventional ceramic mixing processes based on commercial powders are the reproducibility, quality and the cost of the process and raw materials. The issues associated with the reproducibility are determined by the complexity of the synthesis processes while the cost of the process is largely determined by the scale-up and automation.

2.2. Electrical conductivity

In the Ni/YSZ cermet materials, YSZ is an ionic conductor and Ni is an electronic conductor. In a simple diphase system the theory predicts the percolation threshold of ∼30 vol% of the higher conducting phase for the transition from dominant ionic conductivity to dominant electronic conductivity. This is generally true for the electronic conductivity of the composite Ni/YSZ cermet systems. Dees *et al.* [84] studied the relationship between the electrical conductivity and the volume fraction of Ni in the Ni/YSZ cermet measured at 1000°C and showed that the rapid rise in the electrical conductivity corresponds to a ∼30 vol% of Ni in the cermet. However, the position of the S-shape dependence of the conductivity on the Ni volume content and the conductivity appear to be related to the particle size of YSZ phase in the cermet, as shown in Fig. 9. In general, the electrical conductivity of Ni/YSZ materials increases with the YSZ particle size. The rather unusually smooth transition instead of S-shape threshold type for Ni/YSZ cermet prepared by self-propagating high temperature synthesis (SHS) was attributed to the unusual microstructure and good dispersion of the metallic component due to the very high temperature experienced during the SHS process [90]. The much lower threshold of conductivity for Ni/YSZ cermets prepared by using Ni-coated graphite (NiGr/YSZ) was due to the large effective Ni content created by the thin Ni layers in the cermet [89]. This indicates that the electrical conductivity of Ni/YSZ is closely related to the microstructure of the cermet. However, difference in percolation threshold and conductivity may also be affected by the porosity as in conductivity curves shown in Fig. 9 level of porosity has not been taken into account.

Electrical conductivity of Ni/YSZ cermets is strongly dependent on the particle size and distribution of both Ni and YSZ phases and thus the threshold of the volume fraction of Ni in the cermet for the change of the conduction mechanism also changes. Huebner *et al.* [91] showed that with Ni average particle size of ∼0.6 μm, the electrical conductivity reached ∼300 S cm^{-1} at
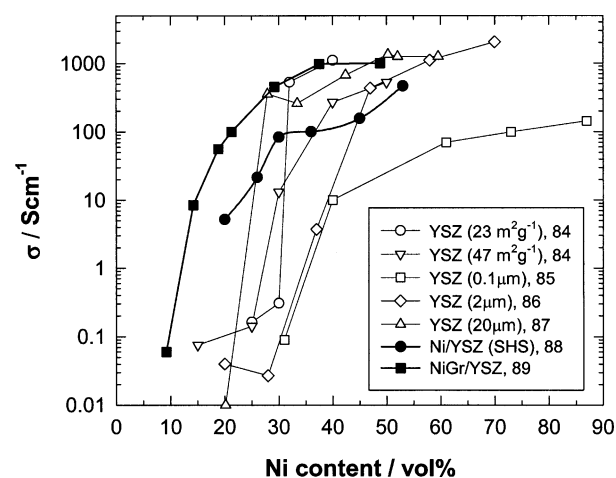
Figure 9 Conductivity of Ni/YSZ cermet as a function of Ni content. The conductivity was measured at 1000°C in humidified H$_2$. Numbers are the references cited. The conductivity value for NiGr/YSZ cermets as reported by Corbin and Qiao [89] was measured at 800°C.

1000°C for 30 vol% Ni and when particle size of Ni increased to ∼16 μm, the threshold volume fraction of Ni to reach electrical conductivity of ∼100 S cm^{-1} at 1000°C increased to 50 vol%. This indicates that the threshold for the transition from the dominant ionic conductivity of the YSZ electrolyte phase to the dominant electric conductivity of the Ni metal phase is related to the YSZ/NiO size ratio. The electrical conductivity of the Ni/YSZ cermet anodes is also dependent on the particle size and particle size distribution of NiO powders. Tietz et al. [45] studied the electrical conductivity of the Ni/YSZ cermet anodes prepared from different commercial NiO powders. The electrical conductivity measured at 800°C varies between 300 S cm^{-1} to 4000 S cm^{-1} with the highest conductivity obtained on NiO powder with small grain size and shrinkage rate of 27%. Tintinelli et al. [87] showed that the electrical conductivity of Ni/8YSZ cermet anodes increases with increase of the 8YSZ/NiO particle size ratio. Itoh et al. [92] studied the relationship between the electrical conductivity and the particle size ratio of coarse YSZ (D_{50} = 10–100 μm), NiO (D_{50} = 1–100 μm) and fine YSZ (D_{50} = 0.4–60 μm). To achieve a good electrical conductivity, weight ratio (NiO/(coarse YSZ + NiO + fine YSZ)) of 8.8% or below is recommended.

For Ni/YSZ cermets to work properly as anodes, certain porosity of the electrode coating is essential for the transportation of fuel gas reactants to the electrode/electrolyte interface region where the fuel oxidation reaction occurs. The porosity is affected by volume fraction of Ni in the cermet as there is a volume reduction of 25% when NiO is reduced to Ni metal under fuel environment. Fig. 10 shows the change of the morphology of Ni anode before and after the NiO
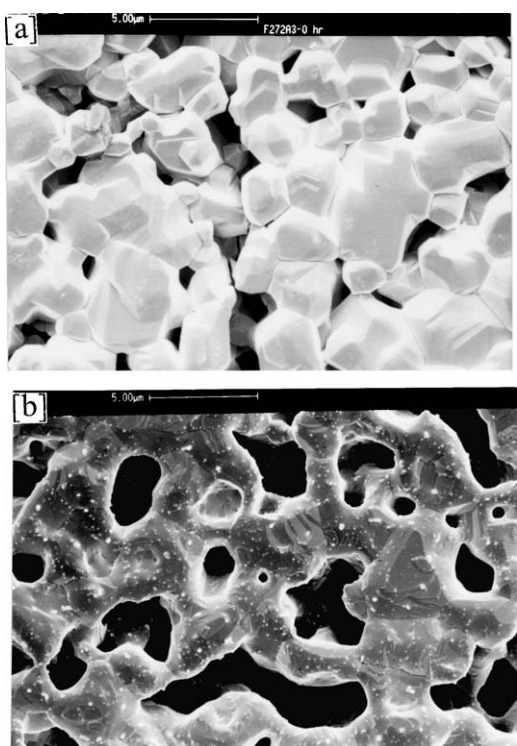
Figure 10 Change of the morphology of Ni anode before and after exposure in humidified 10%H$_2$/90%N$_2$ for 1 h at 1000°C.

reduction in humidified H$_2$. An increase in the porosity is clearly seen. In general, the porosity increases with the increase in the Ni volume fraction and for Ni/8YSZ, a typical porosity of 35% was found for Ni (40 vol%)/8YSZ (60 vol%) and 42% when Ni content increased to 70 vol% [86]. The porosity and pore morphology can also be controlled by adding pore-formers such as carbon fiber, graphite and corn starch. Addition of 10–20 wt% graphite pore-formers would typically increase the porosity by ∼10% [49]. The porosity has strong effect on the electrical conductivity through its impact on the Ni-to-Ni connectivity. Therefore the electrical conductivity of the porous Ni/YSZ cermet coatings is expected to be considerably smaller than that of the Ni/YSZ cermet material. On a porous Ni (50 vol%)/YSZ (50 vol%) cermet coatings screen-printed on a 50 × 50 mm YSZ, the conductivity is ∼254 S cm^{-1} at 800°C in 97%H$_2$/3%H$_2$O, which is much smaller than that of the dense Ni/YSZ cermet specimen with similar volume fraction of nickel [93]. Addition of pore formers with geometric anisotropy such as graphite and carbon fiber can result in the formation of anisotropic porous structure of the Ni/YSZ cermets [94, 95]. The electrical conductivity of Ni/YSZ with anisotropic porous structure is in the range of 150 to 600 S cm^{-1} as compared to ∼1600 S cm^{-1} for the cermet with isotropic porous structure measured at 800°C [94]. This shows that porous structure also has significant effect on the electrical conductivity of the Ni/YSZ cermet anodes in addition to the porosity.

Conductivity of the Ni/YSZ cermet anode coatings in fuel cells is also affected by the heat treatment and sintering temperatures of the anodes. For Ni (50 vol%)/YSZ (50 vol%) cermet anodes prepared from the cermet powder coarsened at 1400°C, the electrical conductivity of the anode was only ∼4 S cm^{-1} at 1000°C for the anode sintered at 1300°C and increased to ∼800 S cm^{-1} when the anode sintering temperature increased to 1500°C [96]. The electrocatalytic activity of the anodes for the H$_2$ oxidation reaction also increased substantially with the increase of the sintering temperature of the anodes. The effect of sintering temperature of Ni/YSZ cermets on the electrical conductivity behavior was also studied by Pratihar et al. [97]. Initial reduction temperature also affects the electrical conductivity as reported by Grahl-Madsen et al. [98]. Electrical conductivity of Ni/8YSZ cermet substrates was twice higher for the anode reduced at 1000°C than that reduced at 800°C. On the other hand, the electrical properties of two phase NiO-YSZ composites were studied in the temperature range of 160–630°C by Park et al. [99].

In comparison to electrical properties, relatively little research has been carried out on the mechanical properties of Ni/YSZ cermets. Selcuk et al. [100] determined the effective Young's and shear moduli and Poisson's ratio of NiO/YSZ cermets as a function of porosity. For 75 mol% NiO-YSZ thick specimen (∼550 μm) sintered at 1350°C with porosity of 31%, the fracture strength of NiO/YSZ is 56 MPa, which is close to 46 MPa of LSM but significantly smaller than 377 MPa reported for dense YSZ [101, 102]. Primdahl et al. [58]

qualitatively studied the effect of sintering temperature of Ni/YSZ cermet anodes on the mechanical properties of the YSZ electrolyte cells. Sintering at temperatures of 1300 to 1400°C significantly reduced the mechanical strength of YSZ electrolyte cell. However, high temperature sintering of Ni/zirconia cermet anodes is essential to reduce the electrode ohmic resistance and electrode polarization resistance. This leaves little room for the compromise of the optimum electrode performance and cell mechanical properties. Sørensen *et al.* [103] showed that fracture of the YSZ electrolyte is most likely initiated by cracks growing from the cermet coating into the YSZ electrolyte. Nevertheless, the residual stress in the NiO/YSZ anodes was much lower as compared to that in LSM cathode due to stress relief by the extensive channel cracking [104]. This explains the observation that the applied load at failure and the stress in the YSZ electrolyte for symmetrical NiO/YSZ and YSZ structure was almost equal to that of YSZ plates [104].

2.3. Performance degradation

Structural and long-term performance stability of Ni/YSZ cermet anodes are critical issues in the development of SOFC anode. Degradation problems in long-term operation of SOFCs are characterized by a gradual decrease in performance of the fuel cell system, measured by the percentage of increased overpotential or decreased cell potential over certain period of operation. As far as the Ni/YSZ cermet anodes are concerned, the most predominant microstructure change is the agglomeration and coarsening of Ni phase [105–107]. The loss of Ni through volatile nickel hydroxide species could also contribute to the performance degradation [108]. The main reason for the agglomeration of Ni in the Ni/YSZ system is probably due to the poor wettability between the metallic Ni and YSZ oxide phase. Nikolopoulos *et al.* [109, 110] studied the wettability and interface reaction between Ni and YSZ system in the temperature range of 1250–1500°C and purified Ar/4%H$_2$ atmosphere. Molten Ni showed no wettability towards YSZ ceramic phase (θ = 117°). Additives such as Ti, Cr, Mn and Pd have certain effect on the wettability between Ni and YSZ [111]. However, the effect on the interfacial energy of the Ni/YSZ system appears to be small. Due to low melting temperature, pure Ni has a high tendency to sinter at SOFC operation temperatures (e.g., 1000°C). The sintering of pure Ni anodes in reducing environment is very rapid, leading to the formation of isolated islands [112]. Therefore, the prevention or reduction of agglomeration and sintering of metallic Ni phase in the Ni/YSZ cermet electrodes rely heavily on the microstructure optimization of the Ni/YSZ cermets.

Simwonis *et al.* [106] studied the structure change of Ni (40 vol%)/8YSZ (60 vol%) cermet anode substrates exposed to humidified Ar/4%H$_2$/3%H$_2$O atmosphere at 1000°C up to 4000 h. The distribution of Ni, 8YSZ and pores of polished cross-section of the substrates were evaluated by quantitative image analysis. After annealing for 4000 h, the average Ni particle size increased
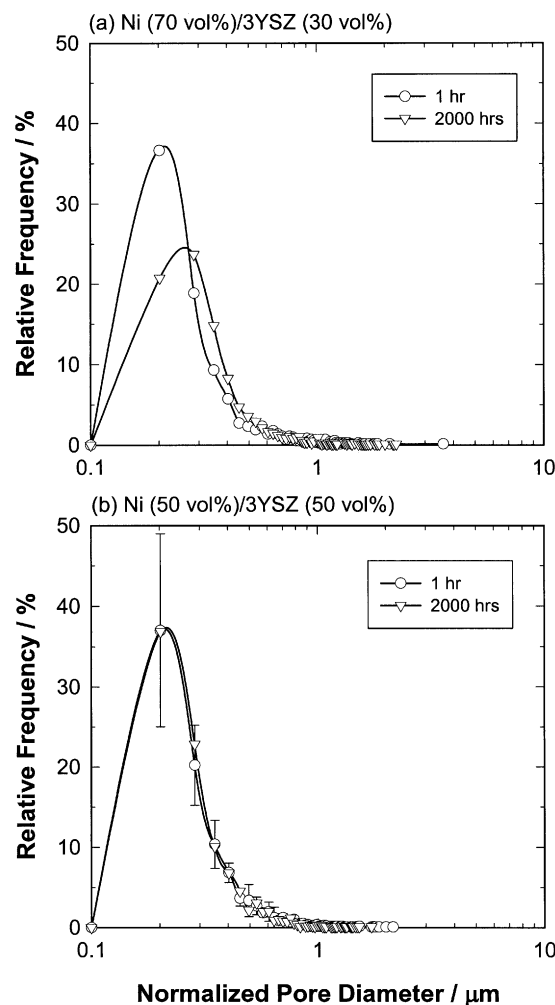
Figure 11 Pore size distribution of Ni (70 vol%)/3YSZ (30 vol%) and Ni (50 vol%)/3YSZ (50 vol%) cermet anodes after sintered at 1000°C in humidified 10%H$_2$/90%N$_2$ for 1 and 2000 h. The pore size distribution was measured by image analysis.

from 2 to 2.57 μm and the number of Ni grain counts decreased from 3421 to 2151. As the result, the electrical conductivity of the anode substrates decreased by 33% due to decreased electronic Ni-to-Ni contacts. There was no change in 8YSZ particle size distribution as expected. The sintering behavior of Ni/3YSZ cermet anodes was also studied as a function of cermet composition [112]. Fig. 11 shows the change of pore size distribution of Ni (70 vol%)/3YSZ (30 vol%) and Ni (50 vol%)/3YSZ (50 vol%) cermet anodes after sintering at 1000°C in wet H$_2$ for 1 and 2000 h. The pore size distribution was measured by image analysis. Fig. 12 shows the corresponding SEM picture of Ni, Ni (70 vol%)/3YSZ (30 vol%) and Ni (50 vol%)/3YSZ (50 vol%) cermet anodes after sintering at 1000°C in wet H$_2$ for 2000 h. Pure Ni anode showed rapid sintering at 1000°C, resulting in the formation of large isolated Ni islands (Fig. 12a). In the case of Ni (70 vol%)/3YSZ (30 vol%) cermet anode, there was a clear increase in large pores and pore size distribution shifted to coarser pores after sintered at 1000°C for 2000 h (Fig. 11a). Ni particles grew out the surface, indicating the significant agglomeration and grain growth of Ni in the cermet (Fig. 12b). As Ni content decreased to 50 vol%, the change in the pore size distribution was very small

4414
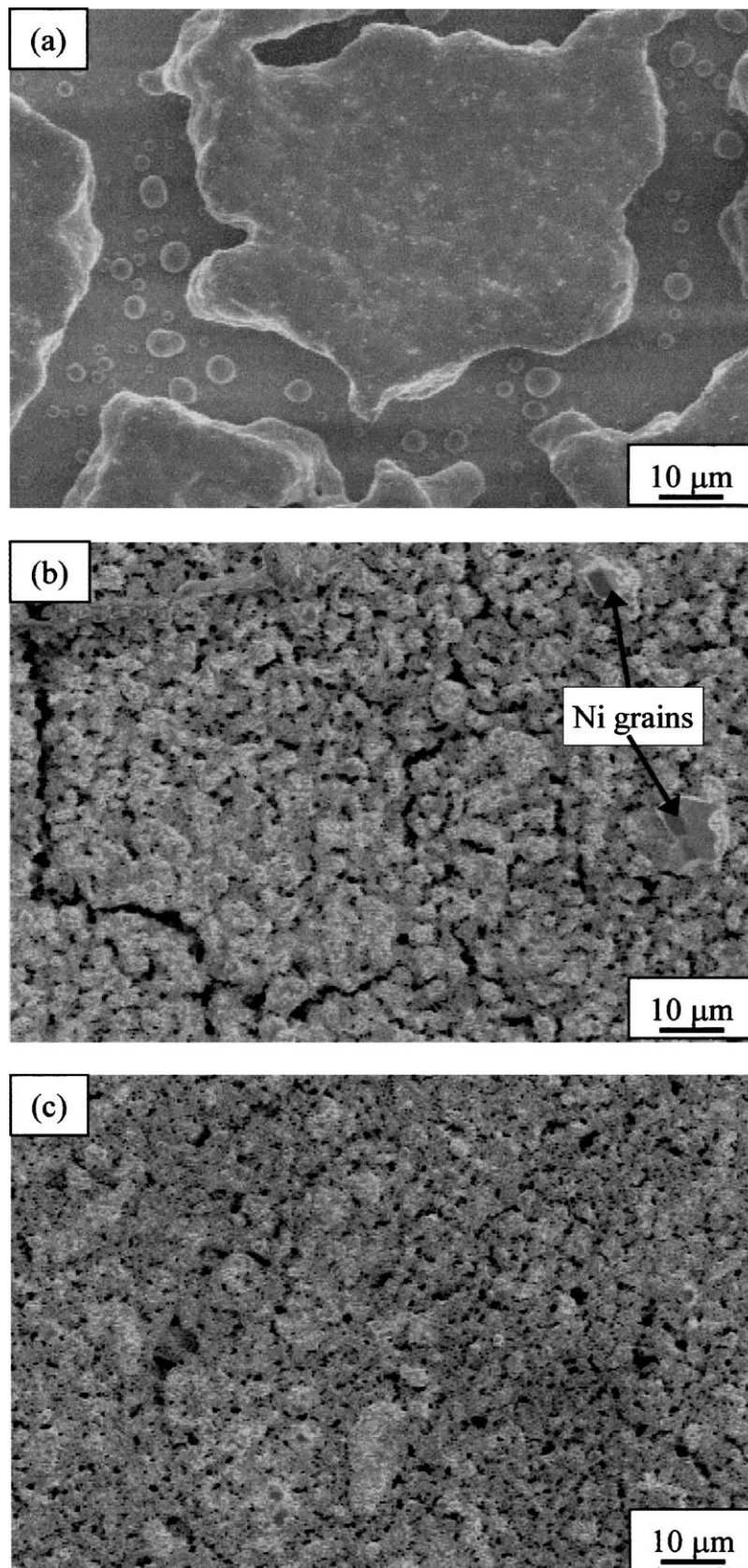
Figure 12 SEM pictures of Ni, Ni (70 vol%)/3YSZ (30 vol%) and Ni (50 vol%)/3YSZ (50 vol%) cermet anodes after sintered at 1000°C in humidified 10%H_2/90%N_2 for 2000 h.

and this is also indicated by negligible change in the morphology of the cermet coating (Figs 11b and 12c). This shows that microstructural stability of Ni/YSZ cermet anodes is critically dependent on the Ni content and Ni and YSZ phase distribution in the cermet. The uniform distribution and homogenization of NiO and YSZ phase in the preparation of NiO/YSZ cermets through effective milling and deagglomeration are also effective in improving the stability of the anodes [113].

Operating conditions of fuel cells also have significant effect on the microstructure of the cermet anodes. Iwata [105] studied the microstructural change

of Ni/8YSZ cermet electrode coatings operating at 0.3 A cm^{-2} and 1000°C. Ni particle size increased from 0.1–1 to 1–10 μm after 1015 h of operation and the specific area of the cermets was decreased by half. The performance degradation rate was 14 mV over 1000 h. This was considered to be caused by the decrease of the contact area at the electrode/electrolyte interface and a decrease of the specific surface area of Ni particles. Müller [114] showed that high current and high fuel utilization can cause the agglomeration of originally fine dispersed Ni in the Ni/YSZ cermet anodes. The agglomeration of Ni phase in the cermet led to the reduction in the three phase boundary and the increase in the polarization resistance of the anode [115].

While in principle it is evident that Ni particles will grow during high temperature operation, a detailed description of the kinetics of the agglomeration and sintering of the Ni/YSZ cermets is difficult due to the complexity of the structure. Two types of materials (Ni and YSZ) plus pores exist in the structure with all of them having multi-modal size distributions. Ioselevich *et al.* [116] and Abel *et al.* [117] used correlated percolation model to describe the degradation of SOFC anodes. In their model, monosized particles are located on a face-centered cubic lattice and sintering between two metal particles occur instantaneously with a certain probability. The result is an unchanged particle and one pore or one dead particle with no more electrochemical contribution to the network. The model gives an insight in the development of active bonds in the anode, the density of three phase boundaries and the transport resistance in anodic materials. A simple two-particles model was used by Vaßen *et al.* [118] to describe the degradation of Ni/YSZ cermet anodes. The model is based on the assumption that the difference in particle size is the driving force for the sintering of the large metal particles and sintering mechanism is dominated by the surface diffusion of metal atoms. From the model, the surface diffusion coefficient of Ni on Ni surface was 1.3×10^{-12} m^2 s^{-1} at 1000°C and a reasonable correlation of the grain growth of Ni particles was observed between the model and experimental data.

When a system breakdown happened, there would be two scenarios for the anode side of the cell: either the reducing atmosphere is preserved with nitrogen (implying nitrogen supply) or the cells stand a redox cycle. Thus, redox stability of anode materials is very important as the large volume change associated with NiO reduction to Ni may cause the disintegration of the cermet structure. The mechanical strength of Ni/8YSZ substrates before and after the reduction in hydrogen was reported to be similar, about 18–20 MPa [98]. However, repeated reduction and oxidation at 1000°C weaken the mechanical strength of Ni/8YSZ membranes [119], indicating the dwindling of bonding between Ni-to-Ni and Ni-to-YSZ in the cermets. Grahl-Madsen *et al.* [98] showed that the redox cycle may have sped up the deterioration of the electrical conductivity of the Ni/8YSZ cermet substrates. This is supported by the significant increase of the electrode ohmic resistance of anode-supported cell after exposing the anode to mild oxidative conditions (normal grade N$_2$ flow) [33]. Addition

of CeGdO$_2$ to the Ni cermet anodes was reported to improve the redox stability of the cell [120].

Antonucci *et al.* [121] studied the stability and performance of Pt/CeO$_2$ anode and Pt/PrO$_2$ cathode of a tubular SOFC stack. Significant chemical and morphological changes occurred in both anode and cathode after 3000 h operation at 950°C. There was a significant depletion of CeO$_2$ and formation of Pt/Ce alloy on the anode side and a strong depletion of PrO$_2$ on the cathode side, leading to the substantial change in the reaction process and the degradation in the stack performance.

2.4. Microstructure optimization

The performance of Ni/YSZ cermet anodes depends on the optimum phase distribution between Ni and YSZ particles that ensures the maximum electronic and ionic paths. Both modeling and experimental approaches are reported in the literature.

2.4.1. Modeling approach

Modeling approach has been adopted by many researchers for optimizing the performance of electrodes. It is known that the microstructure of the electrode plays a critical role in determining the performance of the electrodes, and thus the performance of the cell as a whole. An optimized microstructure of cermet electrode, for example, should have long-range connectivity of respective ionic and electronic conductor chains stretching across the electrode and linking the current collector to the electrolyte; and maximized active sites of three-phase boundary (TPB) for electrochemical reactions. These requirements warrant an optimal ratio of ionic to electronic conductors, in terms of their volume and average grain size, in a properly sintered electrode. In addition to the required microstructure for enhanced conversion of ionic to electronic current taking place at the TPB and transport of these currents along their respective "active bond" (chains), there is other important consideration such as efficient gas diffusion from the bulk into the reaction sites. The latter warrants properly design microstructure in terms of pore size and its distribution, porosity and the diffusion path. In summary, a good electrode must consider the complex interrelationship among the microstructure, electrochemical processes and gas transport phenomena. As one can see the complexity in designing an optimal electrode, micro modeling is a useful approach for researchers to achieve the goal, in particular to guide the design of a high-performance electrode.

Literature review showed that the electrode micro model of SOFCs could roughly be divided into pore model [122], random resistor network model [123–125], and random packing sphere model [126, 127]. In the pore model, the ionic conductor in the electrode is viewed as protruding from the dense electrolyte surface with electronic conducting particles spread over the surface in a connected network and the remaining space is filled by continuous pore structure for the transport of gases. In the random resistor network model,
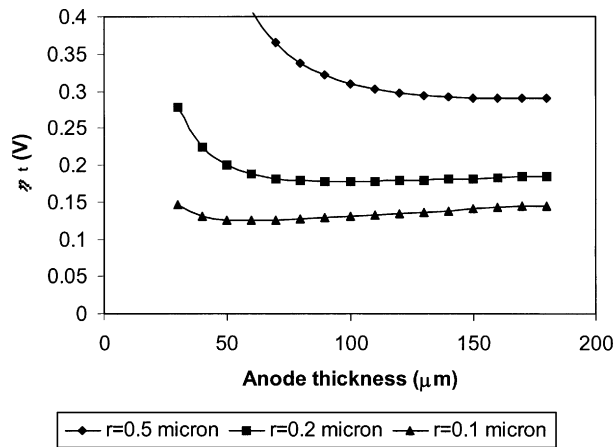
Figure 13 Influence of particle size and anode thickness to the polarization for H_2 oxidation (hydrogen humidified at 50°C, i.e., H_2:H_2O = 87.6:12.4) [128].

the electrode is assumed to consist of grains of the electronic conductors and the ionic conductors packed together so as to form a continuous network. In the random packing sphere model, the electrode is assumed to be a random packing of spheres. The theory of the particle coordination number was applied, together with the percolation theory. However, in this model [126, 127], the complex gas transport phenomena in the electrode were ignored, despite its importance. Although concentration polarization does not play an important role in most cases, especially for a thin anode, it does somehow affect the fuel cell performance significantly if crucial parameters related to microstructure of the anode are not properly chosen. Chan and Xia [128] developed a micro model for the anode that formed by a mixture of electronic and ionic conductors. The model considers the complex inter-relationship among the microstructure, electrochemical processes and gas transport phenomena in the anode. Fig. 13 shows the effect of particle size and anode thickness on the polarization

potential for H_2 oxidation on wet H_2 [128]. The predicted results show that for fixed particle radii of 0.1, 0.2 and 0.5 μm, the polarization reaches the minimum at anode thickness of roughly 50, 100 and 160 μm, respectively. Loselevich and Kornyshev [129] developed a phenomenological model of cermet anode based on a simple macro- and micro-kinetics of charge and gas transport in the electrode. The model considered the transport of hydrogen molecules and oxygen anions to the reaction sites, hydrogen oxidation reaction and the water-product removal.

Apart from above modeling approaches, Chan *et al.* [130] has developed a complete polarization model for SOFC and using it to study the sensitivity of performance to the change of cell component thickness. The study revealed that, for the same materials used, same electrode kinetics and under same operating conditions, the performance of a cathode-supported cell would be no way better than an anode-supported cell even under elevated feedstock pressure conditions. The study also showed that reducing the thickness of all three principal components of the fuel cell (anode, electrolyte and cathode) could improve the operating current density range significantly.

2.4.2. Experimental approach

As shown by Primdahl and Mogensen [66], experimentally the relationship between the electrochemical performance and microstructure of Ni/YSZ cermet anodes is rather complex. However, a general trend does exist between the microstructure, the electrochemical behavior and performance of the anode. Fig. 14 shows the electrochemical impedance arcs for four different anodes measured at 1000°C in 97%H_2/3%H_2O [131]. The particle size of Ni and YSZ of fine and coarse cermet anodes was in the range of 0.5–3 μm and 3–5 μm, respectively (Fig. 14a and b). Ni particles in Ni paste anode
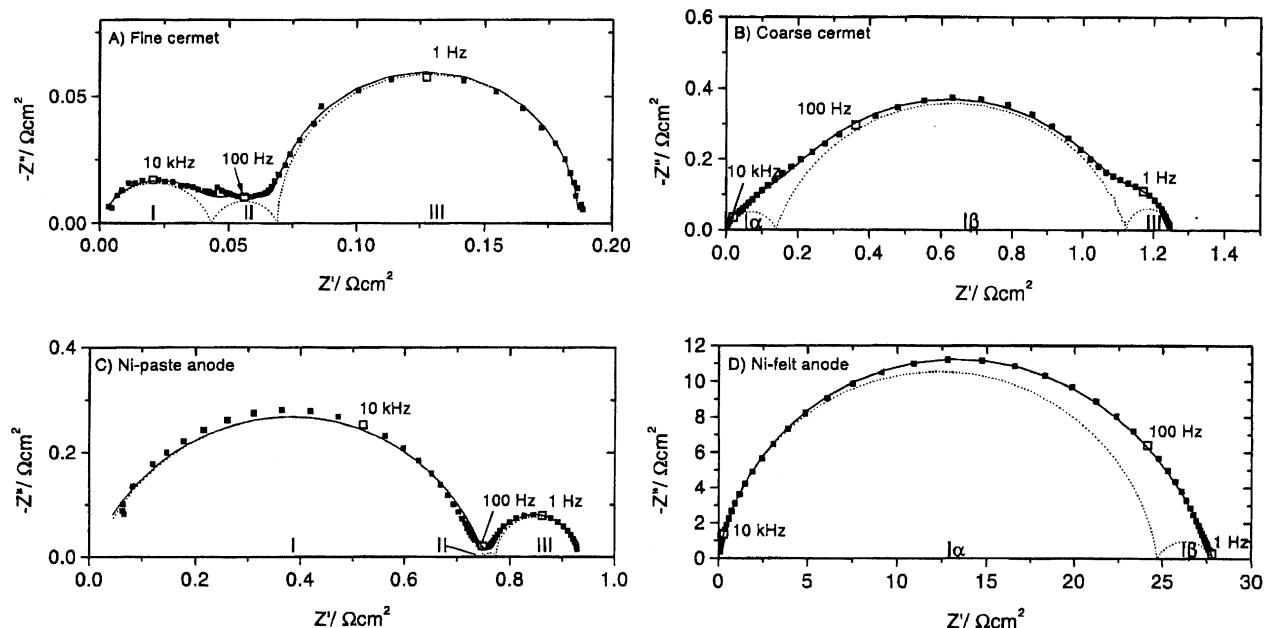
Figure 14 Electrochemical impedance curves measured at 1000°C and open circuit in wet H_2. Points are experimental data and lines are fitted data. (a) fine cermet anode, (b) coarse cermet anode, (c) Ni paste anode and (d) Ni felt anode after Brown *et al.* [131]. Symbols are experimental results and lines are fitted results by equivalent circuit.

were ∼10 μm (Fig. 14c) while Ni felt anode consisted of 50 μm diameter fibers (Fig. 14d). Ni/YSZ cermet anode with fine Ni and YSZ particles and thus fine microstructure had the smallest overall electrode polarization resistance ($R_E = 0.19$ Ωcm^2 at 1000°C, Fig. 14a) and electrode polarization resistance increased as the microstructure became coarser. For Ni felt electrode, R_E increased to 27.8 Ωcm^2 at 1000°C (Fig. 14d). The relationship between microstructure and electrochemical performance of Ni based anodes was also studied by others [132, 133]. The electrode impedance behavior showed strong dependence on the characteristics of the anode microstructure.

The microstructure of Ni/YSZ cermet anodes in turn depends on the development and optimization of the fabrication processes as shown above. On the other hand, due to high temperature processing, certain changes in the microstructure of Ni/YSZ cermet anodes are inevitable. Fig. 15 shows typical microstructure changes of Ni (50 vol%)/3YSZ (50 vol%) cermet anodes in various fabrication stages [134]. In the green state (i.e., the stage of anode coating before sintering), distribution of NiO and 3YSZ particles was very uniform and the particle size was extremely small, in the range of less than 1 μm (Fig. 15a). Pores were also very small. After sintered at 1400°C in air for 2 h, there was clearly significant grain growth for both NiO and 3YSZ particles and increase of porosity (Fig. 15b). In comparison, the grain growth of NiO was substantially higher than that of 3YSZ particles. Before the use as fuel electrodes, NiO in the Ni/3YSZ cermet anode must be reduced to Ni under fuel reducing environment. The volume reduction of 25% in the reduction of NiO to Ni metal leads to further increase in porosity and more importantly there was further grain growth of Ni at operating temperature of 1000°C due to the poor wetability between Ni and zirconia (Fig. 15c). Ni particles were typically in the range of 2 to 5 μm and there was a significant variation in the distribution between fine 3YSZ particles and large Ni particles. In some cases, Ni particles were almost standing alone with little coverage of zirocnia particles. This clearly demonstrates that the sintering and reducing stages at high temperatures play an important role in the formation of the microstructure of Ni/zirconia cermet electrodes.

Ion impregnation was reported to be effective in improving the microstructure of Ni/YSZ cermet anodes during the high temperature sintering and reducing processes [134]. In this method, metal ions usually in nitrate solution such as $Y_{0.03}Zr_{0.97}(NO_3)_x$ or $Sm_{0.20}Ce_{0.80}(NO_3)_x$ was impregnated into semi-fired or as-fired Ni/YSZ cermet anode coatings, followed by decomposition at high temperatures (i.e., fuel cell operating temperatures). As a result, nano-sized $Y_{0.03}Zr_{0.97}O_2$ and $Sm_{0.2}Ce_{0.8}O_2$ particles would deposit on the surface of Ni and YSZ grains. The formation of fine oxide particles inhibits the sintering, grain growth and agglomeration of zirconia and in particular Ni phases during sintering and reducing stages at high temperatures. Fig. 16 shows the SEM pictures of Ni/8YSZ cermet anodes before and after the ion impregnation treatment of $Sm_{0.2}Ce_{0.8}(NO_3)_x$ nitrate solution after fuel cell testing,
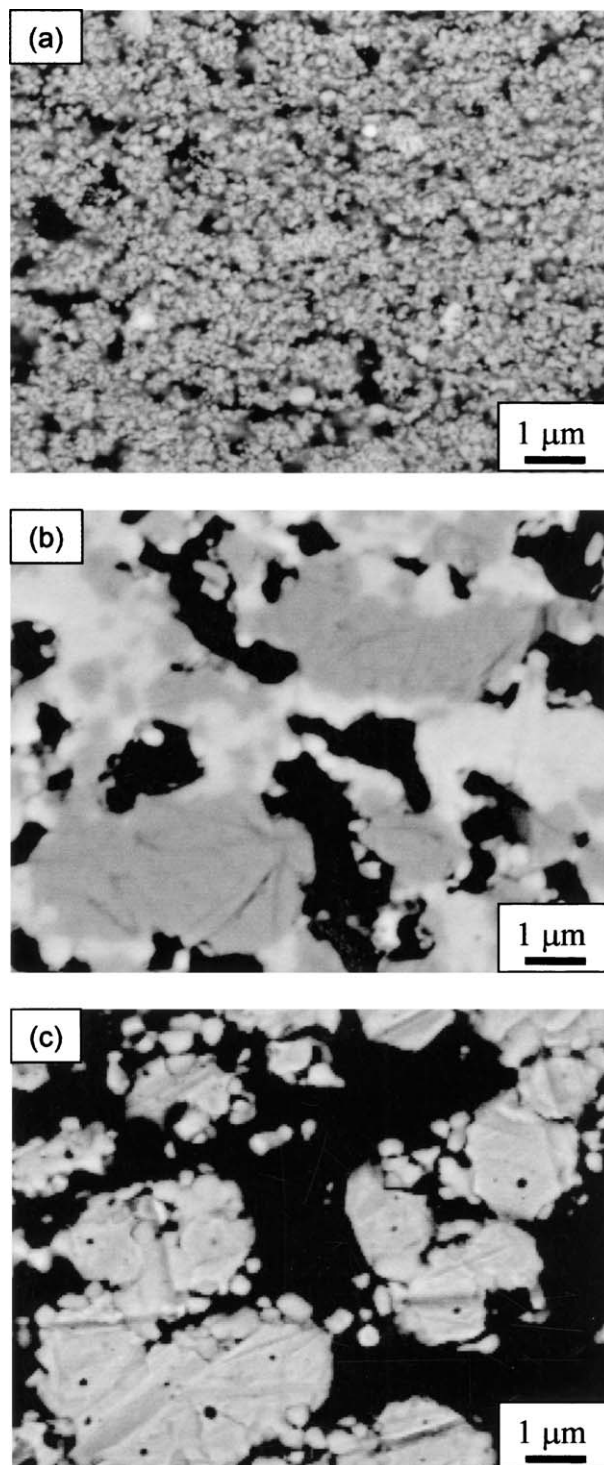
Figure 15 Microstructure evolution of Ni (50 vol%)/3YSZ (50 vol%) cermet anodes in various fabrication stages of (a) green state, (b) after sintered at 1400°C, and (c) after reduction at 1000°C in wet H_2.

and Fig. 17 shows the corresponding electrode performance measured in 97%H_2/3%H_2O at 800°C [134]. After impregnation treatment, Ni particle size was substantially reduced and majority of Ni particles were below ∼2 μm. Furthermore, Ni and YSZ particles were covered by very fine oxide particles. As shown in Fig. 17, polarization losses of impregnated Ni/8YSZ cermet anodes were significantly reduced as compared to those without impregnation. For H_2 oxidation on Ni/8YSZ cermet anode without impregnation, η was 234 mV at 250 mA cm^{-2} and 800°C. After impregnated
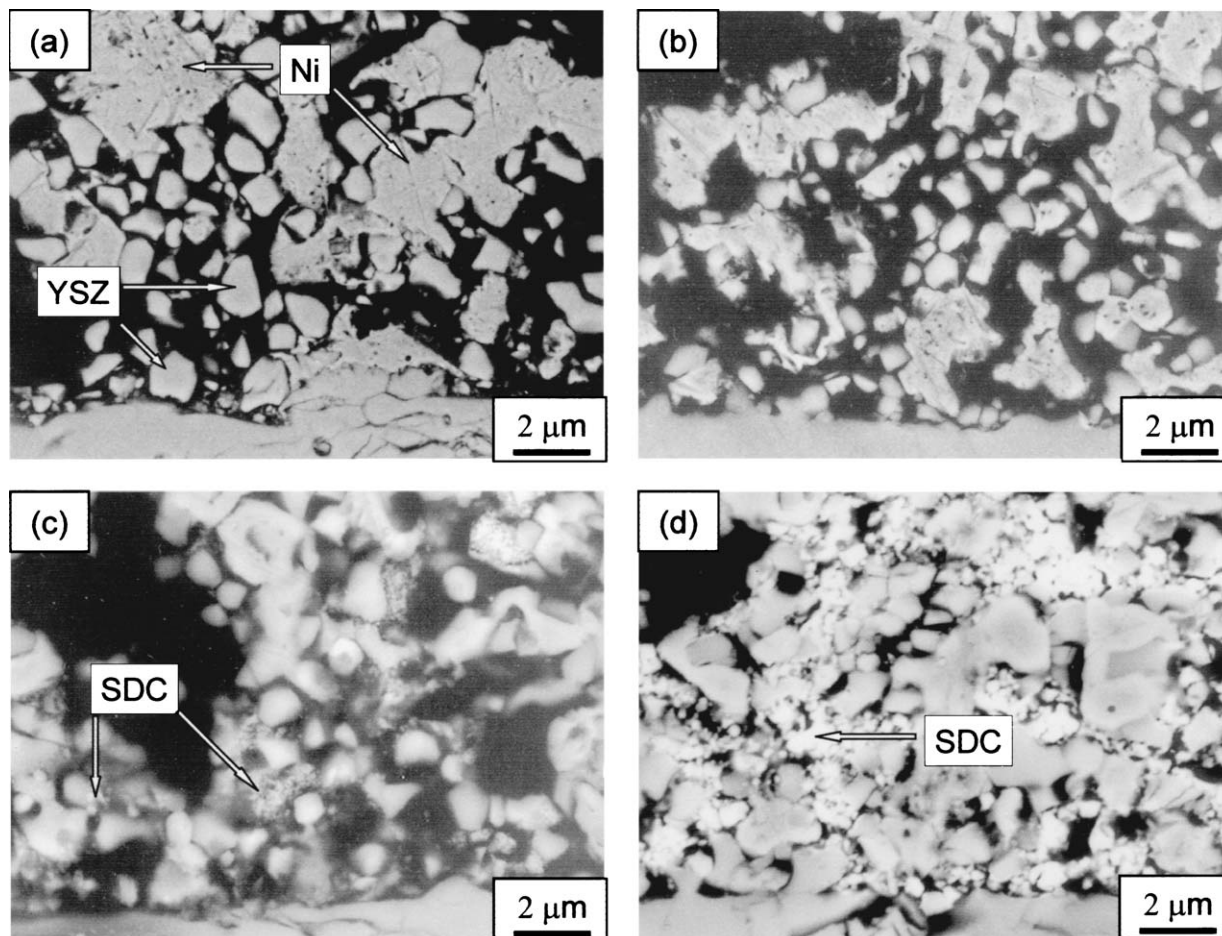
Figure 16 SEM pictures of Ni (50 vol%)/8YSZ (50 vol%) cermet anodes with and without impregnation after fuel cell testing. (a) none, (b) impregnation with 3 M $Y_{0.03}Zr_{0.97}(NO_3)_x$, (c) impregnation with 3 M $Sm_{0.2}Ce_{0.8}(NO_3)_x$ and (d) impregnation three times with 3 M $Sm_{0.2}Ce_{0.8}(NO_3)_x$ nitrate solution.
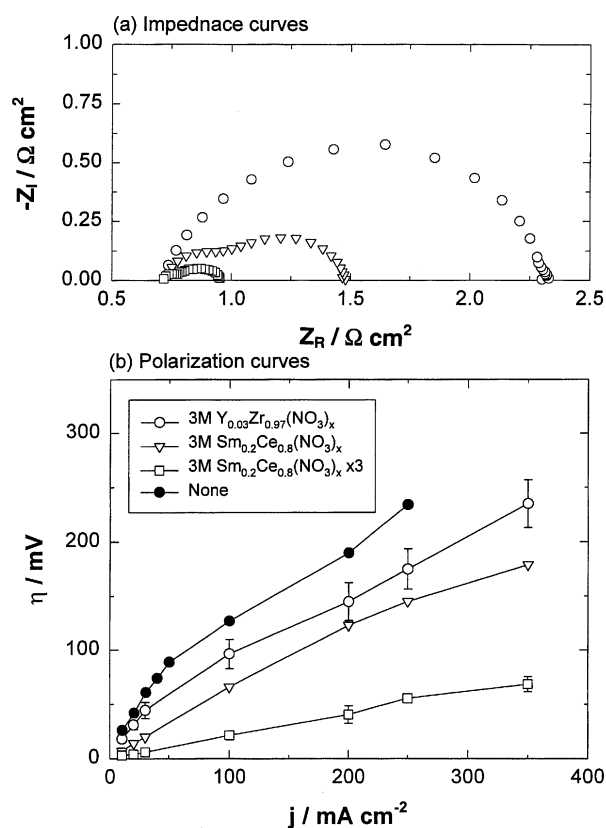
Figure 17 Impedance and polarization performance of Ni (50 vol%)/8YSZ (50 vol%) cermet anodes with and without impregnation. The performance was measured in 97%H_2/3%H_2O at 800°C.

with 3 M $Y_{0.03}Zr_{0.97}(NO_3)_x$ and 3 M $Sm_{0.2}Ce_{0.8}(NO_3)_x$ nitrate solution, η was 175 and 145 mV, respectively, at 250 mA cm^{-2} and 800°C. After three consecutive impregnation with 3 M $Sm_{0.2}Ce_{0.8}(NO_3)_x$ nitrate solution, η was reduced substantially to 56 mV. The results demonstrated that impregnation treatment is effective not only in the inhibition of grain growth and agglomeration of Ni phases in the cermet but also in the promoting of electrochemical reactions. Ion impregnation method is equally effective in the enhancement of the electrode performance of LSM cathodes [135].

Similar to the effect of ion impregnation, Yoon *et al.* [136] observed a significant improvement in the electrode performance of Ni/YSZ cermet anode after the deposition of a thin film of YSZ or samaria-doped ceria (SDC) using a sol-gel coating technique. In this method, as-fired cermet coating was completely dipped into YSZ or SDC sols, followed by calcinations at 600°C for 12 h. The process can be repeated to increase the loading or the thickness of the coating. The process was also used for the improvement of the electrode performance and stability of anode supported electrolyte cells [137]. A process combining slurry coating and pressure infiltration was used by Chou *et al.* [138] to prepare Ni/YSZ cermet anodes over YSZ tubes. Impregnating standard Ni/YSZ cermet anodes with metal catalysts such as Ru improved the power density from 0.35 to 0.48 W cm^{-2} at 800°C [50].

4419

Using electrochemically active interlayer to enlarge the reaction sites for the reaction at the electrode/electrolyte interface has proved to be effective in the promotion of the electrocatalytic activity of both anodes and cathodes. Mixed ionic and electronic conducting materials such as doped CeO_2 are often used as the interlayer [139]. The interlayer layer can also be used to prevent the interfacial reaction between the electrode and the electrolyte in some cases. Combining an interlayer of SDC and impregnated Ru catalysts, the current density achieved at -0.9 V on modified SDC anode structure was more than 4 times higher than that without the interlayer and Ru additives [140]. Using a 0.5 μm thick Y-doped ceria (YDC) interlayer between anode and electrolyte, the electrode polarization resistance for Ni/YSZ anode for methane oxidation was $\sim$1.2 Ωcm^2 at 600°C, which is much smaller than 6.6 Ωcm^2 for the Ni/YSZ cermet anode without the interlayer under the same conditions [41]. Using double anode structure with electrochemically active, composite anode or Ni/YSZ cermet anode with different Ni content and microstructure as anode function layer, polarization performance and power density increased as compared to single anode layer structure [8]. The double layered anode showed good long-term stability [85]. Multilayer anode concept with gradients in composition and microstructure to function as electrochemical active layer, gas diffusion layer and current collector top layer have also been proposed [141]. Müller *et al.* [142] showed that such multilayer anode structure improved the polarization performance and long term stability.

Limitations of the fabrication processes based on the conventional ceramic powder mixing process (see Fig. 1) are the difficulties in achieving optimum phase distribution between Ni and YSZ particles. Several techniques have been developed to achieve better distribution between Ni and YSZ for the preparation of cermet anodes for solid oxide fuel cells. The most notable one was based on electrochemical vapor deposition (EVD) developed by Westinghouse [143]. In Westinghouse tubular cells, the anode is fabricated by slurry coating of nickel and YSZ is incorporated into the Ni skeleton structure by EVD method. The morphology of YSZ intergrowth restricts grain growth and sintering of Ni particles and provides an effective pathway for oxygen ions from YSZ electrolyte to Ni phase [12]. Other deposition techniques reported include sputtering [144], chemical vapor deposition (CVD) [145], a combined EVD/CVD process [145], polarized electrochemical vapor deposition (PEVD) [146, 147], etc. Each of these methods offers advantages in certain aspects but each also presents its own difficulties in terms of cost, reproducibility, scale-up and microstructure control. The objective in the development and optimization of a preparation process of Ni/YSZ cermet anodes is on controlling and tailoring the electrode microstructure to certain degree and thus producing an anode not only with high performance and stability but also with high reproducibility and low cost. The fabrication processes based on cheap and conventional ceramic powder mixing method in conjunction with microstructure improvement processes such as ion impregnation may
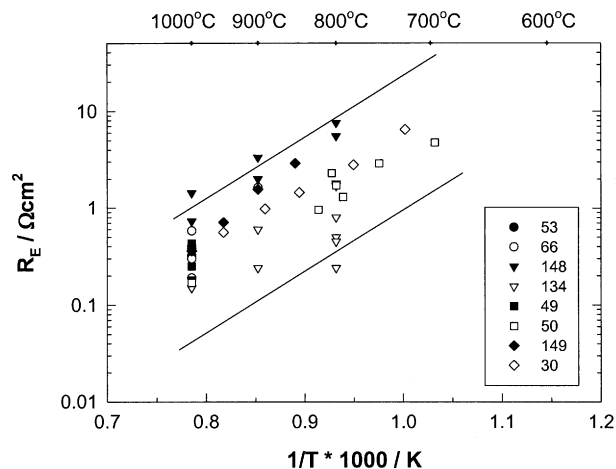
Figure 18 Partial list of the electrode polarization resistance (R_E) of Ni/YSZ cermet anodes measured under moist hydrogen at different temperatures. R_E was measured by electrochemical impedance spectroscopy at open circuit potential. Numbers are the references cited.

offer an effective way to produce high performance and high stable Ni/YSZ cermet anodes.

Fig. 18 is the partial list of the electrode polarization resistance (R_E) of Ni/YSZ cermet anodes measured under moist hydrogen at different temperatures. R_E was measured under open circuit potential by electrochemical impedance spectroscopy and was obtained by the difference of low and high frequency intercepts on the impedance plots. Most of the results reported in the literature are in the medium to high temperature range (800 to 1000°C) and have wide variations in the R_E value. By extrapolating the results to low temperature region, the electrode polarization resistance would be in the range of 1–30 Ωcm^2 at 700°C and 7–200 Ωcm^2 at 600°C for Ni/YSZ based anodes. The electrode polarization resistance is still too high for H_2 oxidation reaction at temepratures below 700°C. However, with modification of Ni/YSZ cermet anodes and with incoporation of YDC interlayer, electrode polarization resistance as low as 0.26 Ωcm^2 at 600°C in wet H_2 was reported [41].

3. Modified Ni/YSZ cermet anodes
Conventional Ni/YSZ cermet materials with and without catalyst modification have been extensively studied for the internal reforming of methane. The internal reforming activity of the anodes is important as it converts methane into more electrochemically active species of H_2 and CO. Unlike polymer electrolyte fuel cells, CO is also a fuel for SOFC. However, the electrochemical activities of Ni/YSZ cermet anodes for the CO oxidation reaction are much lower as compared to that of the anode for the H_2 oxidation reaction [150, 151]. Lee *et al.* [152] studied internal reforming reaction on Ni/YSZ cermet anodes with wide range of porosity and various Ni content. The reaction is of first order with respect to the methane and -1.25 for the steam. Ahmed *et al.* [153, 154] studied the kinetics of internal reforming reaction on Ni/YSZ cermet anodes. On conventional Ni/YSZ cermet anodes, a steam/carbon (S/C) ratio of 2 or higher was required to avoid carbon deposition. At

steam/carbon ratios of 1.5–3, the rate of reforming reaction is 0.84 order with respect to the partial pressure of CH_4 and -0.35 order with respect to the steam on conventional Ni/YSZ cermet anodes at temperatures of $\sim 900°C$. The activation energy of the reforming reaction was 95 kJ mol^{-1} on Ni/YSZ cermet anodes. Activation energy values of 58 to 82 kJ mol^{-1} were also reported for the steam reforming reaction on Ni/YSZ cermet anodes [155, 156]. High activation energy of 118–294 kJ mol^{-1} was reported for the reforming reaction on Ni/YSZ cermet anodes with addition of catalyst such as Ce [157, 158]. Addition of small quantities of molybdenum ($\sim 1\%$) was reported to significantly reduce the carbon deposted on Ni/YSZ anode during mechane reforming [159]. Drescher et al. [160] studied the reforming activities and structural properties of Ni/8YSZ cermet substrates using temperature programmed reduction (TPR), gas adsorption, diffusion and permeation measurements. The methane conversion rate increased linearly with the increase of anode thickness up to 0.6 mm. The gas adsorption experiments showed that the active Ni surface area is about 20% of the total surface area of the cermet. TPR result indicates that the Ni in the cermet would be completely reduced at a temperature of about $500°C$ at sufficient hydrogen supply. This temperature range is close to those reported by Perego et al. [161] and Shirakawa et al. [162].

The effect of carbon deposition on the electrochemical activity of Ni/YSZ cermet anodes in the methane fuel appears to be related to the operating conditions such as current load. Koh et al. [33] showed that at open circuit or low current density, the effect of carbon deposition on the electrocatalytic activity of Ni/YSZ cermet anodes was irreversible. Conversely, under high current load, the polarization performance of the Ni/YSZ was reversible. This indicates the possibility of minimization of the carbon deposition on Ni/YSZ cermet anodes. Weber et al. [163] demonstrated the stability of Ni/YSZ cermet anode up to 1000 h under a current density of 0.4 A cm^{-2} at $950°C$ in dry methane without serious degradation in performance.

Under high current and low concentration (4–9%) of dry methane, methane was reported to be completely oxidized to CO_2 and H_2O without carbon deposition on Ni/YSZ cermet anodes [164, 165]. Under fuel cell operation conditions where methane concentration was high and current was lower than the threshold value, carbon deposition occurs at steam to carbon (S/C) ratio lower than 1 [166]. Liu and Barnett [167] studied the performance and stability of Ni/YSZ anode-supported SOFC operated with wet methane and natural gas at 600–$800°C$. Under a current density of ~ 0.6 A cm^{-2}, the cells showed good stability with limited carbon deposition. Takeguchi et al. [168] studied the carbon deposition and steam reforming of methane on Ni/YSZ anodes modified with alkaline earth addition of MgO, CaO, SrO and CeO_2. CaO, SrO and CeO_2 addition suppressed the carbon deposition while MgO addition promoted the carbon deposition rate and decreased the steam reforming activity of the anodes. High content (~ 2 wt%) of SrO and CeO_2 in the Ni/YSZ cermets also reduced the steam reforming activity significantly. Further study

[169, 170] shows that Ru and Pt addition promotes the reforming activity and supress the carbon deposition. The steam reforming reaction and carbon deposition are also reported by Onuma et al. [171] on Pt electrodes and Horita et al. [172] on Ni/YSZ and Fe/YSZ anodes. Sato et al. [173] studied Ni-Co alloy/YSZ cermet anodes for the oxidation of H_2 and CH_4. Ni-Co alloy was prepared by co-precipitation, followed by sintering at $1100°C$ for 24 h. Co content in Ni-Co/YSZ anodes has little effect on the cell performance with H_2 fed but increases the cell performance with CH_4 fed. The best composition was found to be $Ni_{0.5}Co_{0.5}$/YSZ. The increased activity of Ni-Co/YSZ cermet anodes for CH_4 oxidation was explained by the preferential crystal orientation along (111) plane at the alloy surface, which was not observed for pure Ni powder. The exposure of the most densely packed plane in the face-centered cubic structure could contribute to the formation of surface active sites for the electrochemical oxidation of methane. Ni-Co/YSZ cermet anodes achieved lowest electrode polarization resistance as compared to that of Ni-Cu/YSZ and Ni-Fe/YSZ cermet anodes for H_2 oxidation reaction in wet H_2 [174]. Kim et al. [175] studied the carbon deposition and CH_4 oxidation on Ni-Cu alloy/YSZ cermet anode prepared by ion impregnation of porous YSZ layer with copper and nickel nitrite solution. Carbon was found to deposit on Ni-Cu alloy. However, for Ni-Cu alloy/YSZ cermet anodes with low Ni content such as $Ni_{0.2}Cu_{0.8}$/YSZ, small amount of carbon deposition, in fact, could promote the cell performance, similar to that of pure Cu/YSZ cermet anodes [176]. On the other hand, it was reported that there was no carbon deposition on $Ni_{0.52}Cu_{0.48}$/GDC cermet anodes prepared from very fine $Ni_{0.52}Cu_{0.48}$ alloy after operating in dry CH_4 for ~ 40 h at $800°C$ [177]. Carbon deposition was also found on $Ni_{0.8}Mg_{0.2}$/YSZ cermet anodes after exposure to wet methane [178]. Electrode polarization resistance for the reaction in wet methane on $Ni_{0.8}Mg_{0.2}$/YSZ anode was 9.2 Ωcm^2 at $1000°C$, which is much higher than 1.7 Ωcm^2 in wet H_2.

Presence of sulfur (primarily in the form of H_2S) in the fuel gas can also affect the performance of Ni/YSZ cermet anodes. Geyer et al. [179] reported that the electrode polarization resistance increased by a factor of two by additing only 5 ppm of H_2S at $950°C$ in $97\%H_2/3\%H_2O$. Matsuzaki and Yasuda [180] showed that the poisoning effect of sulfur-containing fuel gas on the electrode performance depends on the total sulfur content and the temperature. The tolerance of the anode towards sulfur poisoning increased with the increasing operation temperature. Study showed that for a sulfur content of 0.02 to 15 ppm, the performance loss caused by the sulfur poisoning could be recovered after switching to the sulfur-free hydrogen fuel. The effect of sulfur impurities on the electrochemical activities of Ni/YSZ cermet anodes was also studied by others [181, 182].

4. Other metal/oxide cermet anodes

Instead of modifying Ni/YSZ cermet anodes, investigations were also performed on the use of

electronic or mixed conducting oxides to make alternative metal/oxide cermets such as ceria stabilized zirconia (CeO_2-ZrO_2), calcium-doped ceria (Ca-CeO_2), yttria-doped ceria (YDC), praseodymium oxide (PrO_x). Mixed results were reported. Kawada et al. [151] studied Ni cermets prepared from CeO_2-ZrO_2, Ca-CeO_2, and Y-CeO_2 and showed no significant improvement in the electrode performance as compared to Ni/YSZ anodes. Relatively high overpotential and high resistance were also observed for ceria related Ni cermet anodes. Eguchi et al. [183], on the other hand, reported the significant improvement in the polarization performance of Ni cermets using samaria-doped ceria (SDC), CeO_x and PrO_x (Ni/oxide ratio was 8/2 in weight) as compared to Ni/YSZ anodes. The activity of the Ni/oxides cermet for hydrogen oxidation was found to be in the following order

$$Ni/YSZ < Ni/CeO_x < Ni/SDC < Ni/PrO_x$$
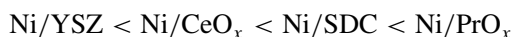
The improved performance was attributed to the increase of the effective reaction area due to the ionic conduction of the oxides. Wang and Tasumi [184] indicated that addition of SDC to Ni anodes led to the increase in activation energy and resulted in high overpotential for H_2 oxidation reactions on Ni/SDC anodes at low temperatures.

Joerger and Gauckler [185] studied the Ni/Gd-doped CeO_2 (Ni/GDC) cermet for H_2 and CH_4 oxidation reaction. Ni/GDC cermet anodes were sintered at 1350°C similar to that of Ni/YSZ cermet anodes. The electrical conductivity of Ni/GDC anodes was 1.7×10^4 S cm^{-1} and electrocatalytic activity of Ni/GDC cermet was much higher than that of Ni/YSZ cermet anodes. At 800°C and 0.5 A cm^{-2}, η of Ni/GDC anode was ~20 mV for H_2 oxidation reaction, significantly lower than ~120 mV obtained on Ni/YSZ cermet anodes. When using methane, η of Ni/GDC anode was ~75 mV at 800°C and 0.25 A cm^{-2}. Activation energies for the H_2 and CH_4 oxidation reaction was also lower on Ni/GDC anodes than those on Ni/YSZ anodes, exhibiting the catalytic and electrocatalytic activities of ceria for the reforming and oxidation of hydrocarbons and hydrogen. Lower overpotential was also reported on Ni/Sm-doped ceria (Ni/SDC) anode as compared to Ni/YSZ anodes for H_2 oxidation at 850°C [186] and the best performance was found on Ni/SDC with 50 vol% Ni content [187]. On Ni/GDC and Ni/15 mol% Y_2O_3-$Ce_{0.7}Zr_{0.3}O_2$ anodes operated below 750°C, no carbon deposition was found when dimethyl ether (DME) was used as the fuel [188]. On the other hand, carbon deposition was found on Ni/GDC anodes with 70 wt% Ni after operating on wet methane at 850°C for about 80 h [189]. With 5 wt% addition of Ru to Ni/GDC anodes, the electrode polarization resistance to CH_4 fuel was reported to be 0.13 Ωcm^2 and a power density of 0.75 W cm^{-2} was recorded in dry CH_4 at 600°C [190]. Hibino et al. [191] also investigated Pd-doped Ni/SDC cermet anodes for partial oxidation of CH_4. With a small addition of Pd (7 wt% PdO), a maximum power density of 0.644 W cm^{-2} at 550°C was achieved on a single-chamber SOFC in CH_4/air mixture, using SDC electrolyte and $Sm_{0.5}Sr_{0.5}CoO_3$ cathode. On the other hand, in a conventional SOFC configuration, a power density of 0.192 W cm^{-2} was reported on Ni/SDC in wet CH_4, using similar electrolyte and cathode materials [192].

The chemical compatibility between YSZ and ceria has been studied by Tsoga et al. [193, 194]. Gd-doped ceria (GDC) and YSZ react and diffuse into each other during sintering process at 1200°C, forming Gd rich phase with ionic conductivity two orders lower than that of YSZ at 800°C [194]. Further study [195] shows that the solid state reaction between YSZ and GDC can be effectively suppressed with an interlayer of $Ce_{0.43}Zr_{0.43}Gd_{0.10}Y_{0.04}O_2$. Chemical compatibility is important for the long-term stability of the multi-layered structure where doped-ceria is often used as interlayer on the cathode side [196] and anode side [41] to protect and to enhance the cell performance. A Ni (40 vol%)/GDC (60 vol%) composition is recommended for the suppression of the reactivity between GDC in the Ni/GDC cermet anode and YSZ electrolyte as the presence of Ni can inhibit the reactivity between YSZ and ceria [194].

Zhang et al. [70] and Ohara et al. [197] studied the effect of sintering temperature on the electrode performance of Ni/SDC anodes on $La_{0.9}Sr_{0.1}Ga_{0.8}Mg_{0.2}O_3$ (LSGM) electrolytes. The best electrode performance (overpotential of 30 mV at 300 mA cm^{-2} and 800°C) was obtained on the anode sintered at 1250–1300°C with Ni content of ~60 vol%. Sintering at 1350°C significantly increased the electrode ohmic resistance and polarization overpotentials, which have been attributed by the significant sintering of the Ni/SDC electrodes and the Ni diffusion into the LSGM electrolyte phase. Kuroda et al. [198] studied the electrode performance of Ni/SDC anodes on $La_{0.8}Sr_{0.2}Ga_{0.8}Mg_{0.15}Co_{0.05}O_3$ (LSGMC) at 650°C and found that the cell polarization were dominated by the loss at the anode. High sensitivity of the sintering temperature of the performance of Ni/SDC cermet anodes on LSGM electrolyte was also observed by Huang et al. [199]. It has been shown that the formation of resistive phase of $LaSrGa_3O_7$, $LaSrGaO_4$ or $LaNiO_3$ between LSGM, NiO and SDC is the main cause for the sensitivity of sintering temperature of the cermet anodes [199–202]. A Ni-free interlayer such as doped-CeO_2 between LSGM and Ni-based anodes could prevent the interfacial reaction [199]. Power density close to 0.9 W cm^{-2} was reported for a 600-μm thick LSGM electrolyte cell at 800°C, using Ni/La_2O_3-doped ceria as the anode [199].

Ni/Ti-doped YSZ cermets were also considered as the anodes for high temperature SOFC [203] due to the attraction of mixed conductivities of TiO_2-doped YSZ under low partial pressure of oxygen [204, 205]. Electrical conductivity of YSZ decreased with Ti doping in YSZ but the bending strength of T-doped YSZ increased. The overpotential of 60 mV at 300 mA cm^{-2} and 1000°C appeares to be compatible with those reported for Ni/YSZ cermet anodes.

Gorte and co-workers [42, 82, 83, 175, 206–208] focused their efforts on the development of Cu/CeO_2/YSZ based anodes. Unlike Ni, copper is inert to

hydrogen or hydrocarbon oxidation and has no catalytic activity for the formation of C—C bonds, thus suppressing the carbon deposition [209]. The primary function of copper in the cermet anodes is to provide electronic conduction path. The melting point of Cu is 1083°C, lower than 1453°C for Ni. Thus Cu-based anodes are suitable for operating temperatures <800°C. However, pure Cu/YSZ anode has very low electrochemical activity for both H_2 and CH_4 oxidation reactions. Ceria catalyst was added to Cu/YSZ cermet to improve the electrode activity [83, 210]. The cells were operated with dry hydrocarbons including methane, butane and synthetic diesel without any carbon deposition. A power output of ~0.15 W cm^{-2} at 700°C was observed in pure C_4H_{10} for a cell with a Cu/CeO$_2$/YSZ anode and a 60 μm thick YSZ electrolyte. Electrode performance of Cu/CeO$_2$/YSZ anodes was significantly improved after exposed to hydrocarbon fuels in particular for the anode with Cu content lower than 30 vol%. This was explained by the effect of the hydrocarbon deposits on the improvement of conductivity of the anode, as shown schematically in Fig. 19 [211]. The effect of lanthanide additives on the Cu/YSZ cermet anodes was also studied, but the performance of Cu/YSZ anodes with lanthanide additives was not as good as that of Cu/ceria/YSZ cermet anodes [212]. In the case of Cu/YSZ based anodes, the oxide catalyst such as ceria

Figure 19 Schematic diagram showing the changes in the three phase boundary and connectivity between metallic particles in Cu/YSZ cermet anode (a) before and (b) after operation in hydrocarbon fuels such as n-butane after McIntosh *et al.* [211].

should be in direct contact with YSZ electrolyte for it to be effective [212]. Because Cu$_2$O and CuO melt at 1235 and 1326°C, respectively, it is not feasible to prepare Cu/YSZ cermets by high temperature sintering as those used for Ni/YSZ cermet anodes. An alternative method was developed for the preparation of Cu/YSZ cermet anodes in which a porous YSZ was produced by acid leaching Ni from Ni/YSZ cermets, followed by addition of Cu and catalysts such as ceria by impregnation [175, 213].

Ruthenium has high melting point (2310°C) as compared to Ni (1453°), thus providing better resistance to sintering and grain growth. Ru/YSZ cermet anodes show high catalytic activity for steam reforming and negligible carbon deposition under internal reforming conditions [214]. Vernoux *et al.* [215] also reached the same conclusion. But its use is prohibited by the high cost and evaporation above 1200°C to produce volatile RuO$_4$ species.

5. Conducting oxides

Mixed ionic and electronic conducting oxides such as gadolinium- or samarium-doped ceria have been investigated as potential anode materials for intermediate temperature SOFC. The major attraction of such mixed ionic and electronic conduction oxides is the possibility of enhanced reaction zone over the three phase boundary due to the high electronic conductivity as compared to conventional YSZ. For example, the oxygen ion conductivity of Sm-doped CeO$_2$ is ~0.1 S cm^{-1} at 800°C is about four times higher than that of YSZ while its electronic conductivity is ~4 S cm^{-1} under H_2 reducing environment [216, 217]. The ceria-based oxides, titanate based oxides, and lanthanum chromite based oxides will be discussed briefly below.

5.1. Ceria-based oxides

Doped-ceria has been extensively investigated as alternative electrolytes to replace YSZ for ITSOFC [218, 219]. The major problem with ceria as electrolyte material is the reduction of Ce^{4+} to Ce^{3+} under the fuel rich conditions of the anode side of electrolyte, introducing electronic conductivity and lattice expansion [218]. The introduced electronic conductivity under fuel reducing environment has been explored for the anode application as it has been shown that CeO$_2$ anode can electrochemically oxidize dry methane as the presence of mobile lattice oxygen reduces the rate of carbon deposition [220, 221]. The high electrocatalytic activity of ceria-based materials for methane oxidation is most likely due to the extraordinary ability of ceria to store, release and transport oxygen ions [222].

The conductivity and activity properties of CeO$_2$-based oxides at 1000°C have been discussed by Mogensen [223] with respect to the application as SOFC anodes. Above 900°C, where grain boundary resistance plays a minor role, the ionic conductivity is mainly determined by the temperature, dopant concentration and dopant metal ion radius. Under reducing conditions like in the anode side, conductivity and dimensional
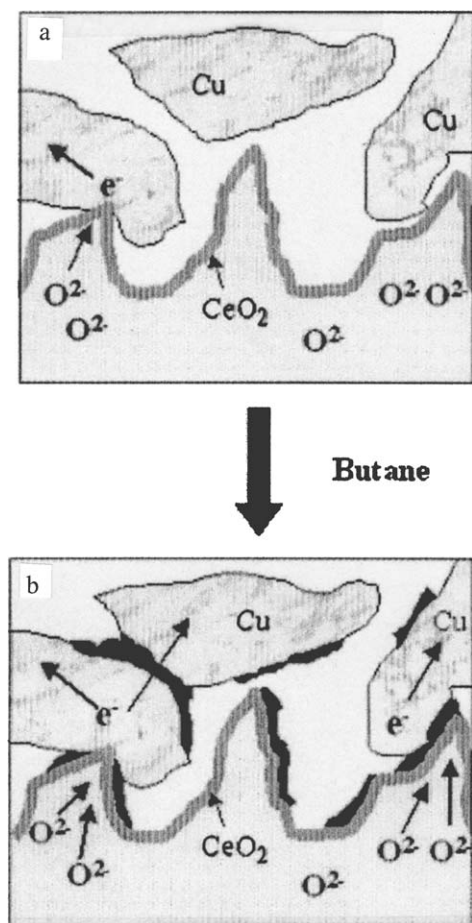
stability of CeO_2-based oxides also relate to the composition and the reducing conditions. Relatively large lattice expansion associated with the loss of oxygen under anodic conditions can result in the anode spilling off the electrolyte and 40% Gd doped CeO_2 is considered to be a reasonable compromise between the conductivity and dimensional stability [224]. Marina *et al.* [225] studied $Ce_{0.6}Gd_{0.4}O_{1.8}$ (GDC) as the anode for both H_2 and CH_4 oxidation reactions at 1000°C. To improve the adhesion between GDC and YSZ electrolyte, an intermediate layer of coarse grain YSZ was sintered on YSZ electrolyte to provide an anchoring effect on the GDC anode. At 1000°C and fuel to steam ratio of 0.13, the cell produced power output of 470 mW cm^{-2} for H_2 and only 80 mW cm^{-2} for CH_4. This indicates that pure GDC has poor electrocatalytic activity for methane oxidation. High electrode polarization resistance of ~11 Ωcm^2 at 800°C was reported for the H_2 oxidation reaction on pure GDC anode [226].

Uchida *et al.* [196, 227, 228] studied the electrocatalytic activity of mixed conducting oxides of Sm-doped CeO_2 (SDC) and Y-doped CeO_2 (YDC) for the H_2 oxidation with and without addition of Ru. SDC and YDC electrodes were sintered at 1150 and 1250°C, respectively. To reduce the electrode ohmic resistance, a gold mesh was use as the current collector. At $\eta = 0.1$ V and 800°C, a performance of 0.2–0.25 A cm^{-2} was obtained on SDC and YDC anodes and the current increased to 0.4–0.5 A/cm^2 with the addition of fine Ru particles. Putna *et al.* [229] also observed enhancing effect of Ru addition on the electrocatalytic activity of ceria anodes. Highly-dispersed Ni in SDC was found to be more effective in promoting the electrocatalytic activity for H_2 oxidation reaction than that of mixed Ni/SDC cermet anodes [230]. Impregnation of 0.75 mg cm^{-2} (or 8 vol%) of nano-sized Ni particles into SDC anodes increased current density to 0.8 A cm^{-2} at overpotential of 0.1 V and 800°C, which is much higher than that of Ni/SDC cermet anodes. This was explained by the significant increase in the number of reactive sites at the nano-sized Ni and SDC boundaries. Significant improvement in the electrocatalytic activity for H_2 oxidation reaction on mixed conductor anodes such as GDC, $La_{0.75}Sr_{0.25}Cr_{0.97}V_{0.03}O_3$ and Ti-doped YSZ with addition of small amounts of Ni (1–2.5 wt%) was also reported by Primdahl *et al.* [231, 232]. On the other hand, a thin layer of yttria-doped ceria (YDC) did not show any significant difference in terms of electrocatalytic activity of Pt electrode for H_2 oxidation as compared to that of pure YSZ electrolyte [233]. This appears to be very different from that of Ni/YSZ cermet anodes. An addition of a thin YDC layer between Ni/YSZ cermet anodes and YSZ electrolyte reduced the electrode interface resistance for methane oxidation by a factor of ~6, as shown in Fig. 20 [41]. This shows that the addition of YDC layer significantly increased the reaction sites for the CH_4 oxidation reaction.

5.2. Titanate-based oxides
Titanate-based oxides are relatively stable in fuel reducing environment and possess certain conductivity
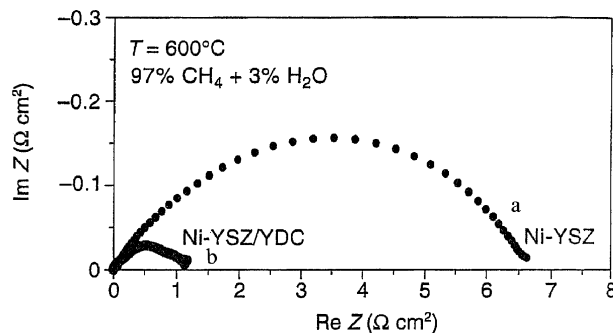
Figure 20 Impedance curves for Ni/YSZ cermet anode (a) without and (b) with a 0.5 μm thick YDC interlayer between anode and YSZ electrolyte. Impedance curves were meaured in 97%CH_4/3%H_2O at 600°C after Murray *et al.* [41].

at low partial pressure of oxygen, making them attractive as potential anode materials. Titanates are electronically conductive and show n-type at low $p_{O_2} (10^{-15}-10^{-2}$ Pa) and p-type at high p_{O_2} (10^0-10^5 Pa). Sutija *et al.* [234] studied the electrical conductivity of Fe-doped calcium titanate and reported that the conductivity was less than 1 S cm^{-1} for $CaFe_xTi_{1-x}O_{3-\delta}$ ($x = 0.1$ to 0.4) even at 1000°C. Holt *et al.* [235] investigated the synthesis and electrical properties of Ti-doped $NdCrO_3$ and found that the solubility of Ti in $Nd(Cr_{1-x}Ti_x)O_3$ is about 20%. The electrical conductivity of Ti-doped $NdCrO_3$ was about 1 S cm^{-1} at 1000°C in low p_{O_2} range. However, the initial electrical conductivity of titanates is somehow related to the sintering conditions. Marina *et al.* [236, 237] studied the electrical and thermal properties of lanthanum strontium titanates (LST) and Ce-doped LST. For air sintered sample, the electrical conductivity is in the range of 1–16 S cm^{-1} and for sample sintered in hydrogen, electrical conductivity of 80–360 S cm^{-1} at 1000°C and partial pressure of 10^{-18} atm. However, electrical conductivity of hydrogen-sintered sample degraded in air and appears to be irreversible. The cell based on $La_{0.4}Sr_{0.6}TiO_3$ anodes showed very rapid performance degradation, i.e., 1/3 of its initial performance after just 1 h of testing at 1000°C in 97%H_2/3%H_2O. Ce-doped LST may in fact consist of a ceria/perovskite assemblage [237].

Electrical properties of titania-doped YSZ were also investigated as potential candidates for alternative anode materials due to the introduced electronic conductivity, their thermal stability and thermal expansion compatibility with YSZ electrolyte [238]. The solubility of titania in YSZ is quite high. But for samples with 15 mol% titania or higher dopant level, Colomer *et al.* [239] reported the appearance of the second phase (e.g., $ZrTiO_4$). They showed that titania additions in excess of 5 mol% are an effective way to promote the electronic conductivity (reduction in ionic transport number) of YSZ under anode working conditions. Total conductivity of 5 mol% titania-doped YSZ is ~0.02 S cm^{-1} at 800°C and decreased with increasing titania content [239, 240]. The reason could be due to the solubility limit effect on the ion vacancy mobility. Yttria-stabilised zirconia-terbia (YSZT) system also showed mixed conductivity under fuel environment. For example, for YSZT containing 30 mol% Tb,

the electric and ionic conductivity were measured as 2.3×10^{-3} S/cm and 2.8×10^{-3} S/cm, respectively, at 800°C in air. The p-type conductivity of YSZT system is only significant in oxidizing atmospheres [241]. Tao and Irvine [242] investigated Y_2O_3-ZrO_2-TiO_2 and Sc_2O_3-Y_2O_3-ZrO_2-TiO_2 systems. In the Sc-Y-Zr-Ti system, $Sc_{0.15}Y_{0.05}Zr_{0.62}Ti_{0.18}O_{1.9}$ showed most promising as potential anode materials with ionic and electronic conductivity of 7.8×10^{-3} and 0.14 S cm^{-1}, respectively, at 900°C. The cubic fluorite structure of YSZ can be maintained even with Ti contents as high as 18% [243]. Cu-stabilized ZrO_2 was also explored as anode materials for SOFC [244]. The catalytic activity of CuO-ZrO_2 samples increased with CuO content up to 20 mol%.

Middleton *et al.* [245] investigated some titanate-based oxides as the potential anodes for methane conversion and oxidation. The oxides under study include rutile-type $Ti_{0.97}Nb_{0.03}O_2$, pseudobrookite-type $Mg_{0.3}Nb_{0.1}Ti_{2.6}O_5$ and $MgTi_{1.95}Nb_{0.05}O_5$, pyrochlore-type $Sm_2Ti_{1.9}Nb_{0.1}O_7$ and V_3O_5-structure type $CrTi_2O_5$. The oxides showed some activities towards the CH$_4$ conversion in the temperature range of 500–700°C and the main product was CO_2. At temperature higher than 800°C, CO was dominated. From steady state catalytic studies, it showed that among the titanates most active catalysts are the compounds with enhanced electronic conductivity, for example pyrochlore-type $Sm_2Ti_{1.9}Nb_{0.1}O_7$ is more active than $Sm_2Ti_2O_7$ and pseudobrookite-type $Mg_{0.3}Nb_{0.1}Ti_{2.6}O_5$ is more active than $MgTi_{1.95}Nb_{0.05}O_5$. All oxides under study showed low C_2 formation except $Ti_{0.97}Nb_{0.03}O_2$. The highest activity in the n-type conducting titanates was observed for $Mg_{0.3}Nb_{0.1}Ti_{2.6}O_5$ generating CO_2 as the main product. No data was reported for the CH$_4$ conversion under SOFC operating conditions.

Fagg *et al.* [246] investigated the possibility of using spinel solid solution series $Mg_{2-y}Ti_{1+y}O_4$, $0 < y < 0.5$ as high temperature anodes for SOFC. Reduced magnesium titanate spinels are stable in the reducing atmosphere and are shown to resist oxidation in air up to 500°C. The conductivity very much depends on the oxidation state of Ti at room temperature, but at fuel cell operation temperatures (e.g., 1000°C), there is little difference in conductivity and the conductivity value was estimated to be in the range of 0.2–2.0 S cm^{-1}. The thermal expansion coefficient of magnesium titanate spinels obtained from the high temperature powder diffraction studies was close to those of the 8 mol% Y_2O_3-doped ZrO_2 ($\sim 10.5 \times 10^{-6}$/K).

Perovskite $SrTiO_3$ doped with La or Nb and niobium based tetragonal tungsten bronzes were evaluated as potential anodes for SOFC [247, 248]. Doped strontium titanates are reported to be stable in reducing environment and the electronic conductivity was ~ 7 S cm^{-1} at 930°C but its ionic conductivity was low [247]. For niobium based tetragonal tungsten bronzes under study, the highest conductivity of ~ 8.3 S cm^{-1} at 10^{-20} bar was observed on $Ba_{0.35}Ca_{0.15}NbO_3$. $Ba_{0.6-x}A_xTi_{0.2}Nb_{0.8}O_3$ (A = Sr, Ca) was considered as a promising anode material as it can be prepared in air and is stable in reducing environment. Layered

perovskite, $La_2Sr_4Ti_6O_{19-\delta}$, was found to have quite high conductivity, 40 S cm^{-1} at 900°C in 5%H$_2$/Ar but its electrode polarization resistances of 3 Ωcm^2 and 9 Ωcm^2 at 900°C in wet H$_2$ and wet CH$_4$, respectively, are still high [249]. Yashiro *et al.* [250] also studied the electrode performance of doped strontium titanates such as $SrTi_{0.97}Nb_{0.03}O_3$, $La_{0.1}Sr_{0.9}TiO_3$ and $La_{0.2}Sr_{0.8}TiO_3$. The observed electrode polarization resistance was in the range of 350 to 700 Ωcm^2 at 800°C. This indicates that doped-$SrTiO_3$ has poor electrocatalytic activity for H$_2$ oxidation reactions despite the high electronic conductivity of doped strontium titanates (e.g., electronic conductivity of $La_{0.1}Sr_{0.9}TiO_3$ was reported to be as high as ~ 200 S cm^{-1} at 800°C [251]).

Yttrium-doped $SrTiO_3$ (YST) showed quite high electrical conductivity under reducing conditions [252, 253]. At partial pressure of 10^{-19} atm and 800°C, the electrical conductivity of dense YST specimen ($Sr_{0.85}Y_{0.10}Ti_{0.95}Co_{0.05}O_{3-\delta}$) is 45 S cm^{-1} and for YST specimen with 30% porosity it is ~ 30 S cm^{-1}. The highest conductivity of 64 S cm^{-1} at 800°C was observed on $Sr_{0.88}Y_{0.08}TiO_{3-\delta}$. The thermal expansion coefficient of YST is in the range of 11–12×10^{-6}/°C, which is compatible with that of YSZ and $(La,Sr)(Ga,Mg)O_3$ electrolyte materials. However, adhesion of YST to YSZ electrolyte was poor and similar to that of ceria based anodes [224], SYT anode coatings delaminated from YSZ electrolyte.

5.3. Lanthanum chromite and other type of oxides

Lanthanum chromites ($LaCrO_3$) based materials have been investigated as interconnector material in SOFC because of its stability towards reduction and its relatively high electrical conductivity and stability in both reducing and oxidizing atmospheres at SOFC operating temperatures [254–257]. The conductivity properties of $LaCrO_3$-based materials are significantly affected by A- and/or B-site doping. For example, Ca doping at the A-sites has significant effect on the electronic conductivity due to the expected charge compensating transitions (Cr^{3+} to Cr^{4+}). Co substitution for Cr also has some positive effect on the electronic conductivity. Co doping causes dramatic increase in TEC, but this can be compensated by the subsequent Ca doping. Conductivity of $(La_{1-x}Ca_x)CrO_3$ materials is independent on the oxygen activity in the high p_{O_2} region and decreased with 1/4 slope at low p_{O_2} range. The conductivity of $La_{0.8}Ca_{0.2}Cr_{0.8}Co_{0.2}O_3$ was 45 S cm^{-1} at high p_{O_2} and reduced to about 4 S cm^{-1} at p_{O_2} of 10^{-16} atm and 1000°C [254–257]. Also, it has been shown that $LaCrO_3$-based materials such as $(La,Sr)CrO_3$ have very low activity towards carbon deposition [36, 258].

Catalytic activity of $LaCrO_3$ for methane oxidation can also be substantially enhanced by doping at A- and B-sites. Sfeir *et al.* [259–261] studied the thermodynamic stability and the catalytic activity of $(LaA)(CrB)O_3$ system (A = Ca, Sr and B = Mg, Mn, Fe, Co, Ni) as alternative anode materials under simulated SOFC operating conditions. Thermodynamically,

Sr and Mn substitution would maintain the stability of the perovskite while other substitutes would destabilize the system. However, transitional metal substituted $LaCrO_3$ did not decompose easily under reducing conditions, indicating that the decomposition of substituted $LaCrO_3$ would be hindered kinetically. Ca and Sr substitution at the A-site improves the catalytic activity and for B-site substitution, Co and Mg showed an inhibiting effect while Mn, Fe and Ni improved the activity. $La_{0.75}Sr_{0.25}Cr_{0.5}Fe_{0.5}$ was shown stable under reducing atmosphere but its electrochemical performance in wet methane was reported to be very poor [262]. Considering the catalytic activity and cracking resistance, $(LaSr)(CrNi)O_3$ with 10% Ni doping was suggested to be most suitable for methane oxidation reactions [263]. On the other hand, Ni exsolution has been found in 10% Ni-doped lanthanum chromites in fuel environment [264] and the surface segregation of Ni from Ni-doped lanthanum chromites may be responsible for the high activity. Liu *et al.* [265] showed that addition of 5% NiO in $La_{0.8}Sr_{0.2}Cr_{0.8}Mn_{0.2}O_3$ (LSCM)/GDC (50 wt%/50 wt%) composite anodes significantly enhanced the anode activity for both H_2 and CH_4 oxidation. The power density of the cell with LSCM/GDC-NiO anode was 0.13 W cm^{-2} at 750°C, much higher than 0.05 W cm^{-2} on the cell with LSCM/GDC anode without NiO addition. Enhancing effect of additing small amount of catalysts such as Ni and Ru on the performance of $LaCrO_3$-based for fuel oxidation reactions was also studied by others [37, 266]. The amount of metal catalysts may be low enough to avoid carbon deposition [265].

Middleton *et al.* [245] studied the activities of $La_{0.8}Ca_{0.2}CrO_3$ for the CH_4 conversion and oxidation reactions. The oxide showed no significant formation of C_2 compounds, but was the most active and selective catalyst for CO_2 formation, with complete conversion below 500°C, as compared with titanate-based oxides [245]. At temperature above 800°C, the conversion of methane dramatically increased, with the concomitant formation of CO and hydrogen. The methane reaction was suggested to occur in two separate ways, i.e., com-

plete oxidation to CO_2 and H_2O by partial methane dissociation (mainly involving surface adsorbed oxygen), and methane dissociation (mainly involving mobile lattice oxygen) to form H and C species on the oxide surface. Methane dissociation was predominant at high temperatures (900–1000°C) with carbon deposition.

Primdahl *et al.* [266] studied the electrocatalytic activity of $(La,Sr)CrO_3$ for H_2 and CH_4 oxidation at 850°C. In the case of $La_{0.8}Sr_{0.2}Cr_{0.97}V_{0.03}O_3$, the electrode polarization resistance (R_E) was ~5 Ωcm^2 for H_2 and ~30 Ωcm^2 in CH_4 with 3%H_2O at 850°C. The presence of second phase formation in $La_{0.8}Sr_{0.2}Cr_{0.97}V_{0.03}O_3$ led to the formation of $SrZrO_3$. This indicates that Sr-doped $LaCrO_3$ has poor electrocatalytic activity for H_2 oxidation and shows little catalytic activity for direct CH_4 oxidation. This is similar to the previous reports on the overall low electrode performance of steam reforming and direct methane oxidation reaction on $LaCrO_3$ and doped $LaCrO_3$ [246, 267–269]. Chromite/titanate based perovskite anodes generally show much poorer electrochemical activity for H_2 oxidation as compared to that of Ni/YSZ cermet anodes despite some of the perovskites have reasonably high electrical conductivity. This may be partially due to the poor adhesion between the perovskite coating and YSZ electrolyte [270]. Insertion of Ru or Mn into the B-site of $LaCrO_3$ was shown to increase the electrochemical activity for the H_2 oxidation as compared to Sr-doped $LaCrO_3$ [271]. The catalytic activity of Ru and V-doped $(LaSr)CrO_3$ for steam reforming of methane was studied in detail as function of stream to carbon ratio at 850°C [272]. It was pointed out that the Sr doping is the key factor in the stability of ruthenium in the chromite perovskite structure [273]. Recently Tao and Irvine [274] reported some promising results of $La_{0.75}Sr_{0.25}Cr_{0.5}Mn_{0.5}O_3$ (LSCM) as anode for SOFC. LSCM is a *p*-type conductor with conductivity of ~38 S cm^{-1} at 900°C at oxygen partial pressure above 10^{-10} atm. The electrode polarization resistance for the oxidation reactions in wet CH_4 and H_2 at 900°C was 0.85 and 0.26 Ωcm^2, respectively. Fig. 21
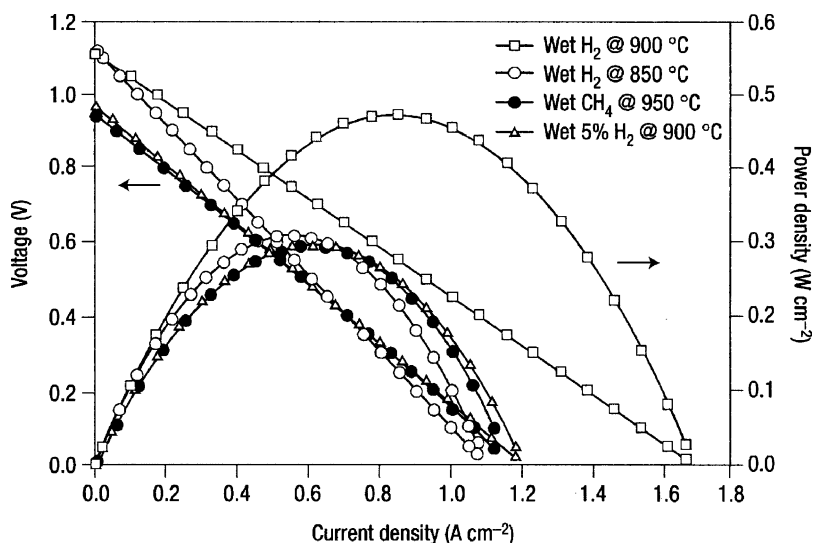
Figure 21 Performance of the cell with $(La_{0.75}Sr_{0.25})_{0.9}Cr_{0.5}Mn_{0.5}O_3$ anode and LSM cathode measured at different temperatures in humidified fuel gases after Tao and Irvine [274]. YSZ electrolyte thickness was 0.3 mm.

shows the performance of a cell with $(La_{0.75}Sr_{0.25})_{0.9}$-$Cr_{0.5}Mn_{0.5}O_3$ anode and LSM cathode measured at different temperatures. The maximum power density was 0.47 W cm^{-2} at 900°C, which is considered to be compatible to the cell based on Ni/YSZ cermet anodes, considering that the YSZ electrolyte used in the cell had a thickness of 0.3 mm.

Mixed ionic and electronic conducting oxides such as $SrFeCo_3O_x$, $SrCo_{0.8}Fe_{0.2}O_3$ and $La_{0.6}Sr_{0.4}Fe_{0.8}Co_{0.2}O_3$ (LSCF) were investigated for their electrochemical activity for the oxidation of H_2 and CH_4 fuels [275, 276]. Different to their high electrocatalytic activity for the O_2 reduction reactions [277], the oxide anodes showed poor electrochemical activity for the oxidation reactions of both H_2 and CH_4. It is well known that LSCF materials without protective layer decompose readily and are not stable in exposing to reducing atmosphere [278]. Other conducting oxides studied as potential anode materials include cubic perovskite Sr_2GaNbO_6 [279], tetragonal tungsten bronze type $A_{0.6}B_xNb_{1-x}O_3$ (A = Ba, Sr, Ca, La and B = Ni, Mg, Mn, Fe, Cr, In, Sn) [280], nonstoichiometric mixed perovskites such as $SrCu_{0.4}Nb_{0.6}O_{2.9}$, $SrMn_{0.5}Nb_{0.5}O_{3-\delta}$ or $Sr_2Mn_{0.8}Nb_{1.2}O_6$ [281, 282], and pyrochlore $Gd_2(Ti_{1-x}Mo_x)_2O_7$ [283]. Table I summarizes the electrical and electrochemical properties of some conducting oxide studied as potential anode materials. Large effort is still needed to understand the conductivity and electrochemical behaviour of conducting oxides under fuel environment and to improve significantly the electrocatalytic activity and stability for the oxidation reaction of H_2 and hydrocarbon fuels such as CH_4 under SOFC operating conditions.

6. Development of anode-supported structures

It is increasingly clear that for the development of commercially viable SOFC technologies, a reduction of the operating temperature from traditionally 1000°C to the range of 600 to 800°C is essential. Low operating temperature not only widens the selection of materials for the electrode, electrolyte, interconnect and manifold components of SOFC but also significantly reduces the risk of thermal shock and interface reactivity between various cell components and thus increases the cell performance stability and reliability. However, lower operating temperature requires high electrode electrocatalytic activity and high ionic conductivity of electrolyte to compensate the cell loss without penalty for the power density achieved at high temperatures. There are two different ways to achieve this objective: one is the development of electrolyte with much higher ionic conductivity than YSZ and the second is to reduce the thickness of YSZ electrolyte using electrode supported structures. Electrode supported cell structure is commonly used to reduce the electrolyte thickness.

The choice of materials for the electrode supported structure is primarily related to a number of important considerations;

- No reactivity with the electrolyte during fabrication process. This is particularly important if the cell structure is formed by co-sintering. As most of electrolyte materials require high sintering temperature (1300 to 1500°C), the reactivity and interface reaction between the electrode support and electrolyte should be none or minimum.
- High strength of the electrode support structure. Cell strength is determined by the strength of the electrode support structure. Sufficient cell strength is needed for easy handling during the cell fabrication and stacking. Also, cell should be strong enough to withstand the thermal and mechanical stress during operation.
- High permeability for the fuel gas and the reaction products H_2O and CO_2. As the electrode support structure is usually in the thickness of 500 to 2000 μm, polarization losses due to gas diffusion can be significant.
- Good sintering compatibility. Sintering behavior of the electrode support and electrolyte must be closely matched to reduce the bending and warping and to increase the production rates.
- High electrical conductivity to reduce the ohmic loss of the cell and high thermal conductivity to respond quickly to temperature swing in the cell and stack.
- Good microstructure, surface and shrinkage properties for easy deposition and densification of thin electrolyte layers.
- Finally the cost of the material and automation of the processing needs to be considered.

Ni/YSZ based electrode materials satisfy most of the considerations for YSZ based electrolyte cells. Ni/YSZ cermets are highly electrically and thermally conductive. Ni/YSZ cermet anodes can be fired with YSZ electrolyte up to 1400°C for the densification of the electrolyte with little reactivity between Ni and YSZ electrolyte. With cathode-supported structure such as Sr-doped $LaMnO_3$, the forming temperature would have to be 1300°C or lower in order to avoid the formation of resistive $La_2Zr_2O_7$ phase at the electrode/electrolyte interface [284–287]. Thus, sintering YSZ thin film on $LaMnO_3$-based oxide substrate is expected to be more difficult than sintering on a Ni/YSZ cermet anode substrate. Gas diffusion limitation is also a less problem on the anode side as compared to that on the cathode side. At 800°C the molecular diffusion coefficient of H_2/H_2O system is $\sim 8.4 \text{ cm}^2 \text{ s}^{-1}$, which is considerably higher than $\sim 2 \text{ cm}^2 \text{ s}^{-1}$ of O_2/N_2 system. The effective binary diffusion coefficients of H_2/H_2O are also considerably higher than those of O_2/N_2 under SOFC operating conditions [288]. Porous structure and porosity of the anode substrates can be controlled by anode composition and addition of pore formers such as rice and corn starch, carbon black and graphite [289]. Primdahl et al. [290] reported that adding 40 vol% corn starch as pore-former to the anode substrates could reduce the electrode polarization resistance from 0.15 to 0.08 Ωcm^2 at 850°C. The cost of Ni/YSZ materials

TABLE I Conductivity and electrochemical properties of selected conducting oxides studied as potential anode materials. Electrode polarization resistance (R_E) was measured at open circuit by electrochemical impedance spectroscopy

Composition	σ/S cm^{-1}		R_E/Ωcm^2		Ref.
	Temp/Re	Temp/Ox	Temp/H$_2$	Temp/CH$_4$	
La$_{0.7}$Ca$_{0.3}$TiO$_3$	2.7 (900°C/Re)[a]				[270]
La$_{0.4}$Sr$_{0.6}$TiO$_3$	60 (900°C/Re)				[270]
La$_{0.7}$Ca$_{0.3}$Cr$_{0.5}$Ti$_{0.5}$O$_3$	0.03 (900°C/Re)				[270]
La$_{0.7}$Ca$_{0.3}$Cr$_{0.5}$Ti$_{0.2}$O$_3$			32 (850°C/H$_2$)[b]		[270]
La$_{0.1}$Sr$_{0.9}$TiO$_3$	3 (1000°C/Re)	1 (1000°C/Ox)[a]	Sintered in air		[236]
La$_{0.2}$Sr$_{0.8}$TiO$_3$	3 (1000°C/Re)	1 (1000°C/Ox)	Sintered in air		[236]
La$_{0.3}$Sr$_{0.7}$TiO$_3$	4 (1000°C/Re)	1.3 (1000°C/Ox)	Sintered in air		[236]
La$_{0.4}$Sr$_{0.6}$TiO$_3$	16 (1000°C/Re)	0.004 (1000°C/Ox)	Sintered in air		[236]
La$_{0.1}$Sr$_{0.9}$TiO$_3$	80 (1000°C/Re)	0.004 (1000°C/Ox)	Sintered in H$_2$		[236]
La$_{0.2}$Sr$_{0.8}$TiO$_3$	200 (1000°C/Re)	0.03 (1000°C/Ox)	Sintered in H$_2$		[236]
La$_{0.3}$Sr$_{0.7}$TiO$_3$	200 (1000°C/Re)	0.01 (1000/Ox)	Sintered in H$_2$		[236]
La$_{0.4}$Sr$_{0.6}$TiO$_3$	360 (1000°C/Re)	0.03 (1000/Ox)	Sintered in H$_2$		[236]
La$_{0.1}$Sr$_{0.9}$TiO$_3$			510 (800°C/H$_2$)		[250]
La$_{0.2}$Sr$_{0.8}$TiO$_3$			350 (800°C/H$_2$)		[250]
SrTi$_{0.97}$Nb$_{0.03}$O$_3$			700 (800°C/H$_2$)		[250]
Sr$_{0.85}$Y$_{0.15}$Ti$_{0.95}$Ca$_{0.05}$O$_3$	37 (800°C/Re)				[252]
Sr$_{0.85}$Y$_{0.15}$Ti$_{0.95}$Co$_{0.05}$O$_3$	45 (800°C/Re)				[252]
Sr$_{0.85}$Y$_{0.15}$Ti$_{0.95}$Zr$_{0.05}$O$_3$	13 (800°C/Re)				[252]
Sr$_{0.85}$Y$_{0.15}$Ti$_{0.95}$Mg$_{0.05}$O$_3$	6 (800°C/Re)				[252]
Sr$_{0.88}$Y$_{0.08}$TiO$_3$	64 (800°C/Re)				[252]
La$_{0.7}$Ca$_{0.32}$CrO$_3$			86 (850°C/H$_2$)		[266]
La$_{0.75}$Ca$_{0.25}$Cr$_{0.9}$Mg$_{0.1}$O$_3$			21 (850°C/H$_2$)		[266]
La$_{0.8}$Sr$_{0.2}$Cr$_{0.97}$V$_{0.03}$O$_3$			5 (850°C/H$_2$)	30 (850°C/CH$_4$)[b]	[266]
La$_{0.75}$Sr$_{0.25}$Cr$_{0.9}$Mg$_{0.1}$O$_3$			2 (850°C/H$_2$)		[266]
La$_2$Sr$_4$Ti$_6$O$_{19}$	~30 (900°C/Re)	8.5 × 10^{-4} (900°C/Ox)	3 (900°C/H$_2$)	9 (900°C/CH$_4$)	[249]
La$_{0.8}$Sr$_{0.2}$CrO$_3$			256 (850°C/H$_2$)		[271]
La$_{0.8}$Sr$_{0.2}$Cr$_{0.8}$Mn$_{0.2}$O$_3$			51 (850°C/H$_2$)		[271]
La$_{0.75}$Sr$_{0.25}$Cr$_{0.5}$Mn$_{0.5}$O$_3$	1.3 (900°C/Re)	38 (900°C/Ox)	0.26 (900°C/H2)	0.85 (900°C/CH$_4$)	[274]
Sr$_{0.6}$Ti$_{0.2}$Nb$_{0.8}$O$_3$	2.5 (930°C/Re)	3 × 10^{-4} (930°C/Ox)			[248]
Sr$_{0.4}$Ba$_{0.2}$Ti$_{0.2}$Nb$_{0.8}$O$_3$	2.5 (930°C/Re)	2 × 10^{-4} (930°C/Ox)			[248]
Sr$_{0.2}$Ba$_{0.4}$Ti$_{0.2}$Nb$_{0.8}$O$_3$	3.2 (930°C/Re)	2 × 10^{-4} (930°C/Ox)			[248]
Ba$_{0.4}$Ca$_{0.2}$Ti$_{0.2}$Nb$_{0.8}$O$_3$	3.1 (930°C/Re)	2 × 10^{-4} (930°C/Ox)			[248]
Ba$_{0.6}$Ti$_{0.2}$Nb$_{0.8}$O$_3$	3.2 (930°C/Re)	1 × 10^{-4} (930°C/Ox)			[248]
Sr$_2$GaNbO$_6$	9 × 10^{-4} (900°C/Re)	7.8 × 10^{-3} (900°C/Ox)			[279]
Ba$_{0.6}$Mn$_{0.067}$Nb$_{0.933}$O$_3$	2.2 (930°C/Re)	4 × 10^{-4} (930°C/Ox)			[280]
Ba$_{0.4}$La$_{0.2}$Mn$_{0.133}$Nb$_{0.867}$O$_3$	0.2 (930°C/Re)	6 × 10^{-4} (930°C/Ox)			[280]
Ba$_{0.4}$Sr$_{0.2}$Mn$_{0.067}$Nb$_{0.933}$O$_3$	1.8 (930°C/Re)	4 × 10^{-4} (930°C/Ox)			[280]
Ba$_{0.6}$Ni$_{0.067}$Nb$_{0.933}$O$_3$	4.5 (930°C/Re)	5 × 10^{-4} (930°C/Ox)			[280]
Ba$_{0.4}$La$_{0.2}$Ni$_{0.133}$Nb$_{0.867}$O$_3$	2.4 (930°C/Re)	2 × 10^{-4} (930°C/Ox)			[280]
Ba$_{0.6}$Mg$_{0.067}$Nb$_{0.933}$O$_3$	1.3 (930°C/Re)	8 × 10^{-5} (930°C/Ox)			[280]
Ba$_{0.4}$La$_{0.2}$Mn$_{0.133}$Nb$_{0.867}$O$_3$	0.5 (930°C/Re)	2 × 10^{-5} (930°C/Ox)			[280]
Ba$_{0.6}$Fe$_{0.1}$Nb$_{0.9}$O$_3$	3.8 (930°C/Re)	1 × 10^{-2} (930°C/Ox)			[280]
Ba$_{0.4}$La$_{0.2}$Fe$_{0.2}$Nb$_{0.8}$O$_3$	1.1 (930°C/Re)	2 × 10^{-4} (930°C/Ox)			[280]
Ba$_{0.5}$La$_{0.1}$Fe$_{0.2}$Nb$_{0.8}$O$_3$	0.7 (930°C/Re)	3 × 10^{-3} (930°C/Ox)			[280]
Ba$_{0.4}$Ca$_{0.2}$Fe$_{0.1}$Nb$_{0.9}$O$_3$	1.2 (930°C/Re)	3 × 10^{-3} (930°C/Ox)			[280]
Ba$_{0.4}$Sr$_{0.2}$Fe$_{0.1}$Nb$_{0.9}$O$_3$	2.3 (930°C/Re)	4 × 10^{-3} (930°C/Ox)			[280]
Ba$_{0.6}$In$_{0.1}$Nb$_{0.9}$O$_3$	1.0 (930°C/Re)	1 × 10^{-4} (930°C/Ox)			[280]
Ba$_{0.4}$Sr$_{0.2}$In$_{0.1}$Nb$_{0.9}$O$_3$	1.5 (930°C/Re)	1 × 10^{-4} (930°C/Ox)			[280]
Ba$_{0.4}$La$_{0.2}$In$_{0.2}$Nb$_{0.8}$O$_3$	0.3 (930°C/Re)	2 × 10^{-5} (930°C/Ox)			[280]
Ba$_{0.6}$Cr$_{0.1}$Nb$_{0.9}$O$_3$	3.6 (930°C/Re)	2 × 10^{-3} (930°C/Ox)			[280]
Ba$_{0.6}$Sn$_{0.2}$Nb$_{0.8}$O$_3$	21 (930°C/Re)	3 × 10^{-4} (930°C/Ox)	Pellet showed signs of decomposition after measurement		[280]
SrCu$_{0.4}$Nb$_{0.6}$O$_{2.9}$	Unstable	1 × 10^{-4} (900°C/Ox)			[281]
Sr$_2$Mn$_{0.8}$Nb$_{1.2}$O$_6$	8 × 10^{-3} (900°C/Re)	0.36 (900°C/Ox)			[281]
SrMn$_{0.5}$Nb$_{0.5}$O$_{3-\delta}$	6 × 10^{-2} (900°C/Re)	1.23 (900°C/Ox)			[282]
Gd$_2$(Ti$_{0.5}$Mo$_{0.5}$)$_2$O$_7$	11 (900°C/Re)				[283]

[a]Re indicates reducing conditions in H$_2$ (e.g., 5%H$_2$/95%Ar or P$_{O_2}$ is $\leq 10^{-20}$) and Ox indicates oxidizing conditions in air.
[b]H$_2$ and CH$_4$ usually indicates moist H$_2$ and CH$_4$ with 3% H$_2$O.

can be reduced by using TiO$_2$ or Al$_2$O$_3$ as cost effective alternatives to YSZ in the anode supported structure [291].

The state-of-the-art anode-supported planar SOFC is based on Ni/YSZ cermet as the support [292–295].

In the last few years, Ni/doped-ceria cermets have been increasingly studied as the supports for the IT-SOFC based on high conductivity electrolyte materials such as doped-ceria [296–298]. Various fabrication techniques have been explored and investigated

in the fabrication of porous anode support substrates. The most common one is probably the tape casting technique.

Tape casting is an established industrial process to make large and flat ceramic tapes, plates and laminated ceramic structure, and thus is suitable for making anode-supported planar solid oxide fuel cell structure. Tape casting involves spreading of ceramic powders and organic ingredients onto a flat surface where solvents are allowed to evaporate. After drying, the resulting tape develops a leather-like consistency and can be stripped off from the casting surface. Typically, tape cast anode layer from 1 to 2 mm thick and tape cast electrolyte layer from 40 to 100 μm thick are produced and these two tapes are laminated and after rolling or calendering, the green laminates are cut to size and sintered at 1400°C in a specially designed kiln furnace to ensure the parts are all flat. The final anode-supported structures are produced with anode thickness of 500–1000 μm and electrolyte thickness of 15–40 μm. Fig. 22 shows typical structure of Ni/YSZ cermet anode-supported thin YSZ electrolyte cell as compared to electrolyte supported cell structure. With tape-calendering process, the YSZ electrolyte thickness can be reduced to 5–10 μm [299–301]. However, shrinkage of anode and YSZ electrolyte materials can be very different [54, 302]. Mismatch in densification of such bilayer structure will cause intolerable bending and/or cracking of the structure during co-firing [291, 303]. Thus, sintering of the laminated anode and electrolyte tapes is critical in producing flat anode-supported structure as the sintering profiles of the anode and electrolyte tapes are very different. Fig. 23 shows the shrinkage profile of Ni/8YSZ cermet tapes and 8YSZ electrolyte tape as function of sintering temperature. Both carbon content and type of 8YSZ powder have significant effect on the shrinkage process of Ni/8YSZ cermet tapes and 8YSZ electrolyte tapes. The bilayer structure based on Ni/YSZ substrates usually tends to warp towards the anode layer during sintering. Alumina is a sintering inhibitor and also has a relatively low thermal expansion coefficient (TEC), which can bring the TEC of the anode substrate close to that of YSZ. Thus, addition of alumina in the Ni/YSZ structure can significantly improve the flatness of the substrate [289]. On the other hand, Müller *et al.* [304] showed that by cofiring screenprinted Ni/YSZ cermet anode and YSZ electrolyte green tape, anode polarization losses were reduced due to the improved contact between the YSZ phase in the cermet and YSZ electrolyte. The mismatch between the anode and YSZ and thus the mechanical stresses in the Ni/YSZ cermet anode layer and YSZ substrate can be reduced by changing the anode coating from a continuous geometry to a large number of small sized individual areas [305]. The best results of the patterned anode layer were observed on the honey-comb design with low curvature and stress. To overcome the sintering profile mismatch, anode substrate tape can also be heated to produce a presintered body strong enough to be handled for electrolyte deposition.

Will *et al.* [306] gave a detailed review on the techniques in the deposition and preparation of thin and dense electrolyte layer on porous anode substrates. This includes vacuum slip casting [307], magnetron sputtering [308], spray and spray pyrolysis [309, 310], screen printing [297], electrophoretic deposition [311–313] and other thin film deposition techniques. For small cells and laboratory investigation purpose, anode-supported structures were often produced by powder compacting and die-pressing [297, 309, 314, 315]. Dense electrolyte film as thin as 8 μm was prepared on porous substrates by dry-pressing process [316]. Yoo *et al.* [317] used compacting and drying of Ni/YSZ slurry to make 50 × 50 mm size anode substrates. Anode-supported cells with diameter of 120 mm were
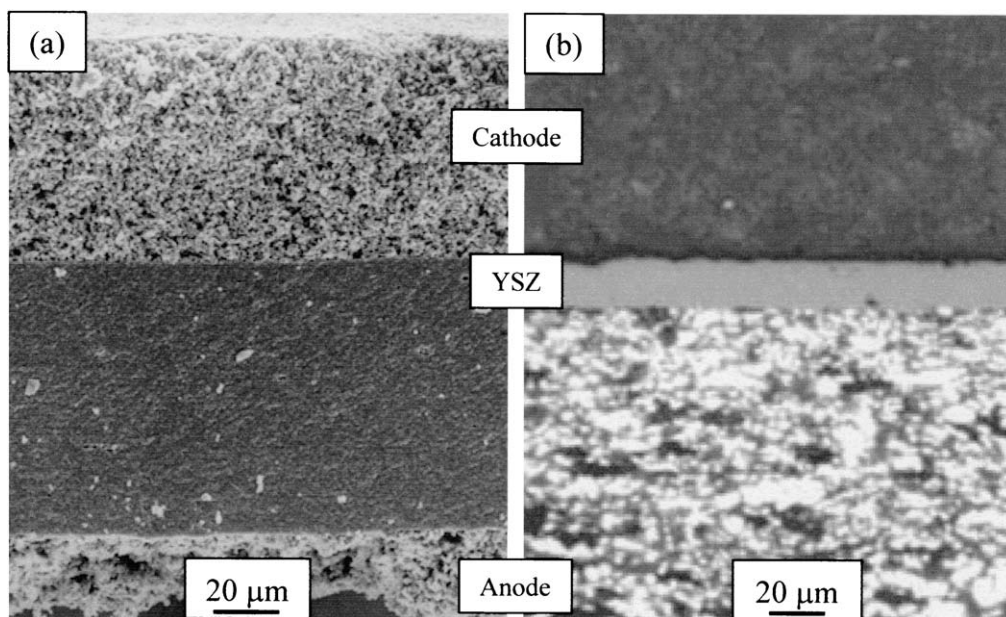
Figure 22 Typical structure of (a) YSZ electrolyte-supported cell and (b) Ni/YSZ cermet anode-supported thin YSZ electrolyte cell prepared by tape casting.
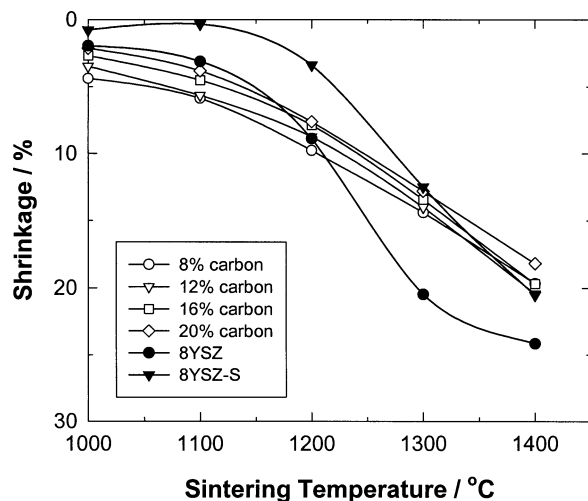
Figure 23 Shrinkage profile of Ni/8YSZ cermet tape with addition of various carbon contents (empty symbols) and 8YSZ tape (filled symbols) as function of sintering temperature.

also sucessfully fabricated by die-pressing technique [318]. Song *et al.* [319] reported the fabrication and performace of anode-supported tubular cell using extrusion technique. Power density in the range of 570 to 800 mW cm^{-2} at 750°C was reported for prototype anode-supported cells based on tape casting technique with Ni/YSZ cermet anode and LSM cathode [293, 307]. Power output as high as 2 W cm^{-2} at 1000°C has been reported on Ni/YSZ anode supported cells [320, 321].

Simwonis *et al.* [322] reported coat-mix (CM) process for the production of porous Ni/YSZ cermet substrates. The powder produced by CM process was characterized by tiny rigid agglomerates and the substrates were prepared by pressing the powder in a die at 120°C. The green plates can be prepared up to the dimensions of 330 × 330 × 2.7 mm. After pre-sintering at 1200°C the porous substrate was coated with a functional layer of Ni and 8YSZ via vacuum slip casting [282]. Electrolyte with thickness of 5–10 μm was deposited by the same technique, followed by sintering at 1400°C. The substrates prepared by CM process were shown to have higher gas permeability, better pore size distribution and pore structure as compared to Ni/8YSZ substrates prepared by tape casting [323]. However, automation of CM process may be of concern. Various pore-former can be added to the anode substrates to improve the porous structure and to improve the cell performance.

Surface morphology of the substrate such as pore size and pore size distribution is critical for the deposition of thin and high dense electrolyte film on the Ni/YSZ anode substrates as the morphology of the deposited film follows that of the substrate surface. Fig. 24 shows the morphology of the YSZ film deposited on YSZ and Ni/YSZ cermet substrate by magnetron sputtering. Thin YSZ film deposited has the same grain and grain boundary pattern as that of the YSZ substrate (Fig. 24a), indicating that the surface morphology of the YSZ thin film follows closely the morphology of the substrate. The large pores on the substrate

surface resulted in open pores on the YSZ electrolyte films deposited (Fig. 24b and c). Thus the pore diameter of the substrate surface needs to be in the order of the grain size of the deposited film to achieve dense and uniform YSZ electrolyte film (Fig. 24d and e). This can be done by using an interlayer or functional layer with finer microstructure and low porosity [282]. The function layer is also used to promote the electrode reaction at the electrode/electrolyte interface. Hobein *et al.* [324] shown that the surface artefacts of the function layer should be smaller than the film thickness in order to avoid the defects on the YSZ film deposited by pulse laser deposition technique. The porous structure of the surface of the function layer can be changed by high temperature annealing [325]. The porosity of both anode substrate and functional layer decreased with increasing annealing temperature and annealing at 1380–1400°C created a dense function layer surface for the deposition of gas-tight YSZ electrolyte film. Kek *et al.* [326] found that the ionic conductivity of deposited YSZ film on Ni/YSZ support varied with the sintering temperature of the anode substrate, but no explaration was given. The structure and stability of the Ni/YSZ cermet substrates are important to the deposition and properties of YSZ thin electrolyte. Cassidy *et al.* [327] studied the effect of the volume change of NiO to Ni in the cermet substrates on the stability of YSZ electrolyte. The initial reduction seems to have a little effect on the stability of YSZ thin electrolyte but the reoxidation of Ni to NiO in the cermet support led to the crack of the YSZ electrolyte.

Preparation and physical properties of Ni/TiO$_2$ cermets were investigated for the anode support for planar SOFC [328]. A thin Ni/YSZ interlayer or function layer was used for the electrochemical reaction at the anode/electrolyte interface. In addition to the cost saving as compared to Ni/YSZ substrates, Ni/TiO$_2$ substrates have thermal expansion coefficient closer to that of YSZ electrolyte and the electrical conductivity is compatible with that of Ni/8YSZ substrates. Softening of the Ni/TiO$_2$ cermet at temperatures above 800°C is also beneficial for the release of stresses introduced during stack manufacturing [329]. Yan *et al.* [330] studied the electrical and microstructural properties of Ni/La$_{0.9}$Sr$_{0.1}$Ga$_{0.8}$Mg$_{0.2}$O$_3$ (Ni/LSGM) anode substrates. The electrical conductivity increased with the Ni content. However, the electrical conductivity appears to be low. For example, the electrical conductivity of Ni (60%)/LSGM (40%) cermet anode was ∼45 S cm^{-1} at 800°C. Among the compositions studied, the substrates with 60% Ni content were considered to have the best microstructure for the deposition of LSGM thin elecrlyte. To avoid the interaction between LSGM and Ni in the substrate, a SDC interlayer with a thickness of 2–5 μm was used. Yan *et al.* [331] also proposed a novel method to prepare Ni/YSZ anode supported LSGM electrolyte thin film cell. In this method, thin LSGM electrolyte film was deposited onto the surface of a porous YSZ substrate, sintered and followed by impregnation of Ni into the porous YSZ substrate to turn it into electrically conducting Ni/YSZ cermet substrate. The
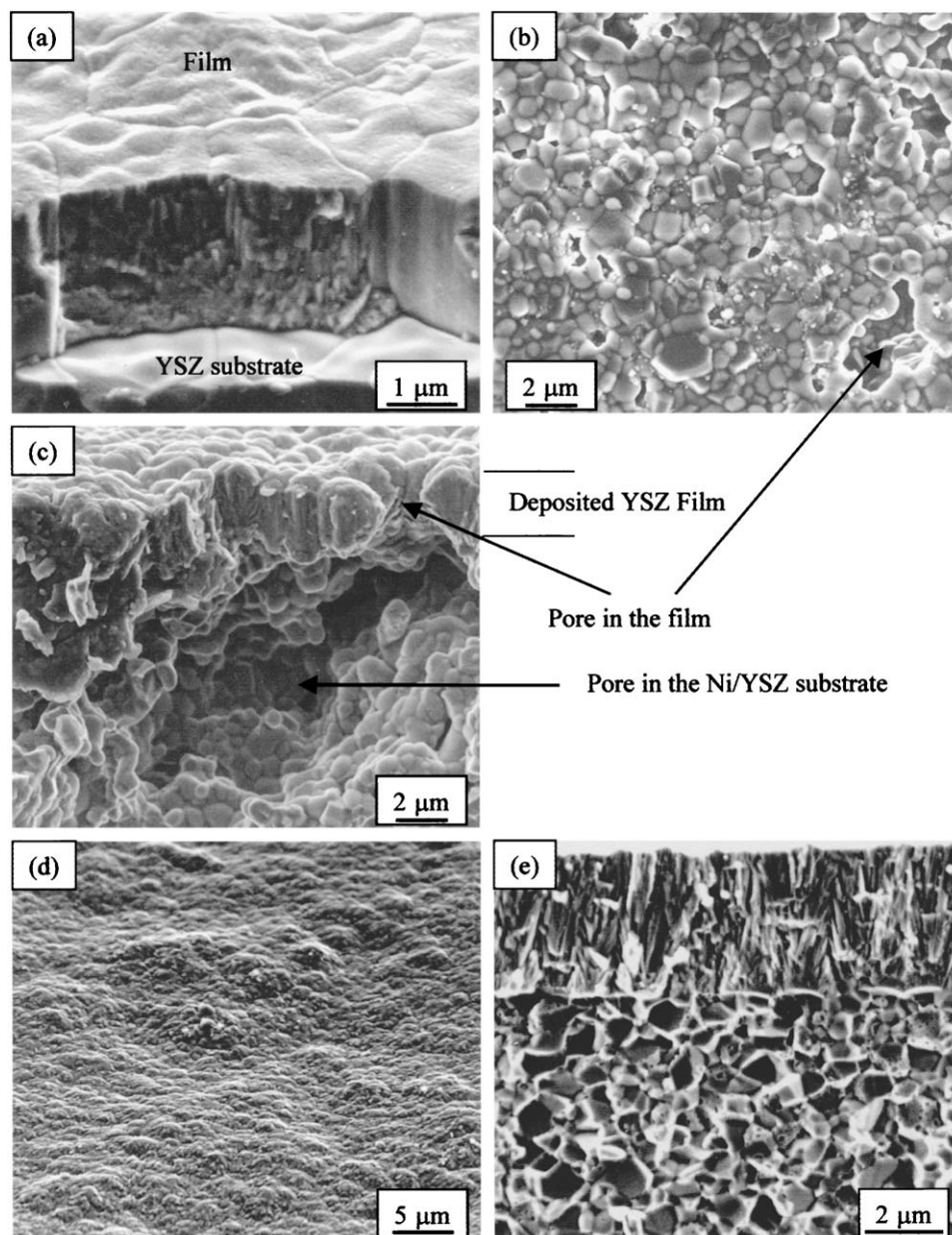
Figure 24 Morphology of the YSZ film deposited on YSZ and Ni/YSZ cermet anode substrate by magnetron sputtering. (a) YSZ film deposited on YSZ substrate, (b) and (c) YSZ film deposited on Ni/YSZ cermet substrate, showing that the defects in the YSZ electrolyte film is due to the large pores on the anode substrate surface, and (d) and (e) dense and uniform YSZ film deposited on Ni/YSZ anode substrate with optimized surface morphology.

maximum power of $0.85\,\mathrm{Wcm^{-2}}$ was achieved at $800°C$ with H_2/air.

Another important property of anode supported electrolyte structure is the structure stability and performance recoverability during reduction-oxidation cycle (or RedOx cycle) either due to accidental system shut-down or system service requirement. Due to the electrochemical and mechanical requirements of the anode supported electrolyte structure, the cell should be able to withstand a significant number (>5/year) of RedOx cycles without significant degradation of the performance [332]. To understand the RedOx behavior of Ni/YSZ cermet materials, Tikekar *et al.* [333] studied the kinetics of reduction and re-oxidation of dense Ni/YSZ cermets at temperature range of 650–800°C. The reduction process is interface controlled, while the re-oxidation kinetics is diffusion controlled.

There was a significant increase in porosity of the re-oxidized sample as compared to the as-sintered sample. The reduction process of NiO in NiO/YSZ cermets is also not a simple one. Mori *et al.* [334] studied the interaction between NiO and YSZ by TPR and identified five different states of NiO species in the NiO/YSZ system. In this respect, porous metallic alloy substrates may be attractive alternatives as electrode-supported structure [335–339]. Different kinds of metallic substrates such as Ni and FeCr alloy were used including felt, foams, nets and porous sintered plates. Ni/YSZ anode, YSZ electrolyte and LSM cathode components were deposited onto porous metallic substrate by a vacuum plasma spray process [335–337] or by conventional ceramic processing techniques such as screen-printing and dip-coating [338, 339]. Cell performance of $280\,\mathrm{mW\,cm^{-2}}$ at 0.7 V and 800°C was achieved in

H$_2$/air with YSZ electrolyte and the power density increased to 430 mW cm^{-2} with the scandia-stabilized zirconia electrolyte [340]. The advantages of metallic substrate-supported cells include low cost, high mechanical strength and the ability in withstanding the rapid thermal cycling.

7. General comments

Ni/YSZ based cermet materials are still the most common anodes in SOFC due to their high electrochemical activity for H$_2$ oxidation reaction and demonstrated long-term stability at SOFC operating conditions. Fabrication and microstructure of the Ni/YSZ cermet materials have been extensively studied and significant understanding and knowledge of the complex inter-relations between the material properties, microstructure, electrochemical process and the fabrication process parameters have been achieved. The electrochemical performance of Ni/YSZ cermet anodes for H$_2$ and CH$_4$ oxidation reactions can be further improved by replacing YSZ with mixed ionic and electronic conductors (MIEC) such as doped ceria or by impregnation or doping of noble metal or MIEC oxide catalyst. Nevertheless, the long-term stability of such modified cermet anodes has not yet been fully demonstrated.

R&D activities in the development of modified Ni-based and/or Ni-free materials for oxidation (or conversion) reactions of hydrocarbon fuels (e.g., methane) in SOFC are increasing significantly since the last decade. However, there are significant discrepancies in the results on the electrical properties and performance of the Ni-based or Ni-free anodes for oxidation reactions of methane under SOFC operation environment, as highlighted recently by Mogensen and Kammer [341]. Steele [40] suggested that anode materials for the electrochemical oxidation of hydrocarbon fuels such as CH$_4$ should have good electronic conductivity of 100 S cm^{-1}, high oxygen surface exchange kinetics, high activity for oxidation of hydrocarbon fuels and stability in reducing environment. From the oxide materials reviewed, there is hardly a material reported so far that satisfies all the requirements for anodes for direct electrochemical oxidation of hydrocarbon fuels. Low electronic conductivity of the anode coatings based on doped ceria, titanate- and chromite-based oxides will pose a serious challenge in the current collector design and probably limit the practical application of the materials as anodes. The low electrical conductivity of ceria-based anodes is partially compensated by using metal paste current collector such as Au [225]. In reality such approach may not be economically and technically viable. In addition to the generally low and, in some cases, unstable conductivity behavior, the overall electrochemical activity of the chromite and titanate based perovskite anodes is poor as compared to that of conventional Ni/YSZ based cermet anodes. The development of Ni-free alternative materials based on various conducting oxides is largely in the laboratory stage and there are significant challenges in the development of effective and stable alternative anodes for the hydrocarbon fuels.

Stability of microstruture and interface at electrode/electrolyte region is an important issue in the development of SOFC technologies. However, stability of individual components in SOFC is not only related to the component itself but also the interfacial reactions between various components of a SOFC stack. For example, in the case of SOFC based on metallic interconnect, the interaction between chromium gaseous species such as CrO$_2$(OH)$_2$ and the cathode materials such as LSM and LSCF can cause significant degradation of the electrocatalytic activities for the O$_2$ reduction reactions on LSM materials [342–344]. As compared to the serious poisoning effect of chromium species on the degradation of the polarization performance on the LSM cathodes, the effect of metallic interconnect on the polarization performance of Ni/YSZ cermet anodes is generally much smaller [345]. Ni/YSZ cermet anodes are also very stable with YSZ electrolyte and there are basically no chemical reactions between Ni and YSZ at the temperature range of the fabrication and fuel cell operation [110]. However, NiO is slightly soluble in YSZ with solubility limit of ~2% NiO in YSZ after heating at 1400°C for 12 h in air [346]. Similar results were also reported for the NiO/YSZ system sintered at 1600°C for 80 h [347]. Linderoth *et al.* [348] investigated the effect of NiO and NiO-to-Ni transformation on the conductivity of YSZ. The presence of NiO reduced the conductivity of 8YSZ by as much as 20% in air. Transformation of NiO to Ni under reducing conditions can cause the cubic to tetragonal phase transformation in YSZ, resulting in further reduction in conductivity. On the other hand, impurities such as Si in the electrode and YSZ electrolyte can have significant effect on the electrode behavior of Ni anodes [349, 350]. Nevertheless, the effect of dissolved Ni in YSZ and impurity segregation at the electrode/electrolyte interface in the case of Ni/YSZ cermet anode on the electrolyte stability, electrode behavior and long-term performance stability is still not clearly understood.

One of the major obstacles in the commercial introduction of SOFC system is the high cost as compared to entrenched power generation technologies. As SOFC stack is the only one component of the SOFC system, the stack cost should only be a fraction of the system cost, which has been targeted to be ~US$400/kW by the US Department of Energy's Solid State Energy Conversion Alliance (SECA) program [351]. Such aggressive cost reduction would preclude the use of expensive or exotic raw materials and complex processing processes for anode and anode substrates. It has been recognized that the fabrication and assembly methods employed in the construction of fuel cell stacks are a significant stack cost element. It is important to select a manufacturing process that is not only cost competitive but also provides a means for stack performance improvement. Reducing the fabrication steps would significantly reduce the production cost. As shown by Rietveld *et al.* [294], tape casting steps for fabrication of anode substrates can be reduced from original three steps to one by adjusting the suspension. Omitting the pre-sintering step for

the anode substrate also improved screenprinting yield from less than 40 to 95% due to the easier handling ability of the tapes. Basu *et al.* [352] shows that by using wet powder spraying instead of vacuum slip casting to deposit the anode function layer, one firing step can be omitted with no effect on the cell performance. Cofiring process is suitable for mass production and to produce anode-supported thin electrolyte cells, reducing material and fabrication cost [353, 354]. However, not all electrode and electrolyte systems are feasible with co-firing processes [353]. On the other hand, the use of low cost metal alloy [335–340] or non-conducting and conventional porous ceramics [355, 356] as cell substrates could reduce the cost and improve the reliability of SOFC stack.

Finally, the studies on the mechanism and kinetics of anodic reactions are primarily concentrated on the H_2 oxidation reaction on Ni/YSZ based cermet anodes and are not covered in this report. However, this does not imply that the reaction processes at the electrode/electrolyte interface are not important. In fact, the fundamental understanding of the electrode processes is critical in the development and optimization of the electrode materials with high performance and long-term stability. Information regarding the mechanism and kinetics of the H_2 oxidation reaction can be found in [17, 25–27, 30, 66, 350, 357–365]. However, in solid oxide fuel cells based on thin electrolyte, study of the reaction and electrode process is hampered by the inability to separate individual electrode polarizations due to the detrimental effect of misalignment and asymmetric interface contact between electrode/electrolyte contact on anode and cathode sides on the reliability and accuracy of the polarization measurement [366–369]. Such inability in polarization separation is probably the main reason for the lack of detailed information on the polarization performance and behavior for fuel oxidation reactions on the anode-supported cells. Separation of anode process in anode-supported cells in most cases is not possible as the measured cathode polarization is almost equal to the total cell polarization in cells with Ni//YSZ cermet substrate anode and LSM cathode [370, 371]. In anode-supported cells, anode electrode area is usually significantly larger than that of the cathode. The usual practice is to normalize the cell performance (power output and current density) to the area of smaller electrode, i.e., cathode in this case. However, as shown by Chung *et al.* [372] recently, such practice could lead to an apparently high power output than symmetric cells. Using a cathode with geometric area significantly less than that of anode can enhance the normalized power density by a factor of two. It was suggested that the Ni/YSZ cermet substrate anodes would be electrochemically superior to screenprinted Ni/YSZ anodes by a factor of two at 800°C [373]. Recently, McIntosh *et al.* [371] reported that electrode impedance could be separable if the characteristic frequencies associated with the anode and cathode processes are significantly different. As the development of ITSOFC based on anode-supported thin electrolyte technology is increasingly important, there is an urgent need to develop ways both numerical and experimental to accurately separate the electrode polarization in order to understand the electrode behavior of anode substrate for the fuel oxidation and/or internal reforming reactions. As the microstructure requirement of thick anode substrates is fundamentally different from that of thin screenprinted anode coating, it is expected that electrode behavior of the thick electrode substrates would be significantly different too [374, 375].

References

1. K. HASSMANN, *Fuel Cells* **1** (2001) 78.
2. N. Q. MINH, *J. Amer. Ceram. Soc.* **76** (1993) 563.
3. H. YOKOKAWA, N. SAKAI, T. HORITA and K. YAMAJI, *Fuel Cells* **1** (2001) 117.
4. H. YOKOKAWA, *Annu. Rev. Mater. Res.* **33** (2003) 581.
5. S. P. S. BADWAL and K. FOGER, *Mater. Forum* **21** (1997) 187.
6. T. KAWADA and H. YOKOKAWA, in "Key Engineering Materials—Electrical Properties of Oxide Materials," edited by J. Nowotny and C. C. Sorrell (Trans Tech Publications, 1997) Vols. 125/126, p. 188.
7. B. C. H. STEELE, *Solid State Ionics* **134** (2000) 3.
8. J. P. P. HUIJSMANS, *Curr. Opin. Solid State Mater. Sci.* **5** (2001) 317.
9. S. P. S. BADWAL, *Solid State Ionics* **143** (2001) 39.
10. L. CARRETTE, K. A. FRIEDRICH and U. STIMMING, *Fuel Cells* **1** (2001) 5.
11. O. YAMAMOTO, *Electrochim. Acta* **45** (2000) 2423.
12. S. C. SINGHAL, *Solid State Ionics* **135** (2001) 305.
13. L. C. DE JONGHE, C. P. JACOBSON and S. J. VISCO, *Annu. Rev. Mater. Res.* **33** (2003) 169.
14. S. C. SINGHAL and K. KENDALL, "High Temperature Solid Oxide Fuel Cells: Fundamental, Design and Applications" (Oxford, UK, Elsevier Ltd. 2003).
15. S. MURAKAMI, Y. AKIYAMA, N. ISHIDA, Y. MIIYAKE, M. NISHIDA, Y. ITOH, T. SAITO and N. FURUKAWA, *Denki Kagaku* **59** (1991) 320.
16. S. P. JIANG, in "Science and Technology of Zirconia V," edited by S. P. S. Badwal, M. J. Bannister and R. H. J. Hannink (Technomic Publishing Company, 1993) p. 819.
17. S. P. JIANG and S. P. S. BADWAL, *J. Electrochem. Soc.* **144** (1997) 3777.
18. J. MIZUSAKI, H. TAGAWA, K. ISOBE, M. TAJIKA, I. KOSHIRO, H. MARUYAMA and K. HIRANO, *ibid.* **141** (1994) 1674.
19. H. UCHIDA, M. YOSHIDA and M. WATANABE, *J. Phys. Chem.* **99** (1995) 3282.
20. M. SUZUKI, H. SASAKI, S. OTOSHI, A. KAJIMURA and M. IPPOMMATSU, *Solid State Ionics* **62** (1993) 125.
21. T. SETOGUCHI, K. OKAMOTO, K. EGUCHI and H. ARAI, *J. Electrochem. Soc.* **139** (1992) 2875.
22. E. IVERS-TIFFÉE, W. WERSING, M. SCHIEBL and H. GREINER, *Ber. Bunsen-Ges. Phys. Chem.* **94** (1990) 978.
23. M. MORI, T. YAMOMOTO, H. ITOH, H. INABA and H. TAGAWA, *J. Electrochem. Soc.* **145** (1998) 1374.
24. T. NORBY, O. J. VELLE, H. LETH-OLSEN and R. TUNOLD, in "SOFC-II," edited by S.C. Singhal and H. Iwahara (Electrochemical Society, Pennington, NJ, 1993) Vol. 93–4, p. 473.
25. J. MIZUSAKI, H. TAGAWA, T. SAITO, T. YAMAMURA, K. KAMITANI, K. HIRANO, S. EHARA, T. TAKAGI, T. HIKITA, M. IPPOMMATSU, S. NAKAGAWA and K. HASHIMOTO, *Solid State Ionics* **70/71** (1994) 52.
26. A. BIEBERLE and L. J. GAUCKLER, *ibid.* **135** (2000) 337.
27. B. DE BOER, M. GONZALEZ, H. J. M. BOUWMEESTER and H. VERWEIJ, *ibid.* **127** (2000) 269.
28. M. MOGENSEN and S. SKAARUP, *ibid.* **86–88** (1996) 1151.
29. S. P. JIANG, *J. Electrochem. Soc.* **148** (2001) A887.
30. P. HOLTAPPELS, I. C. VINKE, L. G. J. DE HAART and U. STIMMING, *ibid.* **146** (1999) 2976.

31. B. C. H. STEELE, *Nature* **400** (2000) 619.
32. A. L. DICKS, *J. Power Sources* **61** (1996) 113.
33. J.-H. KOH, Y.-S. YOO, J.-W. PARK and H. C. LIM, *Solid State Ionics* **149** (2002) 157.
34. P. V. HENDRIKSEN, in "SOFC-V," edited by S. C. Singhal and H. Tagawa (Electrochem. Soc., Pennington, NJ, 1997) Vol. 97–40, p. 1319.
35. W. J. DOLLARD, *J. Power Sources* **37** (1992) 133.
36. P. VERNOUX, J. GUINDET and M. KLEITZ, *J. Electrochem. Soc.* **145** (1998) 3487.
37. P. VERNOUX, M. GUILLODO, J. FOULETIER and A. HAMMOU, *Solid State Ionics* **135** (2000) 425.
38. C. M. CHUN, J. D. MUMFORD and T. RAMANARAYANAN, *J. Electrochem. Soc.* **147** (2000) 3680.
39. K. YASHIRO, K. TAKEDA, T. TAURA, T. OTAKE, A. KAIMAI, Y. NIGARA, T. KAWADA, J. MIZUSAKI and H. YUGAMI, in "SOFC-VIII," edited by S. C. Singhal and M. Dokiya (Electrochem. Soc., Pennington, NJ, 2003) Vol. 2003–07, p. 714.
40. B. C. H. STEELE, *Solid State Ionics* **86–88** (1996) 1223.
41. E. P. MURRAY, T. TSAI and S. A. BARNETT, *Nature* **400** (1999) 649.
42. S. D. PARK, J. M. VOHS and R. J. GORTE, *ibid.* **404** (2000) 265.
43. S. P. JIANG, *Battery Bimonthly* **32** (2002) 133.
44. S. P. JIANG and S. H. CHAN, *Mater. Sci. Tech.*, in press.
45. F. TIETZ, F.J. DIAS, D. SIMWONIS and D. STÖVER, *J. Euro. Ceram. Soc.* **20** (2000) 1023.
46. F. T. CIACCHI, K. M. CRANE and S. P. S. BADWAL, *Solid State Ionics* **73** (1994) 49.
47. T. HIKITA, in "Science and Technology of Zirconia V," edited by S. P. S. Badwal, M. J. Bannister and R. H. J. Hannink (Technomic Publishing Co., Lancaster, PA, 1993) p. 674.
48. S. MURAKAMI, Y. AKIYAMA, N. ISHIDA, T. YASUO, T. SAITO and N. FURUKAWA, in "SOFC-II," edited by F. Grosz, P. Zegers, S. C. Singhal and O. Yamamoto (Commission of The European Communities, Luxembourg, 1991) p. 561.
49. S. P. JIANG, P. J. CALLUS and S. P. S. BADWAL, *Solid State Ionics* **132** (2000) 1.
50. J. VAN HERLE, R. IHRINGER and A. J. MCEVOY, in "SOFC-V," edited by S.C. Singhal and H. Tagawa (Electrochem. Soc., Pennington, NJ, 1997) Vol. 97–40, p. 565.
51. H. ITOH, T. YAMAMOTO, M. MORI, T. HORITA, N. SAKAI, H. YOKOKAWA and M. DOKIYA, *J. Electrochem. Soc.* **144** (1997) 641.
52. S. P. JIANG, *ibid.* **150** (2003) E548.
53. T. KAWADA, N. SAKAI, H. YOKOKAWA, M. DOKIYA, M. MORI and T. IWATA, *ibid.* **137** (1990) 3042.
54. T. MATSUSHIMA, H. OHRUI and T. HIRAI, *Solid State Ionics* **111** (1998) 315.
55. D. D. UPADHYAYA, T. R. G. KUTTY and C. GANGULY, in "Science and Technology of Zirconia V," edited by S. P. S. Badwal, M. J. Bannister and R. H. J. Hannink (Technomic Publishing Co., Lancaster, PA, 1993) p. 310.
56. F. F. LANGE, *J. Amer. Ceram. Soc.* **72** (1989) 3.
57. T. FUKUI, S. OHARA, M. NAITO and K. NOGI, *J. Power Sources* **110** (2002) 91.
58. S. PRIMDAHL, B. F. SØRENSEN and M. MOGENSEN, *J. Amer. Ceram. Soc.* **83** (2000) 489.
59. R. MILLINI and M. F. GAGLIARDI, *J. Mater. Sci.* **29** (1994) 4629.
60. Y. LI, Y. XIE, J. GONG, Y. CHEN and Z. ZHANG, *Mater. Sci. Engng.* B **86** (2001) 119.
61. S. LI, R. GUO, J. LI, Y. CHEN and W. LIU, *Ceram. Intern.* **29** (2003) 883.
62. S. T. ARUNA, M. MUTHURAMAN and K. C. PATIL, *Solid State Ionics* **111** (1998) 45.
63. A. RINGUEDÉ, J. A. LABRINCHA and J. R. FRADE, *ibid.* **141–142** (2001) 549.
64. A. RINGUEDÉ, D. BRONINE and J. R. FRADE, *ibid.* **146** (2002) 219.
65. *Idem.*, *Electrochim. Acta* **48** (2002) 437.
66. S. PRIMDAHL and M. MOGENSEN, *J. Electrochem. Soc.* **144** (1997) 3409.
67. M. MARINSEK, K. ZUPAN and J. MAÈEK, *J. Power Sources* **106** (2002) 178.
68. T. FUKUI, T. OOBUCHI, Y. IKUHARA, S. OHARA and K. KODERA, *J. Amer. Ceram. Soc.* **80** (1997) 261.
69. T. FUKUI, S. OHARA and K. MUKAI, *Electrochem. Solid State Lett.* **1** (1998) 120.
70. X. ZHANG., S. OHARA, R. MARIC, T. FUKUI, H. YOSHIDA, M. NISHIMURA, T. INAGAKI and K. MIURA, *J. Power Sources* **83** (1999) 170.
71. R. MARIC, S. OHARA, T. FUKUI, T. INAGAKI and J. FUJITA, *Electrochem. Solid State Lett.* **1** (1998) 201.
72. C. A.-H. CHUNG, N. J. E. ADKINS and R. M. ORMEROD, in "SOFC-VII," edited by H. Yokokawa and S. C. Singhal (Electrochem. Soc., Pennington, NJ, 2001) Vol. 2001–16, p. 693.
73. F. CHEN and M. LIU, *J. Mater. Chem.* **10** (2000) 2603.
74. V. ESPOSITO, C. D'OTTAVI, S. FERRARI, S. LICOCCIA and E. TRAVERSA, in "SOFC-VIII," edited by S. C. Singhal and M. Dokiya (Electrochem. Soc., Pennington, NJ, 2003) Vol. 2003–07, p. 643.
75. Y. OKAWA, T. MATSUMOTO, T. DOI and Y. HIRATA, *J. Mater. Res.* **17** (2002) 2266.
76. C. XIA and M. LIU, *Solid State Ionics* **152/153** (2002) 423.
77. J. W. MOON, H. L. LEE, J. D. KIM, G. D. KIM, D. A. LEE and H. W. LEE, *Mater. Lett.* **38** (1999) 214.
78. T. FUKUI, K. MURATA, S. OHARA, H. ABE, M. NAITO and K. NOGI, *J. Power Sources* **125** (2004) 17.
79. T. IOROI, Y. UCHIMOTO, Z. OGUMI and Z. TAKEHARA, *J. Electrochem. Soc.* **78** (1995) 593.
80. N. M. SAMMES, M. S. BROWN and R. RATNARAJ, *Mater. Sci. Lett.* **13** (1994) 1124.
81. C. IWASAWA, M. NAGATA and S. YAMAOKA, in "SOFC-IV," edited by M. Dokiya, O. Yamamoto, H. Tagawa and S. C. Singhal (Electrochem. Soc., Pennington, NJ, 1995) Vol. 95–01, p. 686.
82. R. CRACIUM, S. PARK, R. J. GORTE, J. M. VOHS, C. WANG and W. L. WORRELL, *J. Electrochem. Soc.* **146** (1999) 4019.
83. S. PARK, R. CRACIUM, J. M. VOHS and R. J. GORTE, *ibid.* **146** (1999) 3603.
84. D. W. DEES, T. D. CLAAR, T. E. EASLER, D. C. FEE and F. C. MRAZEK, *ibid.* **134** (1987) 2141.
85. H. KOIDE, Y. SOMEYA, T. YOSHIDA and T. MARUYAMA, *Solid State Ionics* **132** (2000) 253.
86. J.-H. LEE, H. MOON, H.-W. LEE, J. KIM, J.-D. KIM and K.-H. YOON, *ibid.* **148** (2002) 15.
87. A. TINTINELLI, C. RIZZO, G. GIUNTA and A. SELVAGGI, in "1st European SOFC Forum," edited by U. Bossel (European Fuel Cells Forum, Lucerne, Switzerland, 1994) p. 455.
88. U. ANSELMI-TAMBURINI, G. CHIODELLI, M. ARIMONDI, F. MAGLIA, G. SPINOLO and Z. A. MUNIR, *Solid State Ionics* **110** (1998) 35.
89. S. F. CORBIN and X. QIAO, *J. Amer. Ceram. Soc.* **86** (2003) 401.
90. U. ANSELMI-TAMBURINI, M. ARIMONDI, F. MAGLIA, G. SPINOLO and Z. A. MUNIR, *ibid.* **81** (1998) 1765.
91. W. HUEBNER, H. U. ANDERSON, D. M. REED, S. R. SEHLIN and X. DENG, in "SOFC-IV," edited by M. Dokiya, O. Yamamoto, H. Tagawa and S. C. Singhal (Electrochem. Soc., Pennington, NJ, 1995) Vol. 95–01, p. 696.
92. H. ITOH, T. WATANABE, D. WADA and K. SUZUKI, in "5th European SOFC Forum," edited by J. Huijsmans (European Fuel Cells Forum, Lucerne, Switzerland, 2002) p. 311.
93. S. P. JIANG, J. G. LOVE and L. APATEANU, *Solid State Ionics* **160** (2003) 15.
94. J.-H. LEE, J.-W. HEO, D.-S. LEE, J. KIM, G.-H. KIM, H.-W. LEE, H. S. SONG and J.-H. MOON, *ibid.* **158** (2003) 225.
95. X. DENG and A. PETRIC, in "SOFC-VIII," edited by S. C. Singhal and M. Dokiya (Electrochem. Soc., Pennington, NJ, 2003) Vol. 2003–07, p. 653.
96. W. HUEBNER, D. M. REED and H. U. ANDERSON, in "SOFC-VI," edited by S. C. Singhal and M. Dokiya (Electrochemical Society, Pennington, NJ, 1999) Vol. 99–19, p. 503.

97. S. K. PRATIHAR, R. N. BASU, S. MAJUMDER and H. S. MAITI, in "SOFC-VI," edited by S. C. Singhal and M. Dokiya (Electrochem. Soc., Pennington, NJ, 1999) Vol. 99–19, p. 513.

98. L. GRAHL-MADSEN, P. H. LARSEN, N. BONANOS, J. ENGELL and S. LINDEROTH, in "5th European SOFC Forum," edited by J. Huijsmans (European Fuel Cells Forum, Lucerne, Switzerland, 2002) p. 82.

99. Y. M. PARK and G. M. CHOI, Solid State Ionics 120 (1999) 265.

100. A. SELCUK and A. ATKINSON, J. Euro. Ceram. Soc. 17 (1997) 1523.

101. A. ATKINSON and A. SELCUK, in "SOFC-V," edited by U. Stimming, S. C. Singhal, H. Tagawa and W. Lehnert (Electrochemical Society, Pennington, NJ, 1997) Vol. 97–40, p. 671.

102. A. SELCUK and A. ATKINSON, J. Amer. Ceram. Soc. 83 (2000) 2029.

103. B. F. SØRENSEN and S. PRIMDAHL, J. Mater. Sci. 33 (1998) 5291.

104. A. SELCUK, G. MERERE and A. ATKINSON, ibid. 36 (2001) 1173.

105. T. IWATA, J. Electrochem. Soc. 143 (1996) 1521.

106. D. SIMWONIS, F. TIETZ and D. STÖVER, Solid State Ionics 132 (2000) 241.

107. H. ITOH, T. YAMOMOTO, M. MORI, T. WATANABE and T. ABE, Denki Kagaku 64 (1996) 549.

108. A. GUBNER, H. LANDES, J. METZGER, H. SEEG and R. STÜBNER, in "SOFC-V," edited by S. C. Singhal and H. Tagawa (Electrochem. Soc., Pennington, NJ, 1997) Vol. 97–40, p. 844.

109. P. NIKOLOPOULOS and D. SOTIROPOULOU, J. Mater. Sci. Lett. 6 (1996) 1429.

110. A. TSOGA, A. NAOMIDIS and P. NIKOLOPOULOS, Acta mater. 44 (1996) 3679.

111. A. NAOUMIDIS, A. TSOGA, P. NIKOPOULOS and H. GRÜBMEIER, in "SOFC-IV," edited by M. Dokiya, O. Yamamoto, H. Tagawa and S. C. Singhal (Electrochem. Soc., Pennington, NJ, 1995) Vol. 95–01, p. 667.

112. S. P. JIANG, J. Mater. Sci. 38 (2003) 3775.

113. R. WILKENBÖNER, TH. KLOIDT and W. MALLÉNER, in "SOFC-V," edited by S. C. Singhal and H. Tagawa (Electrochem. Soc., Pennington, NJ, 1997) Vol. 97–40, p. 851.

114. A. MÜLLER, in "3rd European SOFC Forum," edited by P. Stevens (European Fuel Cell Group, Lucerne, Switzerland, 1998) p. 353.

115. E. IVERS-TIFFÉE, A. WEBER and D. HERBSTRITT, J. Euro. Ceram. Soc. 21 (2001) 1805.

116. A. IOSELEVICH, A. A. KORNYSHEV and W. LEHNERT, J. Electrochem. Soc. 144 (1997) 3010.

117. J. ABEL, A. A. KORNYSHEV and W. LEHNERT, ibid. 144 (1997) 4253.

118. R. VAßEN, D. SIMWONIS and D. STÖVER, J. Mater. Sci. 36 (2001) 147.

119. M. NAGAISHI, K. TAKEUCHI, A. FUKUNAGA, M. EGASHIRA and N. YAMAZOE, J. Ceram. Soc. Japan, Int. Edition 105 (1997) 579.

120. C. VOISARD, U. WEISSEN, E. BATAWI and R. KRUSCHWITZ, in "5th European SOFC Forum," edited by J. Huijsmans (European Fuel Cells Forum, Lucerne, Switzerland, 2002) p. 18.

121. V. ANTONUCCI, E. MODICA, G. MONFORTE, A. S. ARICÒ and P. L. ANTONUCCI, J. Euro. Ceram. Soc. 18 (1998) 113.

122. C. W. TANNER, K. Z. FUNG and A. V. VIRKAR, J. Electrochem. Soc. 144 (1997) 21.

123. S. SUNDE, ibid. 142 (1995) L50.

124. Idem., ibid. 143 (1996) 1123.

125. Idem., ibid. 143 (1996) 1930.

126. P. COSTAMAGNA, P. COSTA and V. ANTONUCCI, Electrochim. Acta 43 (1998) 375.

127. P. COSTAMAGNA, P. COSTA and E. ARATO, ibid. 43 (1998) 967.

128. S. H. CHAN and Z. T. XIA, J. Electrochem. Soc. 148 (2001) A388.

129. A. S. LOSELEVICH and A. A. KORNYSHEV, Fuel Cells 1 (2001) 40.

130. S. H. CHAN, K. A. KHOR and Z. T. XIA, J. Power Sources 93 (2001) 130.

131. M. BROWN, S. PRIMDAHL and M. MOGENSEN, J. Electrochem. Soc. 147 (2000) 475.

132. A. BIEBERLE and L. J. GAUCKLER, Z. Metallkd. 92 (2001) 7.

133. C.-H. LEE, C.-H. LEE, H.-Y. LEE and S. M. OH, Solid State Ionics 98 (1997) 39.

134. S. P. JIANG, Y. Y. DUAN and J. G. LOVE, J. Electrochem. Soc. 149 (2002) A1175.

135. S. P. JIANG, Y. J. LENG, S. H. CHAN and K. A. KHOR, Electrochem. Solid State Lett. 6 (2003) A67.

136. S. P. YOON, J. HAN, S. W. NAM, T.-H. LIM, I.-H. OH, S.-A. HONG, Y.-S. YOO and H. C. LIM, J. Power Sources 106 (2002) 160.

137. S. P. YOON, J. HAN, S. W. NAM, T.-H. LIM, I.-H. OH, S.-A. HONG and Y.-S. YOO, in "5th European SOFC Forum," edited by J. Huijsmans (European Fuel Cell Group, Lucerne, Switzerland, 2002) p. 148.

138. K. C. CHOU, S. YUAN and U. PAL, in "SOFC-III," edited by S. C. Singhal and H. Iwahara (Electrochem. Soc., Pennington, NJ, 1993) p. 431.

139. W. SCHÄFER, A. KOCH, U. HEROLD-SCHMIDT and D. STOLTEN, Solid State Ionics 86–88 (1996) 1235.

140. H. UCHIDA, H. SUZUKI and M. WATANABE, J. Electrochem. Soc. 145 (1998) 615.

141. M. CASSIDY and G. LINDSAY, in "1st European SOFC Forum," edited by U. Bossel (European Fuel Cell Group, Lucerne, Switzerland, 1994) p. 205.

142. A. C. MÜLLER, D. HERBSTRITT and E. IVERS-TIFFÉE, Solid State Ionics 152/153 (2002) 537.

143. U. B. PAL and S. C. SINGHAL, J. Electrochem. Soc. 137 (1990) 2937.

144. L. S. WANG and S. A. BARNETT, Solid State Ionics 61 (1993) 273.

145. Z. OGUMI, T. IOROI, Y. UCHIMOTO, Z. TAKEHARA, T. OGAWA and K. TOYAMA, J. Amer. Ceram. Soc. 78 (1995) 593.

146. E. Z. TANG, T. H. ETSELL and D. G. IVEY, ibid. 83 (2000) 1626.

147. J. L. YOUNG and T. H. ETSELL, Solid State Ionics 135 (2000) 457.

148. X. WANG, N. NAKAGAWA and K. KATO, J. Electrochem. Soc. 148 (2001) A565.

149. S. P. JIANG and Y. RAMPRAKASH, Solid State Ionics 122 (1999) 211.

150. P. HOLTAPPELS, L. G. DE HAART, U. STIMMING, I. C. VINKE and M. MOGENSEN, J. Appl. Electrochem. 29 (1999) 561.

151. T. KAWADA, I. ANZAI, N. SAKAI, H. YOKOKAWA and M. DOKIYA, in Proc. of Sym. On High Temperature Electrode Materials and Characterization, edited by D. Macdonald and A. C. Khandkar (Electrochem. Soc., Pennington, NJ, 1991) Vol. 91–6, p. 165.

152. A. L. LEE, R. F. ZABRANSKY and W. J. HUBER, Ind. Eng. Chem. Res. 29 (1990) 766.

153. K. AHMED, P. SESHADRI, Y. RAMPRAKASH, S. P. JIANG and K. FOGER, in "SOFC-V," edited by S. C. Singhal and H. Tagawa (Electrochem. Soc., Pennington, NJ, 1997) Vol. 97–40, p. 228.

154. K. AHMED and K. FOGER, Catalysis Today 63 (2000) 479.

155. E. ACHENBACH and E. RIENSCHE, J. Power Sources 52 (1994) 283.

156. R. ODEGAARD, E. JOHNSEN and H. KAROLIUSSEN, in "SOFC-IV," edited by M. Dokiya, O. Yamamoto, H. Tagawa and S. C. Singhal (Electrochem. Soc., Pennington, NJ, 1995) Vol. 95–01, p. 810.

157. V. D. BELYAEV, T. I. POLITOVA, O. A. MARINA and V. A. SOBYANIN, Appl. Catal. A 133 (1995) 47.

158. A. L. DICKS, K. D. POINTON and A. SWANN, in "3rd European SOFC Forum," edited by P. Stevens (European Fuel Cell Group, Lucerne, Switzerland, 1998) p. 249.

159. C. M. FINNERTY, N. J. COE, R. H. CUNNINGHAM and R. M. ORMEROD, Catalysis Today 46 (1998) 137.

160. I. DRESCHER, W. LEHNERT and J. MEUSINGER, *Electrochim. Acta* **43** (1998) 3059.

161. C. PEREGO, L. ZANIBELLI, M. CARTRULLO and G. PIRO, in "SOFC-III," edited by S. C. Singhal and H. Iwahara (Electrochem. Soc., Pennington, NJ, 1993) p. 454.

162. T. SHIRAKAWA, S. MATSUDA and A. FUKUSHIMA, in "SOFC-III," edited by S. C. Singhal and H. Iwahara (Electrochem. Soc., Pennington, NJ, 1993) p. 464.

163. A. WEBER, B. SAUER, A. C. MÜLLER, D. HERBSTRITT and E. IVERS-TIFFÉE, *Solid State Ionics* **152/153** (2002) 543.

164. T. AIDA, A. ABUDULA, M. IHARA, H. KOMIYAMA and K. YAMADA, in "SOFC-IV," edited by M. Dokiya, O. Yamamoto, H. Tagawa and S. C. Singhal (Electrochem. Soc., Pennington, NJ, 1995) Vol. 95–01, p. 801.

165. A. ABUDULA, M. IHARA, H. KOMIYAMA and K. YAMADA, *Solid State Ionics* **86–88** (1996) 1203.

166. M. IHARA, C. YOKOYAMA, A. ABUDULA, R. KATO, H. KOMIYAMA and K. YAMADA, *J. Electrochem. Soc.* **146** (1999) 2481.

167. J. LIU and S. A. BARNETT, *Solid State Ionics* **158** (2003) 11.

168. T. TAKEGUCHI, Y. KANI, T. YANO, R. KIKUCHI, K. EGUCHI, K. TSUJIMOTO, Y. UCHIDA, A. UENO, K. OMOSHIKI and M. AIZAWA, *ibid.* **112** (2002) 588.

169. T. TAKEGUCHI, T. YANO, Y. KANI, R. KIKUCHI and K. EGUCHI, in "SOFC-VIII," edited by S. C. Singhal and M. Dokiya (Electrochem. Soc., Pennington, NJ, 2003) Vol. 2003–07, p. 704.

170. T. TAKEGUCHI, R. KIKUCHI, T. YANO, K. EGUCHI and K. MURATA, *Catalysis Today* **84** (2003) 217.

171. S. ONUMA, A. KAIMAI, K. KAWAMURA, Y. NIGAWA, T. KAWADA, J. MIZUSAKI, H. INABA and H. TAGAWA, *J. Electrochem. Soc.* **145** (1998) 920.

172. T. HORITA, N. SAKAI, T. KAWADA, H. YOKOKAWA and M. DOKIYA, *ibid.* **143** (1996) 1161.

173. K. SATO, Y. OHMINE, K. OGASA and S. TSUJI, in "SOFC-VIII," edited by S. C. Singhal and M. Dokiya (Electrochem. Soc., Pennington, NJ, 2003) Vol. 2003–07, p. 695.

174. A. RINGUEDÉ, D. P. FAGG and J. R. FRADE, *J. Euro. Ceram. Soc.* **24** (2004) 1355.

175. H. KIM, C. LU, W. L. WORRELL, J. M. VOHS and R. J. GORTE, *J. Electrochem. Soc.* **149** (2002) A247.

176. H. KIM, C. DA ROSA, M. BOARO, J. M. VOHS and R. J. GORTE, *J. Amer. Ceram. Ceram.* **85** (2002) 1473.

177. A. SIN, A. TAVARES, Y. DOUBITSKY, A. ZAOPO, A. S. ARICÒ, L. R. GULLO, D. LA ROSA, S. SIRACUSANO and V. ANTONUCCI, in "SOFC-VIII," edited by S. C. Singhal and M. Dokiya (Electrochem. Soc., Pennington, NJ, 2003) Vol. 2003–07, p. 745.

178. K. KAMMER and M. MOGENSEN, in "SOFC-VIII," edited by S. C. Singhal and M. Dokiya (Electrochem. Soc., Pennington, NJ, 2003) Vol. 2003–07, p. 781.

179. J. GEYER, H. KOHLMULLER, H. LANDES and R. STUBNER, in "SOFC-V," edited by U. Stimming, S. C. Singhal, H. Tagawa and W. Lehnert (Electrochem. Soc., Pennington, NJ, 1997) Vol. 97–40, p. 585.

180. Y. MATSUZAKI and I. YASUDA, *Solid State Ioincs* **132** (2000) 261.

181. D. STOLFEN, R. SPAH and R. SCHAMM, in "SOFV-V," edited by S. C. Singhal and H. Tagawa (Electrochem. Soc., Pennington, NJ, 1997) Vol. 97–40, p. 88.

182. P. PRIMDAHL, in "SOFC-VI," edited by S. C. Singhal and M. Dokiya (Electrochem. Soc., Pennington, NJ, 1999) Vol. 99–19, p. 530.

183. K. EGUCHI, T. SETOGUCHI, K. OKAMOTO and H. ARAI, in Proc. of the International Fuel Cell Conf. (Makihari, Japan, 1992) p. 373.

184. S. Z. WANG and I. TATSUMI, *Acta Physico-Chimica Sinica* **19** (2003) 844.

185. M. B. JOERGER and L. J. GAUCKLER, in "SOFC-VII," edited by H. Yokokawa and S. C. Singhal (Electrochem. Soc., Pennington, NJ, 2001) Vol. 2001–16, p. 662.

186. C.-J. WEN, T. MASUYAMA, T. YOSHIKAWA, J. OTOMO. H. TAKAHASHI, K. EGUCHI and K. YAMADA, in "SOFC-VII," edited by H. Yokokawa and S. C. Singhal (Electrochem. Soc., Pennington, NJ, 2001) Vol. 2001–16, p. 671.

187. T. INAGAKI, H. YOSHIDA, K. MIURA, S. OHARA, R. MARIC, X. ZHANG, K. MUKAI and T. FUKUI, in "SOFC-VII," edited by H. Yokokawa and S. C. Singhal (Electrochem. Soc., Pennington, NJ, 2001) Vol. 2001–16, p. 963.

188. E. P. MURRAY, S. J. HARRIS and H. JEN, *J. Electrochem. Soc.* **149** (2002) A1127.

189. B. RÖSCH, H. TU, A. O. STÖRMER, A. C. MÜLLER and U. STIMMING, in "SOFC-VIII," edited by S. C. Singhal and M. Dokiya (Electrochem. Soc., Pennington, NJ, 2003) Vol. 2003–07, p. 737.

190. T. HIBINO, A. HASHIMOTO, K. ASANO, M. YANO, M. SUZUKI and M. SANO, *Electrochem. Solid-State Lett.* **5** (2002) A242.

191. T. HIBINO, A. HASHIMOTO, M. YANO, M. SUZUKI, S.-I. YOSHIDA and M. SANO, *J. Electrochem. Soc.* **149** (2002) A133.

192. C. XIA, F. CHEN and M. LIU, *Electrochem. Solid-State Lett.* **4** (2001) A52.

193. A. TSOGA, A. GUPTA, A. NAOUMIDIS, D. SKARMOUTSOS and P. NIKOLOPOULOS, *Ionics* **4** (1999) 234.

194. A. TSOGA, A. NAOUMIDIS, A. GUPTA and D. STÖVER, *Mater. Sci. Forum* **308–311** (1999) 234.

195. A. TSOGA, A. GUPTA, A. NAOUMIDIS and P. NIKOLOPOULOS, *Acta Mater.* **48** (2000) 4709.

196. H. UCHIDA, S. ARISAKA and M. WATANABE, *Electrochem. Solid-State Lett.* **2** (1999) 428.

197. S. OHARA, R. MARIC, X. ZHANG, K. MUKAI, T. FUKUI, H. YOSHIDA, T. INAGAKI and K. MIURA, *J. Power Sources* **86** (2000) 455.

198. K. KURODA, I. HASHIMOTO, K. ADACHI, J. AKIKUSA, Y. TAMOU, N. KOMADA, T. ISHIHARA and Y. TAKITA, *Solid State Ionics* **132** (2000) 199.

199. K. HUANG, J.-H. WAN and J. B. GOODENOUGH, *J. Electrochem. Soc.* **148** (2001) A788.

200. K. HUANG, R. TICHY, J. B. GOODENOUGH and C. MILLIKEN, *J. Amer. Ceram. Soc.* **81** (1998) 2581.

201. S. M. CHOI, K. T. LEE, S. KIM, M. C. CHUN and H. L. LEE, *Solid State Ionics* **131** (2000) 221.

202. X. ZHANG, S. OHARA, H. OKAWA, R. MARIC and T. FUKUI, *ibid.* **139** (2001) 145.

203. M. MORI, Y. HIER, H. ITOH, G. A. TOMPSETT and N. M. SAMMES, *ibid.* **160** (2003) 1.

204. K. KOBAYASHI, Y. KAI, S. YAMAGUCHI, N. FUKATSU, T. KAWASHIMA and Y. IGUCHI, *ibid.* **93** (1997) 193.

205. K. E. SWIDER and W. L. WORRELL, *J. Electrochem. Soc.* **143** (1996) 3706.

206. S. D. PARK, H. KIM, S. MCINTOSH, W. WORRELL, R. J. GORTE and J. M. VOHS, in "SOFC-VII," edited by H. Yokokawa and S. C. Singhal (Electrochem. Soc., Pennington, NJ, 2001) Vol. 2001–16, p. 712.

207. S. PARK, R. J. GORTE and J. M. VOHS, *J. Electrochem. Soc.* **148** (2001) A443.

208. R. J. GORTE, H. KIM and J. M. VOHS, *J. Power Sources* **106** (2002) 10.

209. I. ALSTRUP, M. T. TAVARES, C. A. BERNARDO, O. SØRENSEN and J. R. ROSTRUP-NIELSEN, *Mat. And Corr.* **49** (1998) 367.

210. C. LU, W. L. WORRELL, J. M. VOHS and R. J. GORTE, in "SOFC-VIII," edited by S. C. Singhal and M. Dokiya (Electrochem. Soc., Pennington, NJ, 2003) Vol. 2003–07, p. 773.

211. S. MCINTOSH, J. M. VOHS and R. J. GORTE, *J. Electrochem. Soc.* **150** (2003) A470.

212. *Idem.*, *Electrochim. Acta* **47** (2002) 3815.

213. R. J. GORTE, S. PARK, J. M. VOHS and C. WANG, *Adv. Mater.* **12** (2000) 1465.

214. H. SASAKI, H. SUZUKI, S. OTOSHI, A. KAJIMU and M. IPPOMMATSU, *J. Electrochem. Soc.* **139** (1992) L12.

215. P. VERNOUX, J. GUINDET, E. GEHAIN and M. KLEITZ, in "SOFC-V," edited by U. Stimming, S. C. Singhal,

H. Tagawa and W. Lehnert (Electrochem. Soc., Pennington, NJ, 1997) Vol. 97–40, p. 219.

216. K. EGUCHI, *J. Alloys Comp.* **250** (1997) 486.

217. G. B. BALAZS and R. S. GLASS, *Solid State Ionics* **76** (1995) 155.

218. B. C. H. STEELE, *ibid.* **129** (2000) 95.

219. M. MOGENSEN, N. M. SAMMES and G. A. TOMPSETT, *ibid.* **129** (2000) 63.

220. B. C. H. STEELE, P. H. MIDDLETON and R. RUDKIN, *ibid.* **40/41** (1990) 388.

221. I. S. METCALFE, *ibid.* **57** (1992) 259.

222. N. V. SKORODUMOVA, S. I. SIMAK, B. I. LUNDQVIST, I. A. ABRIKOSOV and B. JOHANSSON, *Phys. Rev. Lett.* **89** (2002) 6601.

223. M. MOGENSEN, in "SOFC-II," edited by F. Gross, P. Zegers, S. C. Singhal and O. Yamamoto (Commission of the European Communities, Brussels, 1991) p. 577.

224. M. MOGENSEN, T. LINDEGAARD, U. R. HANSEN and G. MOGENSEN, *J. Electrochem. Soc.* **141** (1994) 2122.

225. O. A. MARINA, C. BAGGER, S. PRIMDAHL and M. MOGENSEN, *Solid State Ionics* **123** (1999) 199.

226. A. O. STÖRMER, P. HOLTAPPELS, H. TU and U. STIMMING, in "5th European SOFC Forum," edited by J. Huijsmans (European Fuel Cell Group, Lucerne, Switzerland, 2002) p. 343.

227. H. UCHIDA, H. SUZUKI and M. WATANABE, *J. Electrochem. Soc.* **146** (1999) 1667.

228. H. UCHIDA, M. SUGIMOTO and M. WATANABE, in "SOFC-VII," edited by H. Yokokawa and S. C. Singhal (Electrochem. Soc., Pennington, NJ, 2001) Vol. 2001–16, p. 653.

229. E. S. PUTNA, J. STUBENRAUCH, J. M. VOHS and R. J. GORTE, *Langmuir* **11** (1995) 4832.

230. H. UCHIDA, S. SUZUKI and M. WATANABE, in "SOFC-VIII," edited by S. C. Singhal and M. Dokiya (Electrochem. Soc., Pennington, NJ, 2003) Vol. 2003–07, p. 728.

231. S. PRIMDAHL and Y. L. LIU, *J. Electrochem. Soc.* **149** (2002) A1466.

232. S. PRIMDAHL and M. MOGENSEN, *Solid State Ionics* **152/153** (2002) 597.

233. T. HORITA, N. SAKAI, H. YOKOKAWA, M. DOKIYA and T. KAWADA, *ibid.* **86–88** (1996) 1259.

234. D. P. SUTIJA, T. NORBY, PER A. OSBORG and PER KOFSTAD, in "SOFC-III," edited by S. C. Singhal and H. Iwahara (Electrochem. Soc., Pennington, NJ, 1993) Vol. 93–04, p. 552.

235. A. HOLT, E. AHLGREN and F. W. POULSEN, in "SOFC-III," edited by S. C. Singhal and H. Iwahara (Electrochem. Soc., Pennington, NJ, 1993) Vol. 93–04, p. 562.

236. O. A. MARINA, N. L. CANFIELD and J. W. STEVENSON, *Solid State Ionics* **149** (2002) 21.

237. O. A. MARINA and L. R. PEDERSON, in "5th European SOFC Forum," edited by J. Huijsmans (European SOFC Forum, Switzerland, 2002) p. 481.

238. W. L. WORRELL, *Solid State Ionics* **52** (1992) 147.

239. M. T. COLOMER, J. R. JURADO, R. M. C. MARQUES and F. M. B. MARQUES, in Proc. of 2nd Intern. Sym. on Ionic and Mixed Conducting Ceramics (Electrochem. Soc., Pennington, NJ 1994) Vol. 94–12, p. 369.

240. H. NAITO and H. ARASHI, *Solid State Ionics* **53–56** (1992) 436.

241. P. HAN and W. L. WORRELL, in Proc. of 2nd Intern. Sym. on Ionic and Mixed Conducting Ceramics (Electrochem. Soc., Pennington, NJ, 1994) Vol. 94–12, p. 317.

242. S. TAO and J. T. S. IRVINE, *J. Solid State Chem.* **165** (2002) 12–18.

243. A. J. FEIGHERY, J. T. S. IRVINE, D. P. FAGG and A. KAISER, *ibid.* **143** (1999) 273.

244. M. K. DONGARE, A. M. DONGARE, V. B. TARE and E. KEMNITZ, *Solid State Ionics* **152/153** (2002) 455.

245. P. H. MIDDLETON, H. J. STEINER, G. M. CHRISTIE, R. BAKER, I. S. METCALFE and B. C. H. STEELE, in "SOFC-III," edited by S. C. Singhal and H. Iwahara (Electrochem. Soc., Pennington, NJ, 1993) Vol. 93–04, p. 542.

246. D. P. FAGG, S. M. FRAY and J. T. S. IRVINE, *Solid State Ionics* **72** (1994) 235.

247. P. R. SLATER, D. P. FAGG and J. T. S. IRVINE, *J. Mater. Chem.* **7** (1997) 2495.

248. P. R. SLATER and J. T. S. IRVINE, *Solid State Ionics* **120** (1999) 125.

249. J. CANALES-VÁZQUEZ, S. W. TAO and J. T. S. IRVINE, *ibid.* **159** (2003) 159.

250. K. YASHIRO, T. KOBAYASHI, L. Q. HAN, A. KAIMAI, Y. NIGARA, T. KAWADA, J. MIZUSAKI and K. KAWAMURA, in "SOFC-VII," edited by H. Yokokawa and S. C. Singhal (Electrochem. Soc., Pennington, NJ, 2001) Vol. 2001–16, p. 678.

251. R. MOOS, S. SCHÖLLHAMMER and K. H. HÄRDTL, *Appl. Phys.* A **65** (1997) 291.

252. S. HUI and A. PETRIC, *J. Euro. Ceram. Soc.* **22** (2002) 1673.

253. *Idem.*, *J. Electrochem. Soc.* **149** (2002) J1.

254. H. YOKOKAWA, N. SAKAI, T. KAWADA and M. DOKIYA, *Solid State Ionics* **52** (1992) 43.

255. N. SAKAI, K. YAMAJI, T. HORITA, H. YOKOKAWA, T. KAWADA and M. DOKIYA, *J. Electrochem. Soc.* **147** (2000) 3178.

256. M. MORI and Y. HIER, *J. Amer. Ceram. Soc.* **84** (2001) 2573.

257. S. TANASESCU, D. BERGER, D. NEINER and N. D. TOTIR, *Solid State Ionics* **157** (2003) 365.

258. J. VULLIET, B. MOREL, J. LAURENCIN, G. GAUTHIER, L. BIANCHI, S. GIRAUD, J.-Y. HENRY and F. LEFEBVRE-JOUD, in "SOFC-VIII," edited by S. C. Singhal and M. Dokiya (Electrochem. Soc., Pennington, NJ, 2003) Vol. 2003–07, p. 803.

259. J. SFEIR, J. VAN HERLE and A. J. MCEVOY, *J. Euro. Ceram. Soc.* **19** (1999) 897.

260. J. SFEIR, P. A. BUFFAT, P. MÖCKLI, N. XANTHOPOULOS, R. VASQUEZ, H. J. MATHIEU, J. VAN HERLE and K. R. THAMPI, *J. Catal.* **202** (2001) 229.

261. J. SFEIR, *J. Power Sources* **118** (2003) 276.

262. S. TAO and J. T. S. IRVINE, in "SOFC-VIII," edited by S. C. Singhal and M. Dokiya (Electrochem. Soc., Pennington, NJ, 2003) Vol. 2003–07, p. 793.

263. J. SFEIR, J. VAN HERLE and R. VASQUEZ, in "5th European SOFC Forum," edited by J. Huijsmans (European SOFC Forum, Switzerland, 2002) p. 570.

264. A. L. SAUVET and J. T. S. IRVINE, in "5th European SOFC Forum," edited by J. Huijsmans (European SOFC Forum, Switzerland, 2002) p. 490.

265. J. LIU, B. D. MADSEN, Z. JI and S. A. BARNETT, *Electrochem. Solid-State Lett.* **5** (2002) A122.

266. S. PRIMDAHL, J. R. HANSEN, L. GRAHL-MADSEN and P. H. LARSEN, *J. Electrochem. Soc.* **148** (2001) A74.

267. N. GUNASEKARAN, N. BAKSHI, C. B. ALCOCK and J. J. CARBERRY, *Solid State Ionics* **83** (1996) 145.

268. P. VERNOUX, J. GUINDET, E. GEHAIN and M. KLEITZ, in "SOFC-VI," edited by S. C. Singhal and M. Dokiya (Electrochem. Soc., Pennington, NJ, 1999) Vol. 99–19, p. 219.

269. J. SFEIR, J. VAN HERLE and A. J. MCEVOY, in "3rd European SOFC Forum," edited by P. Stevens (European SOFC Forum, Switzerland, 1998) p. 267.

270. G. PUDMICH, B. A. BOUKAMP, M. GONZALEZ-CUENCA, W. JUNGEN, W. ZIPPRICH and F. TIETZ, *Solid State Ionics* **135** (2000) 433.

271. P. VERNOUX, E. DIJURADO and M. GUILLODO, *J. Amer. Ceram. Soc.* **84** (2001) 2289.

272. A.-L. SAUVET and J. FOULETIER, *J. Power Sources* **101** (2001) 259.

273. A.-L. SAUVET, J. FOULETIER, F. GAILLARD and M. PRIMET, *J. Catal.* **209** (2002) 25.

274. S. TAO and J. T. S. IRVINE, *Nature Mater.* **2** (2003) 320.

275. S. WANG, Y. JIANG, Y. ZHANG, W. LI, J. YAN and Z. LU, *Solid State Ionics* **120** (1999) 75.

276. A. HARTLEY, M. SAHIBZADA, M. WESTON, I. S. METCALFE and D. MANTZAVINOS, *Catalysis Today* **55** (2000) 197.

277. S. P. JIANG, *Solid State Ionics* **146** (2002) 1.

278. E. D. WACHSMAN and T. L. CLITES, in "Ionic and Mixed Conducting Ceramics IV," edited by T. A. Ramanarayanan, W. L. Worrell and M. Mogensen (Electrochem. Soc., Pennington, NJ, 2001) Vol. 2001–28, p. 306.

279. T. D. MCCOLM and J. T. S. IRVINE, *Solid State Ionics* **152/153** (2002) 615.

280. P. R. SLATE and J. T. S. IRVINE, *ibid.* **124** (1999) 61.

281. S. TAO and J. T. S. IRVINE, *ibid.* **154/155** (2002) 659.

282. *Idem.*, *J. Mater. Chem.* **12** (2002) 2356.

283. O. PORAT, C. HEREMANS and H. L. TULLER, *Solid State Ionics* **94** (1997) 75.

284. A. MITTERDORFER and L. J. GAUCKLER, *ibid.* **111** (1998) 185.

285. J.-P. ZHANG, S. P. JIANG, J. G. LOVE, K. FOGER and S. P. S. BADWAL, *J. Mater. Chem.* **8** (1998) 2787.

286. S. P. JIANG, Z.-P. ZHANG and K. FOGER, *J. Euro. Ceram. Soc.* **23** (2003) 1865.

287. T. ISHIHARA, K. SHIMOSE, T. KUDO, H. NISHIGUCHI, T. AKBAY and Y. TAKITA, *J. Amer. Ceram. Soc.* **83** (2000) 1921.

288. C. C. WHITE and B. P. MARETT, "Restriction on Planar Solid Oxide Fuel Cell Design," BHP Research Report BHPR/PDR/R/92/023/KH21 (Melbourne, Australia, 1992).

289. S. P. SIMNER, J. W. STEVENSON, K. D. MEINHARDT and N. L. CANFIELD, in "SOFC-VII," edited by H. Yokokawa and S. C. Singhal (Electrochem. Soc., Pennington, NJ, 2001) Vol. 2001–16, p. 1051.

290. S. PRIMDAHL, M. J. JØRGESEN, C. BAGGER and B. KINDL, in "SOFC-VI," edited by S. C. Singhal and M. Dokiya (Electrochem. Soc., Pennington, NJ, 1999) Vol. 99–19, p. 793.

291. R. VABEN, R. W. STEINBRECH, F. TIETZ and D. STÖVER, in "3rd European SOFC Forum," edited by P. Stevens (European Fuel Cell Group, Lucerne, Switzerland, 1998) p. 557.

292. H. P. BUCHKREMER, U. DIEKMANN, L. G. J. DE HAART, H. KABS, U. STIMMING and D. STÖVER, in "SOFC-V," edited by U. Stimming, S. C. Singhal, H. Tagawa and W. Lehnert (Electrochem. Soc., Pennington, NJ, 1997) Vol. 97–40, p. 160.

293. R. DONELSON, S. AMARASINGHE, D. GOBLE, D. HICKEY, S. P. JIANG, J. LOVE and T. QUACH, in "3rd European Solid Oxide Fuel Cells Forum," edited by P. Stevens (European Fuel Cell Group, Lucerne, Switzerland, 1998) p. 151.

294. G. RIETVELD, P. NAMMENSMA and J. P. OUWELTJES, in "SOFC-VII," edited by H. Yokokawa and S. C. Singhal (Electrochem. Soc., Pennington, NJ, 2001) Vol. 2001–16, p. 125.

295. E. TANG, F. MARTELL, R. BRULÈ, K. MARCOTTE and B. BORGLUM, in "SOFC-VIII," edited by S. C. Singhal and M. Dokiya (Electrochem. Soc., Pennington, NJ, 2003) Vol. 2003–07, p. 935.

296. R. DOSHI, V. L. RICHARDS, J. D. CARTER, X. WANG and M. KRUMPELT, *J. Electrochem. Soc.* **146** (1999) 1273.

297. C. R. XIA and M. LIU, *J. Amer. Ceram. Soc.* **84** (2001) 1903.

298. Y. J. LENG, S. H. CHAN, S. P. JIANG and K. A. KHOR, *Solid State Ionics*, in press.

299. N. Q. MINH, T. R. ARMSTRONG, J. R. ESOPA, J. V. GUIHEEN, C. R. HOME, F. S. LIU, T. L. STILLWAGON and J. J. VAN ACKEREN, in "SOFC-II," edited by F. Gross, P. Zegers, S. C. Singhal and O. Yamamoto (Commission of the European Communities, 1991) p. 93.

300. N. Q. MINH, in "SOFC-IV," edited by S. C. Singhal and M. Dokiya (Electrochem. Soc., Pennington, NJ, 1995) Vol. 95–01, p. 138.

301. N. Q. MINH and K. MONTGOMERY, in "SOFC-V," edited by U. Stimming, S. C. Singhal, H. Tagawa and W. Lehnert (Electrochem. Soc., Pennington, NJ, 1997) Vol. 97–40, p. 153.

302. A. C. MÜLLER, A. KRÜGEL and E. IVERS-TIFFÉE, *Mater. Sci. Tech.* **33** (2002) 343.

303. J.-H. JEAN and C.-R. CHANG, *J. Amer. Ceram. Soc.* **80** (1997) 2401.

304. A. C. MÜLLER, D. HERBSTRITT, A. WEBER and E. IVERS-TIFFÉE, in "4th European SOFC Forum," edited by A. J. McEvoy (European Fuel Cell Group, Lucerne, Switzerland, 2000) p. 579.

305. A. C. MÜLLER, A. KRÜGEL, A. WEBER and E. IVERS-TIFFÉE, in "5th European SOFC Forum," edited by J. Huijsmans (European Fuel Cell Forum, Lucerne, Switzerland, 2002) p. 737.

306. J. WILL, A. MITTERDORFER, C. KLEINLOGEL, D. PEREDNIS and L. J. GAUCKLER, *Solid State Ionics* **131** (2000) 79.

307. D. GHOSH, G. WANG, R. BRULE, E. TANG and P. HUANG, in "SOFC-VI," edited by S. C. Singhal and M. Dokiya (Electrochem. Soc., Pennington, NJ, 1999) Vol. 99–19, p. 822.

308. P. K. SRIVASTAVA, T. QUACH, Y. Y. DUAN, R. DONELSON, S. P. JIANG, F. T. CIACCHI and S. P. S. BADWAL, *Solid State Ionics* **99** (1997) 311.

309. Y. J. LENG, S. H. CHAN, K. A. KHOR, S. P. JIANG and P. CHEANG, *J. Power Sources* **117** (2003) 26.

310. D. PEREDNIS and L. J. GAUCKLER, *Solid State Ionics* **166** (2004) 229.

311. T. ISHIHARA, K. SATO, Y. MIZUHARA and Y. TAKITA, *Chem. Lett.* **1992** (1992) 943.

312. J. WILL, M. K. M. HRUSCHKA, L. GUBLER and L. J. GAUCKLER, *J. Amer. Ceram. Soc.* **84** (2001) 328.

313. P. SARKAR and H. RAO, in "SOFC-VIII," edited by S. C. Singhal and M. Dokiya (Electrochem. Soc., Pennington, NJ, 2003) Vol. 2003–07, p. 135.

314. J.-W. KIM, A. V. VIRKAR, K.-Z. FUNG, K. MEHTA and S. C. SINGHAL, *J. Electrochem. Soc.* **146** (1999) 69.

315. P. CHARPENTIER, P. FRAGNAUD, D. M. SCHLEICH and E. GEHAIN, *Solid State Ionics* **135** (2000) 373.

316. C. XIA and M. LIU, *ibid.* **144** (2001) 249.

317. Y.-S. YOO, J.-H. KOH, J.-W. PARK and H. C. LIM, in "5th European SOFC Forum," edited by J. Huijsmans (European Fuel Cell Group, Lucerne, Switzerland, 2002) p. 191.

318. P. HOLTAPPELS, T. GRAULE, B. GUT, U. VOGT, L. GAUCKLER, M. JÖRGER, D. PEREDNIS, K. HONEFFER, G. ROBERT, S. RAMBERT and A. J. MCEVOY, in "SOFC-VIII," edited by S. C. Singhal and M. Dokiya (Electrochem. Soc., Pennington, NJ, 2003) Vol. 2003–07, p. 1003.

319. R.-H. SONG, K.-S. SONG, Y.-E. IHM and H. YOKOKAWA, in "SOFC-VII," edited by H. Yokokawa and S. C. Singhal (Electrochem. Soc., Pennington, NJ, 2001) Vol. 2001–16, p. 1073.

320. S. DE SOUZA, S. J. VISCO and L. C. DE JONGHE, *Solid State Ionics* **98** (1997) 57.

321. A. V. VIRKAR, J. CHEN, C. W. TANNER and J.-W. KIM, *ibid.* **131** (2000) 189.

322. D. SIMWONIS, H. THÜLEN, F. J. DIAS, A. NAOUMIDIS and D. STÖVER, *J. Mater. Proc. Tech.* **92/93** (1999) 107.

323. D. SIMWONIS, A. NAOUMIDIS, F. J. DIAS, J. LINKE and A. MOROPOULOU, *J. Mater. Res.* **12** (1997) 1508.

324. B. HOBEIN, F. TIETZ, D. STÖVER and E. W. KREUTZ, in "Ionic and Mixed Conducting Ceramics IV," edited by T. A. Ramanarayanan, W. L. Worrell and M. Mogensen (Electrochem. Soc., Pennington, NJ, 2001) Vol. 2001–28, p. 164.

325. E. WANZENBERG, F. TIETZ, P. PANJAN and D. STÖVER, *Solid State Ionics* **159** (2003) 1.

326. D. KEK, P. PANJAN, E. WANZENBERG and J. JAMNIK, *J. Euro. Ceram. Soc.* **21** (2001) 1861.

327. M. CASSIDY, G. LINDSAY and K. KENDALL, *J. Power Sources* **61** (1996) 189.

328. F. MESCHKE, F. J. DIAS and F. TIETZ, *J. Mater. Sci.* **36** (2001) 5719.

329. F. TIETZ, F. J. DIAS, B. DUBIEL and H. J. PENKALLA, *Mater. Sci. Eng.* B **B68** (1999) 35.

330. J. YAN, Y. DONG, C. YU and Y. JIANG, in "SOFC-VII," edited by H. Yokokawa and S. C. Singhal (Electrochem. Soc., Pennington, NJ, 2001) Vol. 2001–16, p. 973.

331. J. W. YAN, Z. G. LU, Y. JIANG, Y. L. DONG, Y. YU and W. Z. LI, *J. Electrochem. Soc.* **149** (2002) A1132.

332. G. ROBERT, A. KAISER, K. HONEGGER and E. BATAWI, in "5th European SOFC Forum," edited by J. Huijsmans (European SOFC Forum, Lucerne, Switzerland, 2002) p. 116.

333. N. M. TIKEKAR, T. J. ARMSTRONG and A. V. VIRKAR, in "SOFC-VII," edited by S. C. Singhal and M. Dokiya (Electrochem. Soc., Pennington, NJ, 2003) Vol. 2003–07, p. 670.

334. H. MORI, C.-J. WEN, J. OTOMO, K. EGUCHI and H. TAKAHASHI, *Appl. Catal. A: General* **245** (2003) 79.

335. G. SCHILLER, R. H. HENNE, M. LANG, R. RUCKDÄSCHEL and S. SCHAPER, *Fuel Cells Bulletin* **3** (2000) 7.

336. M. LANG, R. HENNE, S. SCHAPER and G. SCHILLER, *J. Thermal Spray Techn.* **10** (2001) 618.

337. T. FRANCO, R. HENNE, M. LANG, G. SCHILLER and P. SZABO, in "5th European SOFC Forum," edited by J. Huijsmans (European Fuel Cell Group, Lucerne, Switzerland, 2002) p. 647.

338. S. J. VISCO, C. P. JACOBSON, L. C. DE JONGHE, A. LEMING, Y. MATUS, L. YANG, I. VILLAREAL and L. RODRIQUEZ-MARTINEZ, in "Ionic and Mixed Conducting Ceramics IV," edited by T. A. Ramanarayanan, W. L. Worrell and M. Mogensen (Electrochem. Soc., Pennington, NJ, 2001) Vol. 2001–28, p. 368.

339. S. J. VISCO, C. P. JACOBSON, I. VILLAREAL, A. LEMING, Y. MATUS and L. C. DE JONGHE, in "SOFC-VII," edited by S. C. Singhal and M. Dokiya (Electrochem. Soc., Pennington, NJ, 2003) Vol. 2003–07, p. 1040.

340. G. SCHILLER, T. FRANCO, R. HENNE, M. LANG, R. RUCKDÄSCHEL, P. OTSCHIK and K. EICHLER, in "SOFC-VII," edited by H. Yokokawa and S. C. Singhal (Electrochem. Soc., Pennington, NJ, 2001) Vol. 2001–16, p. 885.

341. M. MOGENSEN and K. KAMMER, *Annu. Rev. Mater. Res.* **33** (2003) 321.

342. S. P. JIANG, J. P. ZHANG, L. APATEANU and K. FOGER, *J. Electrochem. Soc.* **147** (2000) 4013.

343. S. P. JIANG, J. P. ZHANG and X. G. ZHENG, *J. European Ceramic Soc.* **22** (2002) 361.

344. W. J. QUADAKKERS, H. GREINER, M. HÄNSEL, A. PATTANAIK, A. S. KHANNA and W. MALLÉNER, *Solid State Ionics* **91** (1996) 55.

345. I. C. VINKE, L. G. J. DE HAART, L. BLUM and D. STOLTEN, in "5th European SOFC Forum," edited by J. Huijsmans (European Fuel Cell Group, Lucerne, Switzerland, 2002) p. 164.

346. T. YAMAMOTO, H. ITOH, M. MORI, T. WATANABE, N. IMANISHI, Y. TAKEDA and O. YAMAMOTO, *J. Power Sources* **61** (1996) 219.

347. A. KUZJUKEVICS and S. LINDEROTH, *Solid State Ionics* **93** (1997) 255.

348. S. LINDEROTH, N. BONANOS, K. V. JENSEN and J. B. BILDE-SØRENSEN, *J. Amer. Ceram. Soc.* **84** (2001) 2652.

349. K. V. JENSEN, S. PRIMDAHL, I. CHORKENDORFF and M. MOGENSEN, *Solid State Ionics* **144** (2001) 197.

350. M. MOGENSEN, K. V. JENSEN, M. J. JØRGENSEN and S. PRIMDAHL, *ibid.* **150** (2002) 123.

351. M. C. WILLIAMS and J. P. STRAKEY, in "SOFC-VII," edited by S. C. Singhal and M. Dokiya (Electrochem. Soc., Pennington, NJ, 2003) Vol. 2003–07, p. 3.

352. R. N. BASU, G. BLAβ, H. P. BUCHKREMER, D. STÖVER, F. TIETZ, E. WESSEL and I. C. VINKE, in "SOFC-VII," edited by H. Yokokawa and S. C. Singhal (Electrochem. Soc., Pennington, NJ, 2001) Vol. 2001–16, p. 995.

353. M. DOKIYA, *Solid State Ionics* **152/153** (2002) 383.

354. F. G. E. JONES and J. T. S. IRVINE, in "5th European SOFC Forum," edited by J. Huijsmans (European Fuel Cell Group, Lucerne, Switzerland, 2002) p. 123.

355. F. J. GARDNER, M. J. DAY, N. P. BRANDON, M. N. PASHLEY and M. CASSIDY, *J. Power Sources* **86** (2000) 122.

356. G. D. AGNEW *et al.*, in "SOFC-VII," edited by S. C. Singhal and M. Dokiya (Electrochem. Soc., Pennington, NJ, 2003) Vol. 2003–07, p. 78.

357. K. WIPPERMANN, in Proc. of IEA Workshop—Materials and Mechanisms, edited by K. Nisanciogly (International Energy Agency, Paris, 1999) p. 31.

358. S. PRIMDAHL and M. MOGENSEN, *J. Electrochem. Soc.* **145** (1998) 2431.

359. S. P. JIANG and S. P. S. BADWAL, *Solid State Ionics* **123** (1999) 209.

360. A. BIEBERLE, L. P. MEIER and L. J. GAUCKLER, *J. Electrochem. Soc.* **148** (2001) A646.

361. A. BIEBERLE and L. J. GAUCKLER, *Solid State Ionics* **146** (2002) 23.

362. M. IHARA, T. KUSANO and C. YOKOYAMA, *J. Electrochem. Soc.* **148** (2001) A209.

363. C. WEN, R. KATO, H. FUKUNAGA, H. ISHITANI and K. YAMADA, *ibid.* **147** (2000) 2076.

364. P. HOLTAPPELS, L. G. DE HAART and U. STIMMING, *ibid.* **146** (1999) 1620.

365. N. NAKAGAWA, K. NAKAJIMA, M. SATO and K. KATO, *ibid.* **146** (1999) 1290.

366. S. H. CHAN, X. J. CHEN and K. A. KHOR, *J. Appl. Electrochem.* **31** (2001) 1163.

367. J. WINKLER, P. V. HENDRIKSEN, N. BONANOS and M. MOGENSEN, *J. Electrochem. Soc.* **145** (1998) 1184.

368. S. B. ADLER, *ibid.* **149** (2002) E166.

369. S. P. JIANG, *J. Appl. Electrochem.*, in press.

370. Y. J. LENG, S. H. CHAN, K. A. KHOR and S. P. JIANG, *ibid.* **34** (2004) 409.

371. S. MCINTOSH, J. M. VOHS and R. J. GORTE, *J. Electrochem. Soc* **150** (2003) A1305.

372. B. W. CHUNG, A.-Q. PHAM, J. J. HASLAM and R. S. GLASS, *ibid.* **149** (2002) A325.

373. R. IHRINGER, S. RAMBERT, L. CONSTANTIN and J. VAN HERLE, in "SOFC-VII," edited by H. Yokokawa and S. C. Singhal (Electrochem. Soc., Pennington, NJ, 2001) Vol. 2001–16, p. 1002.

374. A. V. VIRKAR, J. CHEN, C. W. TANNER and J.-W. KIM, *Solid State Ionics* **131** (2000) 189.

375. Y. JIANG and A. V. VIRKAR, *J. Electrochem. Soc.* **150** (2003) A942.